BIODEGRADATION OF NAPHTHENIC ACIDS IN MICROBIAL FUEL CELL TYPE BIOREACTORS

A Thesis Submitted to the College of

Graduate and Postdoctoral Studies

In Partial Fulfillment of the Requirements

For the Degree of Master of Science

In the Department of Chemical and Biological Engineering

University of Saskatchewan

Saskatoon

By

GUADALUPE MONTSERRAT VALDES LABRADA

© Copyright Guadalupe Montserrat Valdes Labrada, April, 2017. All rights reserved.

PERMISSION TO USE

In presenting this thesis in partial fulfillment of the requirements for a Postgraduate degree from the University of Saskatchewan, I agree that the Libraries of this University may make it freely available for inspection. I further agree that permission for copying of this thesis in any manner, in whole or in part, for scholarly purposes may be granted by the professor or professors who supervised my thesis work or, in their absence, by the Head of the Department or the Dean of the college in which my thesis work was done. It is understood that any copying or publication or use of this thesis or parts thereof for financial gain shall not be allowed without my written permission. It is also understood that due recognition shall be given to me and to the University of Saskatchewan in any scholarly use which may be made of any material in my thesis.

Requests for permission to copy or to make other use of material in this in whole or part should be addressed to:

Head of the Department of Chemical and Biological Engineering

57 Campus Drive

University of Saskatchewan

Saskatoon, Saskatchewan S7N 5A9

Canada

ABSTRACT

Canada has the third largest oil reserves in the world. Close to 96% of these reserves are located in oil sands deposits (CAPP, 2015). Extraction of bitumen from these oil sands is carried out by alkaline hot water process (Clark Process) which results in the generation of large volumes of waters contaminated with naphthenic acids (NAs). These waters are referred to as Oil Sands Process Water (OSPW) and they are maintained in large tailing ponds due to their toxicity and a zero-discharge policy enforced by the Government.

Given the environmental challenges associated with OSPW and tailing ponds, several physicochemical and biological treatments have been evaluated as remediation option. Previous studies in our research group have successfully achieved biodegradation of model NAs in conventional bioreactors of various configurations under aerobic and anoxic conditions (Paslawski et al., 2009; Huang et al., 2012; D'Souza et al., 2014; Gunawan et al., 2014; Dong and Nemati, 2016). Against this background, the current work offer an alternative treatment approach based on anoxic biodegradation of NAs in Microbial Fuel Cells (MFCs). MFCs are unconventional bioreactor in which biodegradation of a contaminant occurs with concomitant generation of energy.

In the present study, biodegradations of a linear (octanoic acid) and a cyclic NA (trans-4-methyl-1-cyclohexane carboxylic acid, trans-4MCHCA) were evaluated in MFCs. Firstly, biodegradation of individual NAs (100, 250 and 500 mg L^{-1}) was carried out in batch operated MFCs with either graphite rod or granular graphite electrodes. Maximum biodegradation rates in the single rod electrode MFCs were achieved during the biodegradation of NAs with highest concentration (1.56 and 2.46 mg L^{-1} h^{-1} for trans-4MCHCA and octanoic acid, respectively). This trend was also observed in MFCs with granular electrodes, where the removal of 500 mg L^{-1} of each individual compound led to the highest biodegradation rates, with values of 7.2 and 22.78 mg L^{-1} h^{-1} for trans-4MCHCA and octanoic acid, respectively. Regardless of the type of employed electrodes, biodegradation of the linear NA occurred at a rate much faster than that of its cyclic counterpart. Moreover, sequential batch operation of MFCs enhanced the biodegradation rate of both compounds.

In continuously operated MFCs with granular electrodes, biodegradation of each individual NAs (trans-4MCHCA or octanoic acid) was assessed at initial concentrations of 100, 250 and 500 mg L^{-1}, with the maximum biodegradation rate again achieved with the highest NA concentration (36.5 and 49.9 mg L^{-1} h^{-1} for trans-4MCHCA and octanoic acid, respectively). Interestingly, the highest current and power densities were attained when the biodegradation rate was at the level, with the values being 481.5 mW m^{-3} and 4296.3 mA m^{-3} for trans-4MCHCA, and 963.0 mW m^{-3} and 6000.0 mA m^{-3} for octanoic acid.

Co-biodegradation of linear and cyclic NAs was also studied using mixtures of NAs with different concentrations in two MFC configurations: batch-wise operated with single rod electrodes and continuously operated with granular electrodes. In batch MFCs with single rod electrodes, it was observed that biodegradation of the linear NA occurred first and biodegradation of the cyclic NA occurred only after complete exhaustion of the linear compound. Contrary to what observed in the batch MFC with rod electrodes, in the continuous flow MFC with granular electrodes biodegradation of cyclic and linear NAs occurred simultaneously, with the biodegradation rate of the linear NA being much faster than that of the cyclic NA.

ACKNOWLEDGEMENTS

I would like to express my sincere gratitude to my supervisor Dr. Mehdi Nemati for his constant support, guidance and motivation throughout my Master's program. I truly appreciate the given opportunity to become part of his research group and collaborate on this project. I would also like to acknowledge the valuable advice and comments of my committee members, Dr. Richard Evitts and Dr. Lifeng Zhang. Additionally I would like to thank Richard Blondin for the continuous support provided and my lab mates for making this experience a remarkable one.

Finally, I would like to acknowledge the University of Saskatchewan, and Natural Sciences and Engineering Research Council of Canada (NSERC) for their financial support for this research work.

DEDICATION

To my parents, Ma. Luisa Labrada and Porfirio Valdes, for all their love and encouragement throughout this project and my entire life.

To my brother, Israel Valdes Labrada, for being the best brother I could ever ask for.

TABLE OF CONTENTS

LIST OF TABLES

LIST OF FIGURES

NOMENCLATURE AND ABBREVIATIONS

Nomenclature

I: Current (mA)

P: Power (mW)

Q: volumetric flow rate of the influent and the effluent (mL h^{-1})

S: residual NAs concentration (mg L^{-1})

So: feed NAs concentration (mg L^{-1})

V: Circuit Potential (mV)

V: working volume of the bioreactor (mL)

Abbreviations

4-MCHAA: 4-methyl-cyclohexane acetic acid

AEM: Anion Exchange Membranes

AEO: Acid-Extractable Organics

BTEX: Benzene, Toluene, Ethylbenzene and Xylenes

CAPP: Canadian Association of Petroleum Producer

CEM: Cation Exchange Membrane

COD: Carbon Oxygen Demand

CPBB: Circulating Packed Bed Bioreactor

CSS: Cyclic Steam Stimulation

CSTR: Continuous Stirred Tank Reactor

ESI-MS: Electron spray ionization-mass spectrometry

FTICR: Fourier Transform Ion Cyclotron Resonance

FTIR: Fourier Transform Infrared

GC: Gas Chromatography

HEPEM: High Exchange Capacity Proton Exchange Membrane

HPLC: High Performance Liquid Chromatography

LC: Liquid Chromatography

LSV: Linear Sweep Voltammetry

MFC: Microbial Fuel Cell

MS: Mass Spectrometry

NAs: Naphthenic Acids

OCP: Open Circuit Potential

OD: Optical Density

OSPW: Oil Sand Process Water

PAHs: Polycyclic Aromatic Hydrocarbons

PEM: Proton Exchange Membrane

RO: Reverse Osmosis

SAGD: Steam Assisted Gravity Draining

TOF: Time of Flight

TPH: Total Petroleum Hydrocarbon

trans-4MCHCA: trans-4-methyl-1-cyclohexane carboxylic acid

CHAPTER 1
INTRODUCTION

The extraction of bitumen from the oil sands in northern Alberta has led to generation of large amounts of contaminated water known as Oil Sand Process Water (OSPW). According to the Canadian Association of Petroleum Producer (CAPP, 2015), in situ and surface mining methods for extraction of bitumen requires 0.3 and 2.8 barrels of fresh water for every barrel of bitumen produced, respectively. During the processing of oil sand, bitumen is separated for further processing and the leftover liquid (mainly composed of salts, clay, residual bitumen, water and most importantly, toxic compounds) is contained in tailing ponds. Tailing ponds enable water recycle and ensure compliance with the zero effluent discharge policy enforced by the Government of Alberta (Alberta Environmental Protection and Enhancement Act, 1993).

The main toxic compounds in OSPW are naphthenic acids (NAs), and their treatment is one of the primary objectives of research related to these waters (MacKinnon and Boerger, 1986; Allen, 2008a). In recent years, several approaches have been evaluated to reduce NAs concentration in OSPW, including advanced oxidation via ozone, coagulation/flocculation, membrane filtration and adsorption, among others (Quagraine et al., 2005; Allen, 2008b). However, NAs were found to be susceptible to natural degradation by indigenous microorganisms in tailing ponds (Herman et al., 1994), which potentially makes biodegradation one of the effective and environmental friendly methods for their treatment (Han et al., 2008).

NAs biodegradation, both aerobic and anoxic, have been extensively studied in previous works in our research group. These included, aerobic biodegradation and co-biodegradation of model NAs (octanoic acid, trans-4-methyl-1-carboxylic acid, and cis and trans isomers of 4-methyl-1-cyclohexane acetic acid) in batch system, continuous stirred tank reactor (CSTR), packed-bed and circulating packed bed bioreactors (CPBB) (Paslawski et al., 2009; Huang et al., 2012; D'Souza et al., 2014). Subsequent studies showed the feasibility of anoxic biodegradation

of trans-4-methyl-1-cyclohexane carboxylic acid using batch, continuous stirred tank reactor (CSTR) and biofilm reactor under denitrifying conditions (Gunawan et al., 2014) and with nitrite as electron acceptor (Dong and Nemati, 2016). It should be emphasized that oxygen in tailing ponds is limited to the surface layers, causing most hydrocarbon degradation to be catalyzed by anaerobic bacteria (An et al., 2013). This fact represents a need to study anaerobic biodegradation, not only to simulate the real OSPW conditions, but also to eliminate the costs associated with aeration needed for aerobic biodegradation.

As can be seen, previous research has focused on the use of conventional bioreactors. The development of microbial fuel cell technology, that converts chemical energy contained in organic or inorganic compounds to electrical energy, offer an unconventional and feasible alternative for anoxic biodegradation of NAs (Du et al., 2007).

In the present work, biodegradation and co-biodegradation of a linear and a cyclic NA (octanoic acid and trans-4-methyl-1-cyclohexane carboxylic acid, respectively) were studied in batch MFCs with single rod electrode and freely suspended bacterial cells. Batch and continuous biodegradation of individual NAs was also evaluated in MFCs with granular graphite electrodes that allowed formation of biofilm and facilitate the transfer of electrons through their extended surface. Co-biodegradation of a linear and cyclic NAs was also studied in continuously operated MFCs with granular electrodes.

The present thesis consists of five chapters including Introduction, Literature Review, Knowledge Gap and Research Objectives, Materials and Methods, Results and Discussion and Conclusions and Recommendations for Future Work.

CHAPTER 2
LITERATURE REVIEW, KNOWLEDGE GAP AND RESEARCH OBJECTIVES

2.1 Oil Sand Industry and Oil Sand Process Water

Canadian oil sands are the third largest reserves of crude oil in the world, covering 142,200 km^2 of land in the Athabasca, Cold Lake and Peace River areas in northern Alberta. Around 166 billion barrels of bitumen can be recovered from these oil sands (CAPP, 2015). The oil sands consist of bitumen (~12 wt%), sand, silts, clays (mineral content ~85 wt%), and water (3–6 wt%) (Pramanik, 2016). Mining and in situ methods are used to recover bitumen from the oil sands. The choice depends on the depth of oil reserves. When bitumen is deposited at depths less than 70 meters, it can be surface mined; however about 80 percent of the recoverable bitumen is buried too deep and can only be recovered by in situ methods (Government of Alberta, 2015).

During the surface mining, oil sand are mined and crushed for size reduction, followed by the addition of caustic hot water as part of the modified Clark Process (Clark and Pasternack, 1932; Kannel and Gan, 2012). The mixture is transported via hydrotransport to extraction plant where bitumen is extracted in separation vessels. In situ methods include the injection of steam into the reservoir, combustion or other heating methods to warm the bitumen and pumped it to the surface through recovery wells. Practical approaches for this approach include cyclic steam stimulation (CSS) and steam assisted gravity draining (SAGD) (CAPP, 2015).

Both methods of bitumen recovery require water. Despite the fact that oil sands industry recycles 80-95% of water used, the Canadian Association of Petroleum Producers (CAPP, 2015) reported that oil sands fresh water use in 2014 was about 168 million m^3. In order to reduce the use of fresh water and to prevent environmental contamination, oil sand process water (OSPW) is stored in dyke systems known as tailing ponds. Tailing ponds not only allow water to be separated and continuously recycled, but also act as storage systems to meet the zero effluent discharge

policy established by the Government of Alberta due to toxicity of the OSPW constituents (Alberta Environmental Protection and Enhancement Act, 1993). The total area of existing tailings ponds is around 220 km^2 (CAPP, 2015).

OSPW is highly alkaline with elevated concentrations of salts, dissolved solids, suspended solids, and toxic compounds. The toxic compounds include heavy metals, organic compounds, residual bitumen and naphthenic acids (NAs), the latter being the main contributors to toxicity. NAs are toxic to a variety of organisms including plants, fish, mammals, zooplanktons, phytoplanktons and amphibians (Kannel and Gan, 2012) and they can be can be highly toxic even at low concentrations (Allen, 2008a).

2.2 Naphthenic Acids

NAs are transferred into the water during the Clark Process and their concentration in the tailing ponds typically range between 40 and 120 mg L^{-1} (Holowenko et al., 2001). NAs consist of a complex mixture of alkyl-substituted acyclic and cycloaliphatic carboxylic acids, with the general chemical formula $C_nH_{2n+Z}O_2$, where n indicates the carbon number and Z that is either zero or negative, specifies the hydrogen deficiency resulting from the ring formation (Clemente and Fedorak, 2005). Therefore, NAs contain one or more cycloalkane rings (five- or six-carbon), an aliphatic side chain of various lengths, and a carboxylic group (Herman et al., 1994). NAs found in OSPW are in the range of n= 7-30 and Z= 0 to -12 (Whitby, 2010).

Naphthenic acids are weak acids, with a *pka* in the range of 5-6 (Headley and McMartin, 2004). Because of the alkalinity of OSPW, NAs remain water-soluble in the tailing ponds. Table 2.1 summarizes physicochemical properties of NAs.

NAs exhibit characteristics of surfactants, since they are composed of hydrophobic alkyl groups and a hydrophilic carboxylic group (Brient et al., 2000). This surfactant nature is associated with their toxicity, since NAs are able to easily penetrate the cell wall of organisms and cause membrane disruption (Headley and McMartin, 2004). Factors such as dissolved oxygen (DO), temperature, salinity, hardness, and the presence of additional contaminants may increase or decrease the sensitivity of biota to NAs, or cause toxicity themselves (Siwik et al., 2000).

Table 2.1 Summary of the physical and chemical properties of NAs (Quinlan & Tam, 2015)

Parameter/Property	General description
Color	Pale yellow to dark amber
State	Viscous liquid
Molecular weight	140–450 g mol^{-1}
Density	0.97–0.99 g cm^{-3}
Water solubility	<50 mg L
Dissociation constant	5-6
Boiling point	250-350 ºC

Identification and quantification of NAs is an important aspect of research in the field of OSPW treatment. Several analytical methods have been used to characterize NAs as individual compound or in a mixture. These include Fourier Transform Infrared (FTIR) spectroscopy, Gas Chromatography (GC), Mass Spectrometry (MS), Electron spray ionization-mass spectrometry (ESI-MS) and High performance liquid chromatography (HPLC) (Clemente and Fedorak, 2005). MS or GC-MS have provided some of the most accurate information to date and therefore are widely used to analyze NAs mixtures. Complete isolation and characterization of individual NAs in OSPW has not been achieved because of the extreme complexity of the NAs mixture in OSPW. However, emerging techniques such as HPLC coupled with time of flight (TOF)-MS, GC x GC/MS, LC x LC (Comprehensive Liquid Chromatography)/MS, LC/MS/MS, Orbitrap MS, and ESI Fourier Transform Ion Cyclotron Resonance (FTICR) MS are being studied (Headley et al., 2013).

As far as the treatment of OSPWs is concerned, it is crucial to develop methods that not only promote a decrease in OSPW toxicity, but also allow effective water recycle. As reviewed by Quinlan and Tam (2015), various physical and chemical methods such as advanced oxidation, coagulation/flocculation, membrane filtration, adsorption and bioremediation have been applied for reducing NA toxicity. Simulated wetlands have also been studied (Quagraine et al., 2005; Allen, 2008b). Among these treatment options, bioremediation, both aerobic and anaerobic, has been identified as one of the most cost-effective method for removing NAs from OSPW (Scott et al., 2008) and will be discussed in detail in the following sections.

2.3 Biodegradation of NAs

Microorganisms are naturally found in tailing ponds and include a wide variety of aerobic and anaerobic microbial species (Golby et al., 2012; An et al., 2013). The activities of microbial communities depend on the depth in tailing ponds. For instance, it is known that the activities of aerobic bacteria are limited to the surface water, while the rest of the tailing ponds are largely dominated by anaerobic species (Ramos-Padrón et al., 2011; An et al., 2013). Despite the awareness of the anaerobic nature of tailing ponds, most biodegradation studies focus on aerobic processes with the aim of conducting the bioremediation externally and in aerobic systems (Whitby, 2010). Some disadvantages of these aerobic systems include high aeration costs and high biomass production.

2.3.1 Aerobic biodegradation

Important findings about the impact of the structure of NAs (naturally found in OSPW and commercially available) on their biodegradability have been revealed through several studies. Cyclic molecular structures have been shown to be more recalcitrant than linear compounds (Quagraine et al., 2005). Moreover, highly branched NAs appear more resistant to biodegradation than less branched NAs (Smith et al., 2008). The *trans*-isomer of model NA compounds, has been reported to be more easily degraded than the *cis*-isomer (Headley et al., 2008; Huang et al., 2012; D'Souza et al., 2014). In the same context, commercial NAs mixtures have been completely removed by aerobic tailing cultures, while no complete removal has been achieved in the case of NAs mixtures obtained from OSPW (Clemente et al., 2004; Scott et al., 2005; Del Rio et al., 2006).

Environmental factors such as oxygen concentration, pH, salinity, redox potential and sunlight may influence NAs degradation (Whitby, 2010). Nutrient availability is another factor that impacts the biodegradability of NAs (Herman et al., 1994; Lai et al., 1996). Finally, temperature has proven to have a significant effect on microbial activity which directly influences the biodegradation kinetics (Headley and McMartin, 2004; Paslawski et al., 2009).

Several approaches have been developed to promote aerobic NAs biodegradation. Different types of biofilm reactors, batch wise and continuously operated, have been studied for biodegradation of NAs and for removing the toxicity from oil sand process water. Previous studies

in our research group have successfully degrade a surrogate NA (trans-4-methyl-1-cyclohexane carboxylic acid, trans-4MCHCA) in batch system, continuously stirred tank reactor (CSTR) and packed bed biofilm reactor (Paslawski et al., 2009). In these studies, different factors affecting the biodegradation rate were evaluated and it was found that the highest rate of biodegradation (4.75 mg L^{-1} h^{-1}) was achieved at a temperature of 23 °C for initial substrate concentration of 500 mg L^{-1}. Moreover, the maximum specific growth rate, biodegradation rate and cell yield were obtained at pH 10. In a follow-up study, Huang et al. (2012) evaluated batch and continuous biodegradation of trans-4MCHCA, a mixture of cis- and trans-4-methyl-cyclohexane acetic acid (4-MCHAA), and mixture of these three naphthenic acids in a CPBB. The results of this work revealed that the biotransformation of the NAs was influenced by the carbon number and the spatial arrangement of the alkyl side branch, with the cis- and trans- 4-methyl-cyclohexane acetic acid biodegradation rates being much lower than that obtained with trans-4-methyl-cyclohexane carboxylic acid as a substrate. Moreover, the maximum biodegradation rate of trans-4MCHCA (209 mg L^{-1} h^{-1}) was observed during the continuous mode of operation. D'Souza et al. (2014) investigated the continuous co-biodegradation of a linear (octanoic acid) and three cyclic NAs (trans-4MCHCA, and cis- and trans-4-MCHAA) in the same reactor configuration (CPBB). The outcomes of this study indicated that in a mixture, biodegradation of the linear NA proceeded with the fastest rate, followed by trans-4MCHAA, and cis-4MCHAA. In addition, it was reported that co-biodegradation of the most recalcitrant NAs (cis- and tran-4MCHAA) with octanoic acid, led to higher biodegradation rates of these cyclic NAs.

As seen, aerobic biodegradation has been studied extensively; however, no biodegradation study has achieved complete removal of NAs in oils sand process water (Brown and Ulrich, 2015). Hence, there is an evident need to evaluate complementary techniques that promote a more effective treatment of these waters. Recent works have evaluated the use of ozone oxidation and adsorption as a pre- or post-treatment options for NAs biodegradation.

According to Martin et al. (2010) ozonation of OSPW prior to biodegradation, led to the removal of the most recalcitrant NAs (high carbon numbers and cyclicity), thereby microbial population were able to easily break drown the remaining NA compounds. Other studies have reported that ozonation followed by biodegradation achieved a much higher removal of NAs compared to that achieved with biodegradation itself. Hwang et al. (2013) reported an increase of

NAs removal from 18.5% to 99% when ozone treatment was applied prior to biodegradation in a biofilm reactor. Similarly, Shi et al. (2015) found that the removal of NAs in moving bed biofilm reactors can be increased from 34.8 to 78.8% as a result of pre-treatment with ozone. The combined adsorption and biodegradation processes through the use of granular activated carbon (GAC) and biofilm with or without ozonation pre-treatment was evaluated by Islam et al. (2016). The outcomes of this work indicated that biodegradation and adsorption contributed 14% and 63% in removal of NAs in raw OSPW, respectively. With ozone pre-treatment, 18% of NAs were removed by microbial communities and 73% by adsorption, reaffirming the improved NAs removal achieved with ozonation processes.

Despite the benefits listed above, the high cost associated with ozone oxidation and the formation of toxic byproducts from metals in tailings water have been indicated as the main limitations of this technique (Martin et al., 2010).

2.3.2 Anaerobic biodegradation

As previously mentioned, oil sands tailing ponds are aerobic at the surface but turn anaerobic at depth of approximately 1 m below the surface and lower (Ramos-Padrón et al., 2011; Clothier and Gieg, 2016). Depending on the tailing ponds depth, compounds rather than oxygen are available that could serve as electrons acceptors (Ramos-Padrón et al., 2011). This anaerobic nature of tailing ponds in conjunction with the high aeration cost of aerobic processes have resulted in studies on anaerobic biodegradation of NAs.

Folwell et al. (2016) investigated the anaerobic biodegration of two polycyclic aromatic hydrocarbons (pyrene and 2-methylnaphthalene), a model NA (adamantane-1-carboxylic acid) and a mixture of NAs from OSPW. Results from this work indicated that the only compound amenable to biodegradation was 2-methylnaphthalene, with a removal percentage of 40% and 25% under sulfate-reducing and methanogenic conditions, respectively. No significant biotransformation of the evaluated NAs was observed. In contrast to these findings, Clothier and Gieg, (2016), showed that anoxic biodegradation of five surrogate NAs (cyclohexanecarboxylic acid, cyclohexaneacetic acid, cyclohexanepropionic acid, cyclohexanebutyric acid, and cyclohexanepentanoic acid) was attainable with a variety of electron acceptors. Removal of a mixture of the five surrogate NAs

was either partially or fully achieved when nitrate and sulfate were used as electrons acceptors. Under iron-reducing conditions, all surrogate NAs were partially removed, with removal percentages from 40% (cyclohexaneacetic acid) to 78% (cyclohexanepentanoic acid). Under methanogenic conditions, only cyclohexanecarboxylic acid was completely biodegraded.

Earlier works in our research group have also focused on anoxic biodegradation of a model NA (trans-4MCHCA) in CSTR and packed bed biofilm reactor. For instance, Gunawan et al. (2014) found that anoxic biodegradation coupled to reduction of nitrate was not only feasible but also achieved higher or comparable removal rates to those obtained under aerobic conditions. In a follow-up study, Dong and Nemati (2016) replaced nitrate with nitrite as electron acceptor during removal of this NA. Although the results confirmed the effectiveness of this approach, it was demonstrated that higher loading and removal rates were achieved when nitrate was used in the bioreactors. In other words, the superiority of nitrate as an electron acceptor for anoxic biodegradation of NAs was demonstrated.

2.4 NAs Treatment in Microbial Fuel Cells

In addition to conventional biodegradation approaches for the treatment of NAs, there is potential for improving the feasibility of NA biodegradation using microbial fuel cell (MFC) type bioreactors that represent an unconventional bioreactor operated under anoxic conditions. The advantage of this technology is the treatment of contaminated water with simultaneous generation of energy.

2.4.1 Fundamentals of MFCs technology

Biodegradable organic matter found in wastewater contains energy that could be used to sustain their treatment. However, existing treatment methods invest much more additional energy to treat these waters. For instance, at a conventional wastewater treatment plant in Toronto, Canada, the amount of energy present in the wastewater was estimated to be 9.3 times the energy that was required for its treatment (Shizas and Bagley, 2004; Logan, 2008). Microbial fuel cell (MFCs) is a promising technology that would allow the utilization of the energy contain in

wastewater treatment systems would eliminate the aeration cost and reduce sludge production, among other advantages (Logan, 2008).

A MFC is a bioreactor that converts chemical energy in organic or inorganic compounds to electrical energy through the reactions catalyzed by microorganisms under anaerobic conditions (Du et al., 2007). As seen in Figure 2.1, a typical MFC consists of anode and cathode chambers, separated by a proton exchange membrane (PEM). The fuel, which is the carbon source or organics in wastewater, is oxidized by anaerobic microorganisms and as a result of this reaction, electrons and protons are released. Electrons travel through an external circuit to reach the cathodic chamber where an electron acceptor is reduced. At the same time, protons pass through the proton exchange membrane to the cathodic chamber (Oh and Logan, 2006; Rahimnejad et al., 2015).

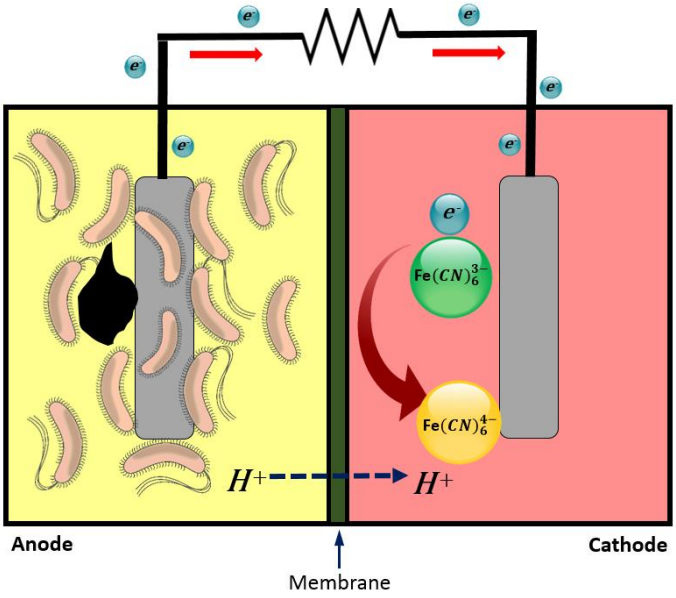

Figure 2.1 Schematic of a typical dual chamber MFC.

In order to understand how this process works, it is first necessary to understand how bacteria capture and process energy for its growth. Some bacteria can transfer the electrons that are generated as part of their metabolism to the outside the cell (exogenously) to a material that is not the immediate electron acceptor. This is done by using either electron shuttles, outer membrane proteins and/or nanowires; these bacteria are called *exoelectrogens*. Many microorganisms can only transfer electrons to soluble compounds such as oxygen, nitrate or sulfate that can diffuse

across the cell membrane and into the cell. Exoelectrogenic bacteria are distinguished from these microorganisms by their ability to directly transport electrons outside the cell which permits them to function in a MFC (Logan, 2008). As an example, *Geobacter* and *Shewanella* species have been extensively utilized in MFCs for electric power generation (Gorby et al., 2006; Watson and Logan, 2010). Similary, *Pseudomonas* species are the other group that have been evaluated. *Pseudomonas putida* have been used for fatty acids and phenol degradation in MFCs (Moreno et al., 2015, 2017), while *Pseudomonas aeruginosa* has been proved to be capable of generating electricity in a glucose fed biofuel cell (Rabaey et al., 2004). It is important to note that MFCs that use mixed cultures achieve greater power outputs than those with pure cultures (Rabaey et al., 2004; Logan et al., 2006).

2.4.2 MFCs Designs

MFCs are constructed with a wide range of materials and different configurations, which will be discussed in the following sections. Depending on the configuration, the number of chambers or the mode of operation, MFCs are classified in three main categories: two-chamber, single-chamber or stacked MFCs. A very common design, mainly for research purposes, is the two-chamber "H" type system, which consists of two chambers connected by a tube containing a separator which is usually a cation exchange membrane (CEM) or a salt bridge (Oh and Logan, 2006). The membrane employed for this configuration must allow protons to pass between the chambers, but not the substrate or the catholyte solution. The H-shape configuration is very useful for basic research such as the measurement of the electrochemical performance using new materials of construction or new substrates in the anodic chamber. However, the power density produced by these systems is typically limited by high internal resistance and electrode-based loses which can be overcome by using a good electron acceptor such as ferricyanide at high concentrations in the cathodic chamber (Oh and Logan, 2006).

In the case of the single-chamber configuration, there is only one anodic chamber coupled with a porous air cathode that is exposed directly to the air, either in the presence or absence of a membrane. The potential elimination of the membrane may lead to a significant internal ohmic resistance reduction (Liu and Logan, 2004; Buitrón and Moreno-Andrade, 2014). Protons and electrons are transferred from the anolyte solution to the cathode (Du et al., 2007; Tharali et al.,

2016), which results in a reduction of the mass transport loss by minimizing the energy required to drive the hydrodynamic flow (Buitrón and Moreno-Andrade, 2014).

Finally, a stacked microbial fuel cell refers to a group of MFCs connected in series or in parallel in order to enhance the electrochemical outputs. Aelterman et al. (2006), compared the performance of MFCs in parallel and series and reported that at the same volumetric flow rate, six times higher electrochemical outputs (voltage and current) were achieved in the parallel system, indicating that higher biochemical reaction rates occurred with this MFC configuration.

2.4.3 MFC Components

Anode and anodic chambers. The materials used in the anodic chamber has a direct effect on key performance parameters, such as microbial adhesion, electron transfer and substrate oxidation (Sonawane et al., 2016). The required characteristics of an anodic material include: corrosion resistant, high specific surface area (area per volume) and high porosity, low electrical resistance and most important, high electrical conductivity (Logan, 2008; Sonawane et al., 2016). The most frequently used materials in anode are made of carbon materials, namely graphite fiber brush, carbon cloth, graphite rod, carbon paper, reticulated vitreous carbon (RVC) and carbon felt. Graphite granules and granular activated carbon have also been widely studied (Moreno et al., 2015, 2017; Rahimnejad et al., 2015).

Graphite rods have been used in several MFC studies as they are highly conductive and have high surface areas and low internal porosity. The reported conductivity of a common graphite rod is 0.2 Ω/cm. Similarly, graphite granules have been extensively used in electrochemical studies in reported diameters of d= 1.5 to 5 mm with specific surface areas estimated to range from 820 to 2700 m^2/m^3 and a porosity θ=0.53. This porosity can be related to specific surface area using $A_s = 6\ \theta/d$. The reported granules conductivity is 0.5 – 1 Ω/granule. It should be pointed out that the granules must make good electrical contact with each other to make the complete bed conductive (Rabaey et al., 2005; Logan, 2008).

In order to improve the performance of MFCs, modification of anode materials through the use of different nanoengineering techniques has been carried out. These new materials not only allow an easier electron transfer, but also enhance the power output of the system. Graphite

composite with polymers, conductive polymer coatings, stainless steel and graphene based anodes are some examples of the new materials that have been studied in recent years (Rahimnejad et al., 2015).

Cathode and cathodic chambers. Oxygen has usually been used as the final electron acceptor in the cathodic chamber due to its accessibility, intense oxidation potential (0.805 V), and the fact that it does not led to toxic by-products. However, due to the slow rate of oxygen reduction on plain graphite, the use of Pt catalyst is needed (Logan et al., 2006; Rahimnejad et al., 2015).

The most used catholyte in MFCs next to oxygen is ferricyanide ($Fe(CN)_6^{3-}$), which has a standard potential of 0.361 V and is highly soluble in water. In contrast to oxygen, no catalyst is needed when potassium ferricyanide ($K_3[Fe(CN)_6]$) is used in the cathode. The main advantage of this electron acceptor is the low overpotential on plain carbon electrodes, resulting in cathode working potential close to its open circuit potential. Despite these advantages, one of the main difficulties associated with the use of ferricyanide in the cathodic chamber is the insufficient reoxidation by oxygen and thus the need for regular replacement (Logan, 2008).

Biocathodes in which reduction reactions are catalyzed by microorganisms represent another option to overcome the catalysis requirement (Watanabe, 2008). Compared with abiotic cathodes, biocathodes have the advantage of self-regeneration of the catalyst, low cost, sustainability and may generate valuable products or remove unwanted by-products (Zhang et al., 2012). Toxic nature of ferricyanide is the other drawback.

Membrane. Membrane is an essential component of a MFC. They are primarily used in two-chambered systems to separate the anodic and cathodic liquids. Membranes must be selectively permeable so that protons produced at the anode can migrate to the cathode. Ion exchange membranes are classified into anion exchange membranes and cation-exchange membranes depending on the type of ionic groups attached to the membrane matrix. Cation exchange membranes (CEM) contain negatively charged groups and allow the passage of cations but reject anions. On the other hand, anion exchange membranes (AEM) contains positively charged groups, allowing the passage of anions but rejects cations (Peighambardoust et al., 2010).

One of the first characteristics to consider when choosing a membrane for the use in MFCs is the proton conduction. Resistive loss is proportional to the ionic resistance of the membrane and

high conductivity is essential for the performance at high current densities (Peighambardoust et al., 2010). The proton transport in a membrane can be explained through a vehicular mechanism. In this mechanism, the water connects to protons ($H^+(H_2O)_x$) and as a result of the electroosmotic drag carry one or more molecules of water with them through the membrane. This is possible due to the existence of free volumes within polymeric chains in proton exchange membrane which allows the transferring of the hydrated protons through its structure.

Different kinds of materials have been used as CEM in MFCs including Ultrex, Nafion, bipolar membranes, dialyzed membranes, glass wool, nano-porous filters and microfiltration membranes (Rahimnejad et al., 2015). Among these, the most widespread used is Nafion, a perfluorosulfonic acid membrane consisting of hydrophobic fluorocarbon backbone ($–CF_2–CF_2–$) to which hydrophilic sulfonate groups sulfonate groups (SO_3^-) are attached. Nafion membranes have high specific conductivity for protons and a long lifetime. Aditionally, they also have an appropriate level of hydration and thickness, which contribute to the better performance of MFCs (Oh and Logan, 2006; Rahimnejad et al., 2015). Despite these advantages, the high cost of Nafion have led to use of Ultrex membranes in MFC systems as a cost-effective alternative for Nafion membranes (Logan, 2008; Rahimnejad et al., 2015).

2.4.4 MFCs for wastewater treatment

Treatment of different types of wastewaters have been evaluated in various MFC designs, reporting parameters such as columbic efficiency, COD, removal rate and the maximum power and current densities (ElMekawy et al., 2015). Besides domestic wastewater, contaminated water from food-processing, dairy, agro-processing, livestock, mining, pharmaceutical, paper, textile, refinery and petrochemical industries have been investigated as substrates in MFCs (Pandey et al., 2016). Among these, the wastewaters from the refinery and petrochemical industries are relevant to the present work due to the presence of pollutants that are also found in the OSPW.

Petroleum hydrocarbon contamination in groundwater is a major environmental problem, therefore biodegradation of these compounds have been assessed in MFCs. BTEX (benzene, toluene, ethylbenzene and xylenes), PAHs (polycyclic aromatic hydrocarbons), and TPH (total petroleum hydrocarbon) have been evaluated as substrates in MFCs (Wang et al., 2015). Likewise,

there are a few studies on the treatment of refinery wastewaters, petroleum sludge and oil-contaminated soil (Srikanth et al., 2016), which are summarized in Table 2.2.

In this context, the oil sands industry in Canada has emerged as one of the main sources of water pollutants. The next section describes the latest approaches to treat OSPW in MFC bioreactors.

Table 2.2 Summary of reported studies on refinery wastewater treatment in MFCs.

Reference	**MFC configuration**	**Operation Mode**	**Culture**	**Treatment efficiency**	**Power and/or current output**
Ren et al., 2013	Single chamber mini-MEC	Batch	Indigenous microorganisms in refinery and domestic wastewater	79% COD 82% HBOD	2.1±0.2 A m^{-2}
Majumder et al., 2014	Single chamber with air-cathode	Sequential batch	*Pseudomonas putida* (BCRC 1059)	30% COD	0.005 $mWcm^{-2}$ 0.015 $mAcm^{-2}$
Zhang et al., 2014	Air-cathode MFC	Batch	Acclimated domestic wastewater	84% Total COD 73% Soluble COD 92% HBOD	280±6 mWm^{-2}/ 16.3±0.4 Wm^{-3}
Guo et al., 2015	Double-chambered MFC	Sequential batch	Wastewater treatment plant sludge	61.92% COD 83.6 % Oil removal	310.8 mW m^{-3}
Guo et al., 2016	Dual chambered aerated cathode	Batch	Wastewater treatment plant sludge	64±4% COD 84±3% Oil removal	330.4 $mWcm^{-3}$
Srikanth et al., 2016	Single chamber with open air–cathode	Batch	Mixed culture from corrosion site	84.4±0.8% Total COD	225 ± 1.4 mWm^{-2}
Yu et al., 2017	Single-chamber air cathode	Batch	Wastewater treatment plant sludge	96.4% COD	746 mW m^{-2}/ 241 W m^{-3}

2.4.5 OSPW treatment in Microbial Fuel Cells

As previously mentioned, OSPW is contaminated with NAs which is the main cause of its toxicity. However, it also contains other solid and dissolved components such as heavy metals, organics and bitumen residue. Therefore, the treatment of this water with concomitant generation of energy in microbial fuel cells has been proposed.

In a recent study, Jiang et al. (2013) reported successful generation of electricity through the treatment of OSPW in MFCs. In this study, four dual-chambered MFCs were constructed and the maximum power density achieved was 392 ± 15 mW/m^2. The chemical oxygen demand (COD) and total acid-extractable organics (AEO) removals were 27.8% and 32.9%, respectively. In addition, effective removal of eight heavy metals was achieved (Se, Ba, Sr, Zn, Mo, Cu, Cr and Pb).

Similarly, Choi and Liu (2014) examined OSPW treatment and voltage generation in a single chamber air-cathode MFC under different conditions of inoculant (anaerobic sludge, mature fine tailings), temperature (ambient, mesophilic) and co-biodegradation with acetate. The results of this work indicated that with an anaerobic sludge inoculum, addition of acetate and mesophilic temperatures (36 ± 0.1 °C) led to an improved performance of the MFC system in terms of treatment efficiency and voltage generated. The maximum power density achieved was 1.33 W/m^2, and the maximum COD and AEO removal efficiencies were 13.7% and 27.5%, respectively.

As can be seen, the outcomes of these previous studies reported naphthenic acids removal in terms of total acid-extractable organics which not only includes classical NAs ($C_nH_{2n+Z}O_2$), but also oxy-NAs ($C_nH_{2n+Z}O_x$) and other acid organics (Grewer et al., 2010). Moreover, high AEO removal efficiencies have not yet been achieved. This, along with the fact that there is not much information available on the NAs biodegradation kinetics in MFCs bioreactors, makes the need to further study NAs biodegradation in MFC essential in order to elucidate the biodegradation kinetics and electrochemical outputs in terms of various operating conditions including NA concentration and loading rate.

2.5 KNOWLEDGE GAP AND RESEARCH OBJECTIVES

As previously mentioned, bioremediation has been considered a feasible method to remove naphthenic acids from oil sand process water. It is known that degradation of NAs is more effective under aerobic conditions. However, earlier work in our research group has shown that anoxic biodegradation is also a viable option. MFCs could offer a feasible alternative for treatment of NA-contaminated water whereby the energy required for the treatment could be supplied as part of the treatment process. Against this background, the main objectives of the present research were as follows:

1. To assess the effect of NAs molecular structure on biodegradation in a MFC using a linear and a cyclic naphthenic acid in batch MFCs with single rod electrode and freely suspended cells.

2. To evaluate co-biodegradation of a linear and a cyclic NAs in batch MFCs with single rod electrode and freely suspended cells.

3. To assess the performance of MFC with granular electrodes and immobilized cells both in batch and continuous mode of operation with individual and mixture of NAs.

CHAPTER 3
MATERIALS AND METHODS

3.1 Surrogate Naphthenic Acids

Two model NAs, one linear and one cyclic, were used in this study to assess the effects of molecular structure on the biodegradation process and electrochemical outputs of MFC. Trans isomer of 4-methyl-1-cyclohexane carboxylic acid (trans-4MCHCA, $C_8H_{14}O_2$, CAS No.: 13064-83-0; Alfa Aesar) was selected as the cyclic model compound (Figure 3.1, (A)). Octanoic acid, with the same carbon number ($C_8H_{16}O_2$, CAS NO. 124-07-2; Alfa Aesar) was chosen as the linear NA compound (Figure 3.1, (B)). Previous works have investigated both model compounds under aerobic (Paslawski et al., 2009; Huang et al., 2012; D'Souza et al., 2014) and anoxic conditions (Gunawan et al., 2014; Dong and Nemati, 2016) in conventional bioreactors which allows the comparison of the kinetic data obtained in MFCs with that of conventional systems.

A

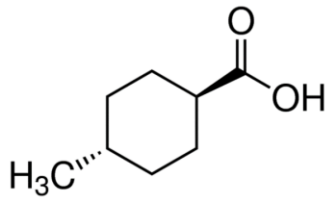

B

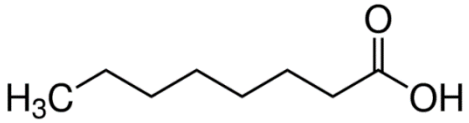

Figure 3.1 Molecular structure of model NAs. Trans-4-methyl-1-cyclohexane carboxylic acid (A) and octanoic acid (B) (Sigma Aldrich Co., 2015).

3.2 Microbial culture and medium

A mixed culture originated from the soil of an industrial site contaminated with heavy hydrocarbons was used for all experiments. As part of earlier works, this mixed culture had been acclimated to anoxic degradation of naphthenic acids using nitrate (Gunawan et al., 2014) and nitrite (Dong and Nemati, 2016) as the terminal electron acceptor. The composition of culture had been

examined earlier by a commercial lab (EPCOR-Quality Assurance Lab, Edmonton, Canada) and the two dominant species identified in this mixed culture were *Pseudomonas aeruginosa* and *Variovorax paradoxus* (Huang et al., 2011).

Cultures were maintained in 150 mL serum bottles containing 90 mL of modified McKinney's medium with 100 mgL^{-1} of trans-4MCHCA and 10mM of nitrate (KNO_3). Previous studies reported a maximum solubility of 1,000 mgL^{-1} for trans-4MCHCA at room temperature in modified McKinney's medium whereby complete dissolution needed vigorous and extended mixing (Paslawski et al., 2009). Based on this, vigorous mixing for three hours was necessary to completely dissolve the trans-4MCHCA. After mixing, purging with nitrogen was carried out to ensure the absence of oxygen and prevailing of anoxic conditions. The nitrogen gas was introduced to the medium through a nylon membrane with the pore diameter of 0.2 μm (VWR) to maintain the sterile conditions of the medium. Following purging with nitrogen, 10 mL of inoculum taken from a 7 days old culture prepared under similar conditions were added to the serum bottle (10% v/v). Subculturing was carried out every two weeks.

Modified McKinney's medium (Paslawski et al., 2009) was used to provide the nutrients necessary for culture growth and biodegradation experiments. Modified McKinney's medium was prepared in reverse osmosis water (RO water) and had the following composition: KH_2PO_4 (840 mg L^{-1}), K_2HPO_4 (750 mg L^{-1}), $(NH_4)_2SO_4$ (474 mg L^{-1}), NaCl (60 mg L^{-1}), $CaCl_2$ (60 mg L^{-1}), $MgSO_4.7H_2O$ (60 mg L^{-1}) and Fe $(NH_4)_2(SO_4)_2.6H_2O$ (20 mg L^{-1}). Trace solution was added to the modified McKinney's medium at 0.1% (v/v). The composition of trace solution was as follows: H_3BO_3 (600 mg L^{-1}), $CoCl_3$ (400 mg L^{-1}), $ZnSO_4.7H_2O$ (200 mg L^{-1}), $MnCl_2$ (60 mg L^{-1}), $NaMoO_4.2H_2O$ (60 mg L^{-1}), $NiCl_2$ (40 mg L-^{1}) and $CuCl_2$ (20 mg L^{-1}).The medium was autoclaved prior to use at 121 °C for 15 minutes.

3.3 MFC Bioreactors

H-type microbial fuel cell type bioreactors were used in this study. This MFC configuration consists of two identical glass chambers (285 mL each) which were used as the anodic and cathodic chambers. Each chamber was equipped with inlet and outlet ports and a flanged glass extension near the bottom, which enabled to attach the chambers by a metallic clamp and a rubber O ring

that avoided leakage**.** The anodic and cathodic chambers were separated by a Nafion high exchange capacity proton exchange membrane (0.09 mm thick, HEPEM, NE-1035 Alfa Aesar). Each chamber had a sampling port in the middle which was capped with a rubber septum. Both chambers were capped with a rubber stopper. As shown in Figure 3.2, two different types of graphite electrodes were used in this work, single rod graphite (L= 102 mm, D= 6.15 mm) and graphite granules (d= 2.9 to 4.0 mm). When the experiments were conducted with freely suspended cells, single graphite rod electrode was used. In the case of experiment with immobilized cells (biofilm), granular graphite electrode was employed. In order to connect these granules to the electrode terminal, a graphite rod was inserted into both chambers (previously filled with the granular electrode). It should be pointed out that granular graphite electrode provided a large surface area that promoted the formation of biofilm and facilitated the transfer of electrons.

The electrodes in anodic and cathodic chambers were connected by chrome wires to the multimeter terminals. The different components of the MFC bioreactor are shown in Figure 3.3. Keithley 2700 multimeter was used together with a 7700 data logger (Keithley Instruments Inc., Cleveland, USA) and relevant software (ExceLINX) together with a laptop computer were employed for monitoring circuit potential.

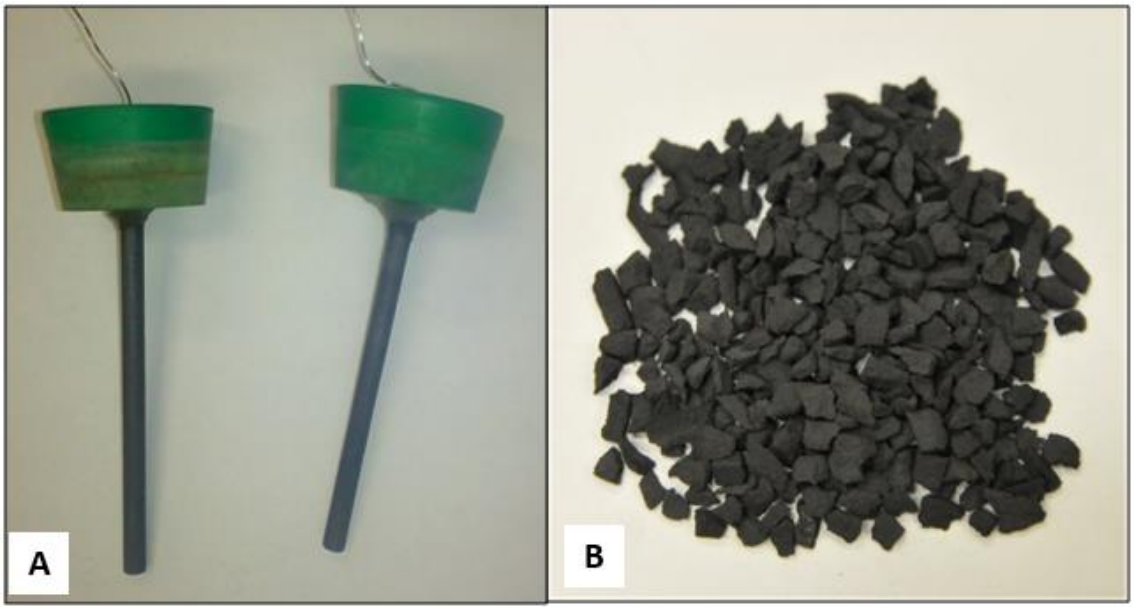

Figure 3.2 Graphite electrodes used in MFC. Single rod (A) and granular (B) electrodes

Figure 3.3 Microbial Fuel Cell components. (A) Flanged glass extension (B) Metallic clamp (C) Rubber O Ring (D) Nafion high exchange capacity proton exchange membrane (E) Sampling port (F) Rubber stopper.

For experiments where single rod electrode was employed, the system was operated in batch mode. Modified McKinney's medium and different concentrations of NAs were mixed together in the anodic chamber. Proper mixing was ensured using a magnetic stirrer under each chamber. Figure 3.4 shows the MFC set-up with single rod electrodes.

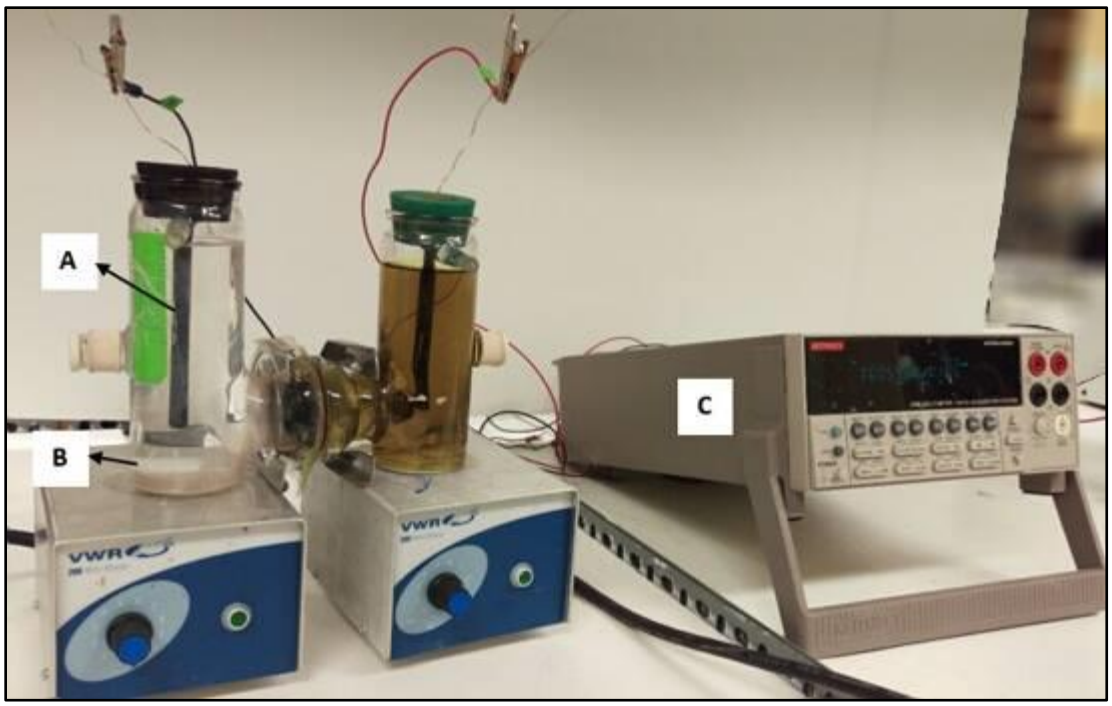

Figure 3.4 MFC with single rod electrode operated batchwise. (A) Single rod electrode (B) Magnetic stirrer (C) Multimeter.

When the experiments were performed with granular electrodes, the system was first operated batchwise to promote biofilm formation and increase of biomass hold-up in the granular graphite matrix. Granular graphite particles were prepared by crushing graphite blocks typically used as conductor for electric motors followed by sieving to obtain granules with sizes in the range of 2.9 to 4.0 mm (Moreno et al., 2015). This size selection was based on previous studies where the size range of 1.5 mm to 5 mm have been reported (Aelterman et al., 2006; Logan, 2008). In an earlier study, Moreno et al. (2017) determined the pore size, pore volume and BET surface area of the fresh (unused) graphite granules using an ASAP 2020 Surface Area and Porosity Analyzer (Micromeritics Instrument Corp., Norcross, GA, USA). The pore volume and surface area of fresh granules were 0.0032 cm^3g^{-1} and 1.10 m^2g^{-1}, respectively.

Granular electrodes were placed in the anodic and cathodic chambers occupying approximately 70% of the volume, resulting in a working volume of 135 ml. Stirring in the system was not possible due to the presence of the granular particles; consequently, mixing in the anode was achieved by a recirculating loop generated by a peristaltic pump (the liquid content was

withdrawn from the top and reintroduced into the bottom). The recirculation flow rate was approximately 3000 mLh^{-1}, which has been reported to be the highest flow rate that did not cause motion of the granules (Moreno et al., 2015).

The electron acceptor in the cathodic chamber was potassium ferricyanide. The potassium ferricyanide solution was prepared by adding 50 mM of potassium ferricyanide ($K_3[Fe(CN)_6]$, 98% purity) and 100 mM for potassium phosphate as buffering agent to RO water. During the experimental runs, cathodic potential was monitored to ensure that it did not decrease below 250 mV, which represents 25% decrease in the potential compared to the initial potential of a fresh potassium ferricyanide solution (Moreno et al., 2015). Once a decrease in cathodic potential below this value was observed, replenishment with fresh solution was carried out to assure that only progress of biodegradation in the anodic chamber affected the overall potential. More details of measurement of cathodic potential are provided in section 3.6.3. All experiments were conducted at room temperature (24$\pm$2 °C).

3.4 Biodegradation of naphthenic acids in MFC with single rod electrode and freely suspended cells

3.4.1 Batch mode of operation with individual naphthenic acids

Biodegradation of individual octanoic acid and trans-4MCHCA were evaluated first. Batch experiments were performed to evaluate the effect of initial NA concentration on biodegradation kinetics and power output. Sequential addition and of each individual compound was conducted as part of these experiments. The initial concentrations evaluated were 100, 250 and 500 mgL^{-1} for both trans-4MCHCA and octanoic acid. In all experiments, 200 mL of modified McKinney's medium were mixed with the specific amount of NA to give the designated concentration of naphthenic acid in the anodic chamber. After purging the anodic chamber with nitrogen for ten minutes, inoculum consisting of 20 mL of a 7 days old stock culture (10% v/v) was added to the anode. Regular sampling of the liquid content of anodic chamber was done to monitor naphthenic acid and biomass concentrations. First sample was taken immediately after the inoculation, while the following samples were taken once a day for high initial concentration (250 and 500 mgL^{-1}) and twice per day for low initial concentration (100 mgL^{-1}). The experiments started with the

lowest concentration of 100 mg L^{-1} NA, once the complete degradation occurred the anode was replenished with 100 mg L^{-1} NA and sequential biodegradation took place. This procedure was also performed with 250 mgL^{-1} and 500 mgL^{-1}. Open circuit potential was continuously monitored and recorded at 15 minutes intervals using the multimeter as described in the previous section.

3.4.2 Co-biodegradation of mixture of naphthenic acids in batch mode of operation

The co-biodegradation of a linear and a cyclic NAs (octanoic acid and trans-4MCHCA, respectively) was also carried out to assess the performance of the MFC bioreactor in terms of biodegradation kinetics and electrochemical outputs. These experiments were performed by introducing modified McKinney's medium with the desired concentration of both NAs into the anodic chamber. Then, this chamber was purged with nitrogen for 10 minutes and inoculated with 20 mL of culture, as described in the previous section. Sampling of the liquid contents of the anodic chamber was carried out twice a day for those combination containing 100 mg L^{-1} octanoic acid, and once a day for all other combinations. The NAs combinations that were tested in the MFC with single rod electrodes are presented in the Table 3.1.

Table 3.1 NAs mixtures used in co-biodegradation.

Octanoic acid (mgL^{-1})	**trans-4MCHCA (mgL^{-1})**
100	250
	500
	100
250	100
500	
100	

3.5 Biodegradation of naphthenic acids in MFC with granular electrode

3.5.1 Batch mode of operation with individual naphthenic acids

Granular graphite electrodes were used in MFCs to increase the surface area of the electrode, which allows biofilm formation (cell immobilization) and results in higher biodegradation rates. At the same time, a larger surface area could led to more efficient electron transfer and electrochemical outputs.

Two identical MFC set-ups were used in experiments with granular electrodes (as described in section 3.3). Each of these MFCs was used with only one NA (either trans-4MCHCA or octanoic acid). This allowed the development of biofilm adapted to different NAs of different structures (linear or cyclic molecular structure).

Batch biodegradation of model NAs were evaluated in these MFCs at the same initial concentration as those tested in the MCF with single rod electrode (100, 250, 500 mgL^{-1}). This allowed the comparison of biodegradation data obtained in MFC bioreactor with single rod and granular.

Similar to previous experiments, modified McKinney's medium containing individual naphthenic acid (octanoic acid or trans-4MCHCA) were placed into the anodic chamber and purged with nitrogen gas. Following this, the anodic chamber was inoculated with 20 mL of a 7 day old culture. Samples were taken three times per day for low initial NAs concentration (100 mgL^{-1}) and twice a day for higher concentration (250 and 500 mgL^{-1}). The use of granular electrode and presence of biofilm in the system caused fast biodegradation thus more frequent sampling was required. Once the NA concentration dropped to zero, the anodic chamber was replenished with a second batch with the same initial NA concentration and progression of sequential biodegradation was monitored. It should be pointed out that the addition of consecutive batches in the anodic chamber promoted biofilm formation. For these experiments, circuit potential was recorded at 15 minutes intervals.

3.5.2 Continuous mode of operation with individual NAs

After completion of batch experiments and once biofilm was stablished in the granular electrode matrix, both MFCs bioreactors were switched to continuous mode of operation. Effect of NA concentration and loading rate on biodegradation of each individual NA and MFC electrochemical output were investigated by varying the feed flow rate and NA concentration in the feed (see Appendix C). Various concentrations of trans-4MCHCA and octanoic acid, namely 100, 250 and 500 mgL^{-1} were examined using the procedure described below in each MFC. Feed was prepared using modified McKinney's medium containing the desired NA concentration and purged with nitrogen gas for ten minutes before being used to ensure anoxic conditions prevailed. The feed was transfer to the anodic chamber using a variable flow peristaltic pump which allowed gradual increase of the feed flow rate. An intermediary glass device was installed along the feed line to avoid bacterial contamination from the anodic chamber to the feed. To ensure that feed concentration remains constant, samples were regularly collected and analyzed from the feed line. The flow rate was initially set at a low value of 1.3 mL h^{-1} for an initial concentration of 100 mg L^{-1} NAs and increased incrementally until MFC performance started to deteriorate (decrease in biodegradation rate). This procedure was repeated with feeds containing 250 and 500 mg L^{-1} of designated NA (either trans-4MCHCA or octanoic acid). Overall six different flow rates, were tested for each concentration of both individual NAs (Table 3.2).

Table 3.2 Range of flow rates tested in continuous MFC with granular electrodes.

Feed Concentration (mg L^{-1})	Feed Flow Rate (mL h^{-1})	
	trans-4MCHCA	Octanoic acid
100	1.3 - 108	1.5 - 150
250	3.2 - 34	3.8 - 54
500	3.6 - 26	3.8 – 39

The effluent from the anodic chamber was sampled for measuring residual NA concentration, and each flow rate was maintained until steady state conditions were achieved in the system. Samples were collected at least once a day at low flow rates and sampling frequency

was increased as higher flow rates were applied (up to 3 samples a day). Steady state conditions were assumed when the NA concentration varied by less than 10% over three consecutive sampling events. Subsequently, the MFC was run at the same flow rate for three additional residence times and then the flow rate was increased. The data obtained at steady state conditions were used to calculate the average values and associated standard deviations. The experimental setup for continuous biodegradation of NAs with granular electrodes is shown in Figures 3.5 and 3.6.

MFC circuit potential was constantly monitored and recorded at 15 minutes intervals. For determination of current and power output, polarization curves were developed by conducting Linear Sweep Voltammetry (LSV) at different loading rates of trans-4MCHCA or octanoic acid (section 3.6.3).

When granular graphite was employed as the electrode, biomass measurement was not possible due to interference of particle turbidity in measurement of optical density. Furthermore, the optical density reading would not have represented the total biomass hold-up in the system due to the attachment of cells to the granular matrix (biofilm).

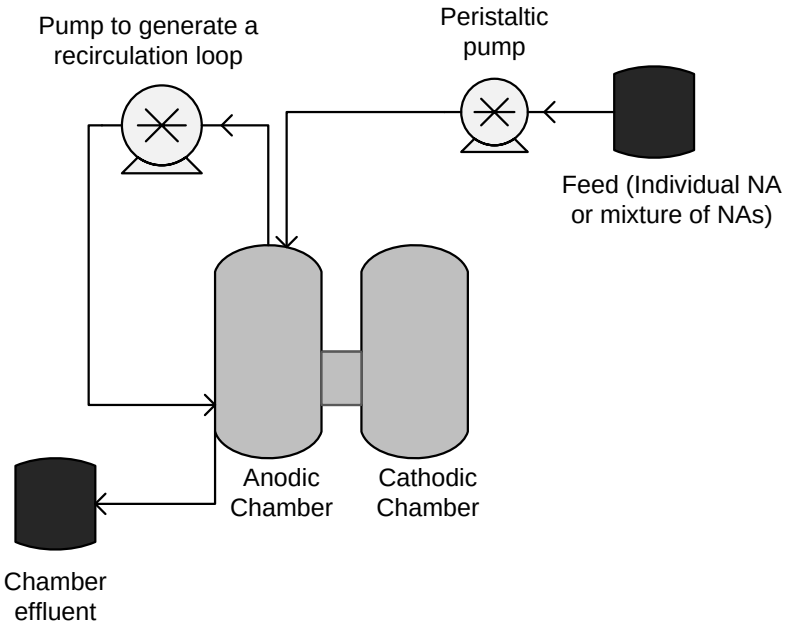

Figure 3.5 Schematic diagram of experimental setup of continuously operated MFC with granular graphite electrodes.

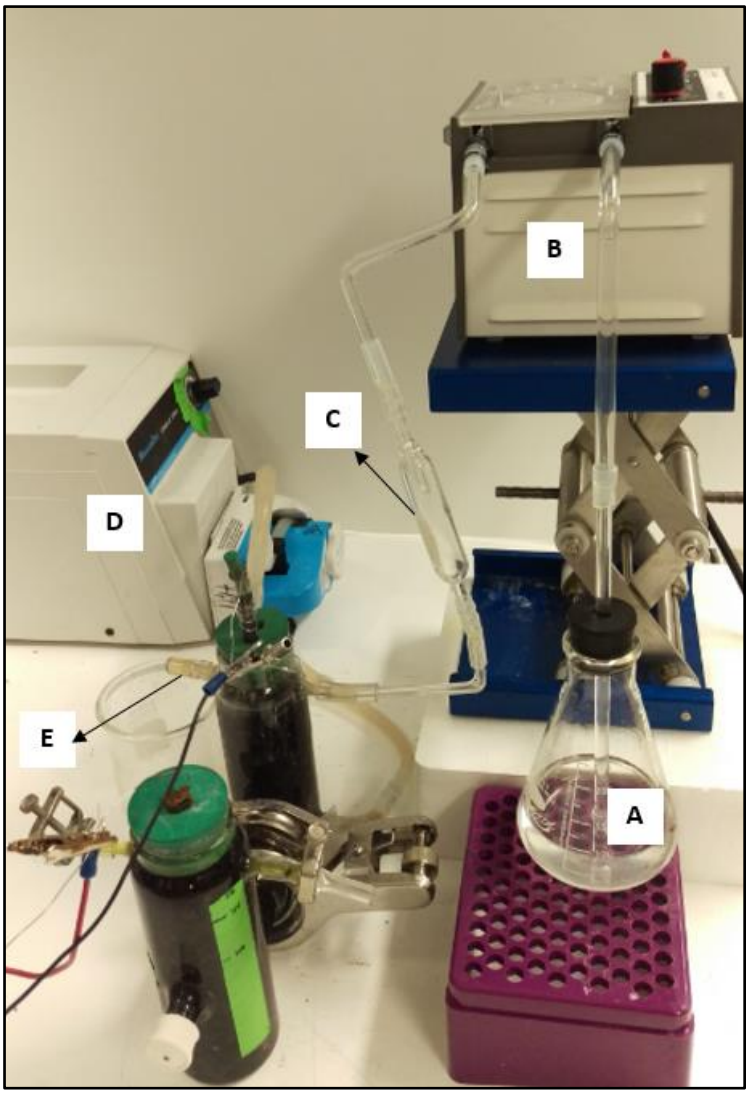

Figure 3.6 MFC with granular graphite electrode operated continuously. (A) Feed, (B) peristaltic pump, (C) intermediary glass device to prevent bacterial contamination, (D) pump to generate a recirculation loop, (E) chamber effluent.

3.5.3 Continuous co-biodegradation of octanoic acid and trans-4MCHCA

After completion of experiments with individual NAs, co-biodegradation of a mixture of 50 mg L^{-1} of trans-4MCHCA and 50 mg L^{-1} of octanoic acid was evaluated in each MFC. These concentrations were chosen to represent the actual NAs concentration range in OSPW. Effect of NA loading rates on performance of MFC was evaluated by varying the flow rates in a range of 9 to 100 mL h^{-1}. This was carried out in both MFC set-ups that had been used for biodegradation of

either trans-4MCHCA and octanoic acid, allowing to assess the potential adaptation of microbial culture to biodegradation of different types of NAs (linear and cyclic). In other words the aim was to find out whether the biofilm developed with linear NA (octanoic acid) as the sole substrate had the ability degrade the cyclic NA (trans-4MCHCA) and vice versa.

At the end of these experiments, a biofilm sample was taken from each MFC and bacterial community analysis was conducted at a commercial laboratory.

3.6 Analytical Methods

3.6.1 Naphthenic Acid Concentration

Previous research (Paslawski et al., 2009; Huang et al., 2012; D'Souza et al., 2014; Gunawan et al., 2014; Dong and Nemati, 2016) has demonstrated that gas chromatograph with flame ionization detector (GC-FID) is effective to analyze octanoic acid, trans-4MCHCA and mixtures of both compounds. The gas chromatograph used for this study was a Varian-430 GC with Agilent J&W DB-FFAP column. The specifications of the column are as follows: length: 30 m, inside diameter: 0.250 mm and film thickness > 0.5 µm. Helium (He) was used as the carrier gas. The equipment was operated under the following conditions: H_2 flow rate of 30 mL min^{-1}; He flow rate of 30 mL min^{-1}; air flow rate of 300 mL min^{-1}, injector splitless, injector and detector temperatures of 250 °C. The column oven had initial temperature of 40 °C which then was increased to 210 °C. The run time of the system, for each injection, was 7 minutes. Samples were taken from the MFC port by using a 5 ml glass syringe and a stainless steel needle. The liquid sample inside the syringe was filtered through a 0.22 µm pore diameter nylon membrane filter placed inside a stainless steel cartridge. Following this, the filtered solution was transferred to 2 mL vials and analyzed three times to determine the NAs concentration. The injection volume was 5.0 µl. Two Millipore water injections were necessary before each running sequence and after 6 sample injections in order to avoid the accumulation of naphthenic acid in the column. The retention time was 5.89 ± 0.5 minutes for octanoic acid and 6.72 ± 0.5 min for trans-4MCHCA. A calibration curve for both octanoic acid and trans-4MCHCA was developed using six standard solutions (10, 20, 40, 60, 80 and 100 mg L^{-1}) in modified McKinney's medium. The correlation

coefficient of the calibration curve was 99.6% for octanoic acid and 99.34% for trans-4MCHCA. Corresponding calibration curves are presented in Appendix A.

3.6.2 Biomass Measurement

In order to determine the optical density (OD) of the samples from MFC with single rod electrode, a Mini Shimadzu spectrophotometer (Model 1240) was used. The wavelength was 620 nm and modified McKinney's media was used as blank. Samples were tested in triplicate. A calibration curve developed in previous studies was used in this work to determine the biomass concentration (Dong, 2014).

3.6.3 Electrochemical tests

In all experiments, MFC circuit potential was continuously recorded by a Keithley 2700 multimeter, equipped with 7700 data logger (Keithley Instruments Inc., Cleveland, USA). This monitoring equipment was connected to a computer and operated using Excelinx software.

Fluke 27 multimeter (Fluke, Everett, WA, USA) was used to measure the cathodic chamber potential. The positive terminal was connected to the cathode and the negative terminal to a calomel reference electrode (Cole-Parmer, Vernon Hills, IL, USA).

For those experiments conducted in MFCs with granular graphite electrodes and under continuous mode of operation polarization and power curves were developed using a Gamry R600 potentiostat (Gamry Instruments, Warminster, USA). Linear Sweep Voltammetry (LSV) was performed at different NA loading rates. With trans-4MCHCA as substrate, the range of the sweep was from -500 mV to 10 mV. With octanoic acid, the range was from -700 mV to 10 mV. In both cases, the scan rate was set at 0.1 mVs^{-1}. This low scan rate was chosen since it minimizes the electron transfer kinetic effects and allows to focus on effects related to microorganisms' effects (enzymatic processes). Furthermore, low scan rates allow to achieve the maximum number of chemical conversion of substrate at each applied potential step (Marsili et al., 2008). Potential range used in each case was based on the OCP observed during batch experiments. For all LSV

runs, the anode was used as the working electrode and the cathode as both the counter and reference electrodes. After each measurement, polarization curves (current – potential) and power curves were generated. From this data and employing the Ohm's law equation (3.1), power curves were developed.

$$P = VI \qquad (3.1)$$

Where, P is the Power (mW), V is the circuit potential (mV) and I is the corresponding current (mA).

3.6.4 Bacterial Community Analysis

At the end of experiments in continuously operated MFCs with granular electrodes, a biofilm sample was taken from each MFC (acclimated to either trans-4MCHCA or octanoic acid) and bacterial community analysis had been conducted at a commercial laboratory (Contango Strategies – Saskatoon, Canada). The MoBIO PowerLyzer PowerSoil DNA Isolation Kit was used and sequence analysis of the 16S ribosomal RNA (rRNA) was carried out.

3.6.5 Reproducibility and Data Uncertainty

In batch wise operated MFCs with single rod electrodes, the average values of the biomass and residual NAs concentration were calculated from three different samples and the associated standard deviations were used as error bar in presenting the results. When granular electrodes were employed in the system, biomass concentration was not determined due to interference of particle turbidity in measurement of optical density and the fact that majority of biomass was attached. In other words, the optical density would not have represented the total biomass hold-up in the anodic chamber.

With continuously operated MFCs, once steady-state conditions were established at each applied flow rate, the experiments were continued for three additional residence times at the same flow rate and three samples were collected over this period of time. The data obtained from these samples were used to calculate the average values and associated standard deviations.

CHAPTER 4
RESULTS AND DISCUSSION

This chapter presents the results of biodegradation of trans-4MCHCA and octanoic acid in MFCs bioreactors. Results of batch operated MFCs with single rode electrodes are presented first. This is followed by the results of batch and continuously operated MFC with granular electrodes. For both MFCs configurations, two different types of substrates were evaluated: individual NA compounds and mixtures of NAs.

4.1 Batch Biodegradation of naphthenic acids in MFC with single rod electrodes and freely suspended cells

4.1.1 Batch biodegradation of individual NA compounds

Biodegradation of trans-4MCHCA and octanoic acid were carried out to investigate the effect of initial concentration of each individual NA and the effect of sequential addition of NA on biodegradation kinetics.

Three different concentrations of each individual compound were evaluated: 100, 250 and 500 mg L^{-1}. Profiles of biodegradation of trans-4MCHCA and octanoic acid as sole substrate are shown in Figures 4.1 and 4.2, respectively.

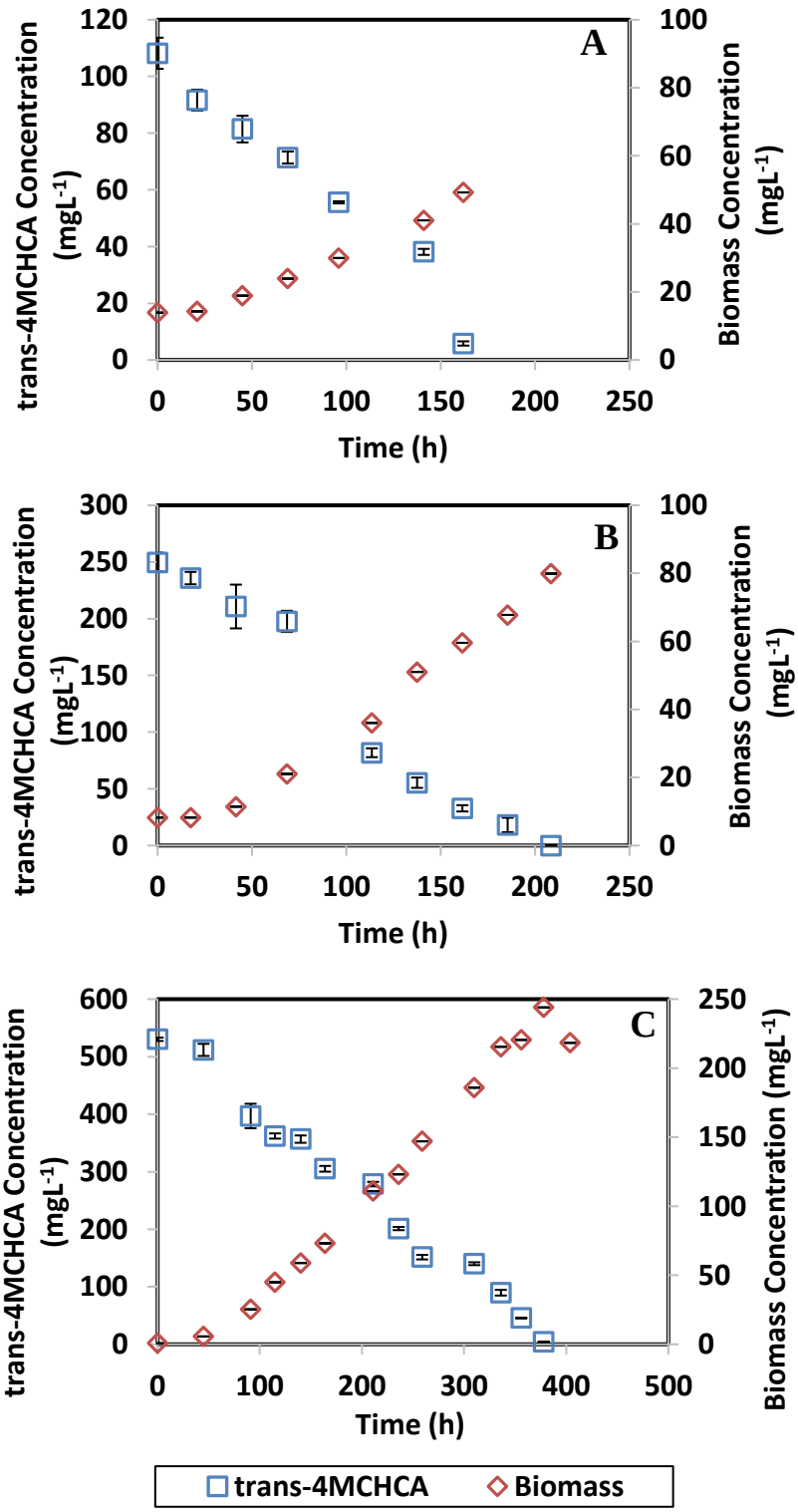

Figure 4.1 Biomass growth and biodegradation profiles obtained with various initial concentrations of trans-4MCHCA in batch operated MFC with single rod electrodes. Panel (A) 100 mg L^{-1}, Panel (B) 250 mg L^{-1}, Panel (C) 500 mg L^{-1}. The error bars represent the standard deviations of three samples taken from the anodic chamber.

Figure 4.1 shows that in general there is a direct relationship between the bacterial growth and trans-4MCHCA biodegradation (substrate utilization); whereby bacterial growth was accompanied by a decline in NA concentration. With trans-4MCHCA as substrate, higher initial concentrations (250 and 500 mg L^{-1}) resulted in longer lag phase in microbial activity but higher final biomass concentrations. A lag phase of around 50 h was observed with 250 and 500 mg L^{-1} trans-4MCHCA which was considerably longer than 20 h that was observed with 100 mg L^{-1} trans-4MCHCA. Following the lag phase, bacterial cells exhibited their metabolic activity during the exponential phase, which resulted in a continuous and linear decrease in trans-4MCHCA concentration until it was completely exhausted. Figure 4.1 (Panel A) shows that with an initial concentration of 100 mgL^{-1} trans-4MCHCA, the biomass concentration reached the maximum value of 49 mg L^{-1} at around 162 h, while with 250 and 500 mg L^{-1} trans-4MCHCA, the maximum biomass concentrations were 80 and 244 mg L^{-1} and achieved at around 209 and 378 h, respectively (Figure 4.1 Panels B and C). In Figure 4.1 (Panel C) after complete consumption of 500 mg L^{-1} trans-4MCHCA, biomass growth levelled off and started to decline (i.e. at 404 h when the NA concentration dropped to zero and the microbial concentration decreased from its maximum value of 244 to 218 mg L^{-1}).

As illustrated in Figure 4.2, when MFC was operated with different initial concentrations of octanoic acid, no lag phase was observed. This could be explained by the fact that octanoic acid is a linear compound amenable to biodegradation and therefore bacteria did not require an extended adaptation period. Once bacterial cells started to grow (increase in biomass concentration), octanoic acid concentration declined. It was also observed that higher initial concentration of octanoic acid resulted in longer periods for complete biodegradation of substrate and higher biomass concentrations. For an octanoic acid initial concentration of 100 mg L^{-1}, the biomass concentration reached the maximum value of around 100 mg L^{-1} after 64 h (Figure 4.2 Panel A), while with 250 and 500 mg L^{-1} octanoic acid, the highest biomass concentrations were approximately 102 and 180 mg L^{-1} and observed at 125 h (Figure 4.2 Panel B) and 270 h (Figure 4.2 Panel C), respectively. Similar to trans-4MCHCA, these maximum biomass concentrations were achieved when the octanoic acid concentration was completely consumed. As seen, the pattern observed for both individual NAs is that initial concentrations of 100 and 250 mg L^{-1} led to close maximum values of biomass concentration, however, with an initial concentration of 500 mg L^{-1} NA, markedly higher maximum biomass concentrations were achieved. Figure 4.2 (Panel

C), shows that the microbial activity decreased after reaching its peak when the octanoic acid was completely depleted. At 291 h, the biomass concentration value decreased from 178 to 161 mg/L.

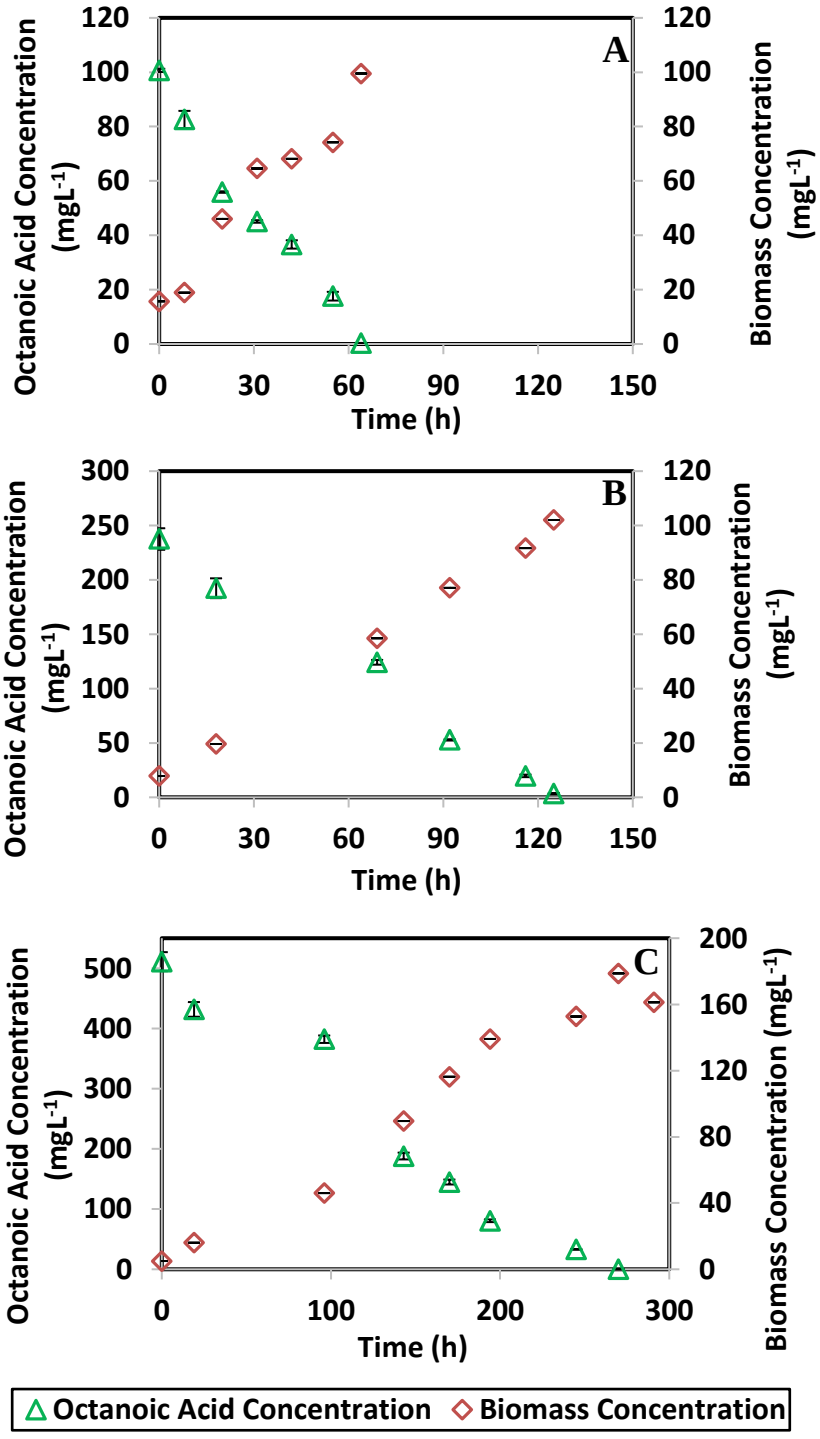

Figure 4.2 Biomass growth and biodegradation profiles obtained with various initial concentrations of octanoic acid in batch operated MFC with single rod electrodes. Panel (A) 100 mg L^{-1}, Panel (B) 250 mg L^{-1}, Panel (C) 500 mg L^{-1}. The error bars represent the standard deviations of three samples taken from the anodic chamber.

Using the slopes of the linear parts of trans-4MCHCA and octanoic acid concentration profiles, biodegradation rates of both NAs were calculated at different NA initial concentrations and presented in Table 4.1.

Table 4.1 Effect of initial concentration of trans-4MCHCA and octanoic acid on their biodegradation rate.

Initial NA Concentration ($mg\ L^{-1}$)	**Biodegradation Rate of trans-4MCHCA ($mg\ L^{-1}\ h^{-1}$)**	**Biodegradation Rate of Octanoic Acid ($mg\ L^{-1}\ h^{-1}$)**
100	0.56 (0.97)*	1.46 (0.97)*
250	1.32 (0.97)*	1.85 (0.98)*
500	1.38 (0.98)*	1.93 (0.97)*

* The number in the parentheses represents R^2 values.

Data compiled in Table 4.1 showed a marked increase in biodegradation rates of both trans-4MCHCA and octanoic acid when their initial concentration was increased from 100 mg L^{-1} to 250 mg L^{-1}. However, biodegradation rates at initial concentration of 250 and 500 mg L^{-1} were close. It can also be observed that for all tested initial NAs concentrations, octanoic acid biodegradation proceeded at a faster rates than that of trans-4MCHCA, indicating that a NA with a linear structure can be degraded easier by the microbial culture when compared with the NA with a cyclic structure.

4.1.2 Effect of Sequential Addition of NA

Figure 4.3 shows the microbial growth and biodegradation profiles of trans-4MCHCA during sequential addition of trans-4MCHCA. As seen, replenishment of the anodic chamber with fresh medium led to an initial decrease in biomass concentration due to dilution of medium. Moreover, after the addition of NA to the anodic chamber, the biomass concentration that had been decreased due to exhaustion of substrate in previous batch increased and reached its maximum

value after complete exhaustion of the second batch of trans-4MCHCA. As seen in Figure 4.3 (Panel A), the maximum value of biomass concentration achieved during biodegradation of the second addition of 100 mg L^{-1} trans-4MCHCA was around 72 mg L^{-1}, which was higher than the maximum value of 49 mg L^{-1} achieved at the end of the first batch. The same pattern was observed for the sequential addition of 250 mg L^{-1} trans-4MCHCA (Figure 4.2 Panel B), where the maximum value of biomass concentration achieved were around 80 mg L^{-1} and 106 mg L^{-1} for the first and second batches, respectively. By contrast with 500 mg L^{-1} trans-4MCHCA, due to substantial decrease in biomass concentration after exhaustion of NA in the first batch, highest biomass concentration achieved during the second addition was close to that in the first batch (237 vs 244 mg L^{-1}) as shown in Figure 4.3 (Panel C). A faster and linear decrease in trans-4MCHCA concentration was observed after the addition of the second batch, resulting in shorter times required to achieve complete depletion of the substrate (i.e. 90, 138 and 313 h for the removal of 100, 250 and 500 mg L^{-1} trans-4MCHCA, respectively).

Using the slope of trans-4MCHCA concentration profile during sequential addition, trans-4MCHCA biodegradation rates for 100, 250 and 500 mg L^{-1} were determined as 1.07, 1.57 and 1.74 mg L^{-1} h^{-1} for the second batch. These biodegradation rates were markedly higher than those obtained during degradation of trans-4MCHCA in the first batch. Interestingly no lag phases were observed during sequential addition of trans-4MCHCA, even at the highest applied concentration of 500 mg L^{-1}.

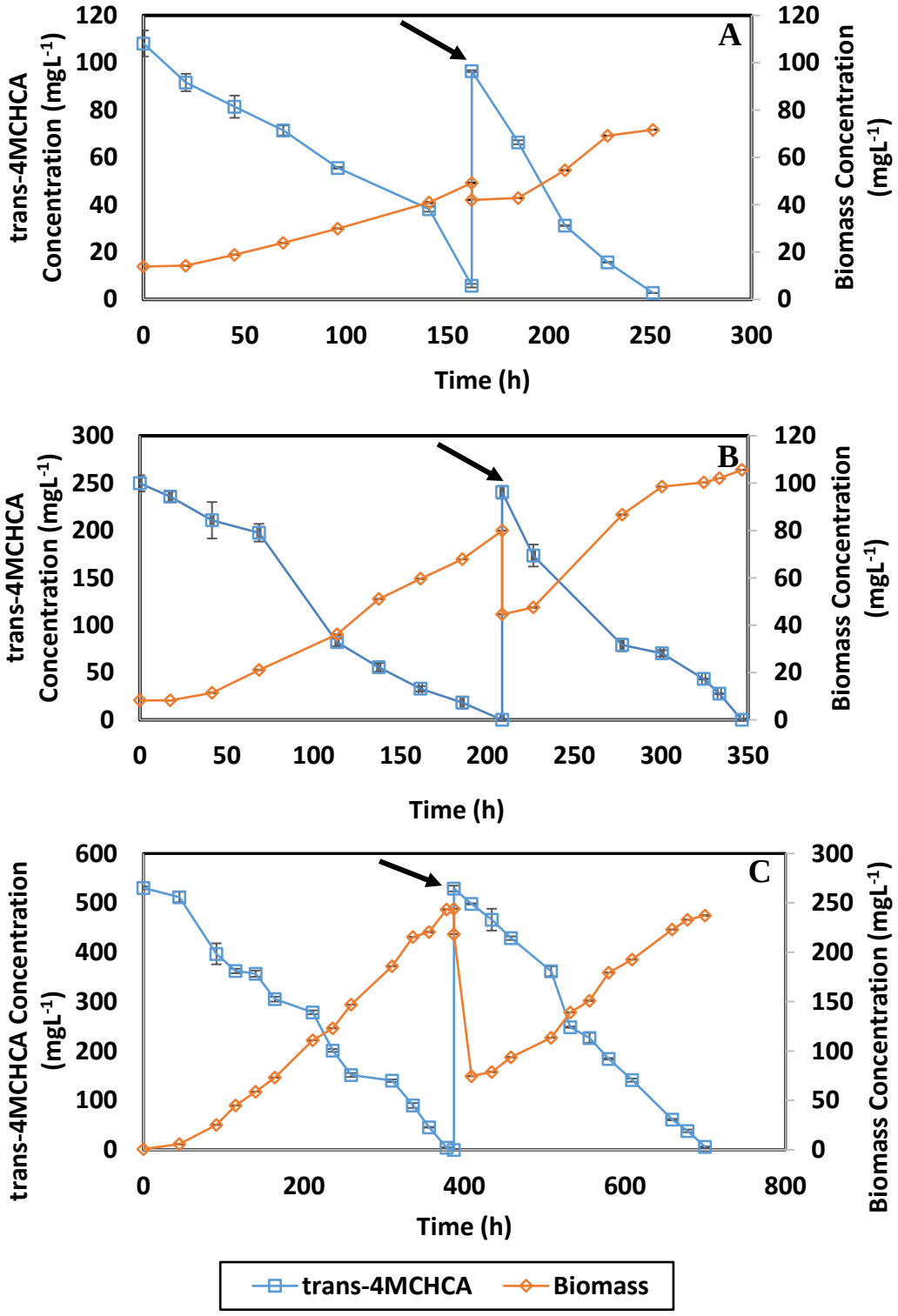

Figure 4.3 Profiles of trans-4MCHCA and biomass concentrations during the sequential batch biodegradation. Panel (A) 100 mg L^{-1}, Panel (B) 250 mg L^{-1}, Panel (C) 500 mg L^{-1} in MFCs with single rod electrodes. Arrows indicate addition of trans-4MCHCA. The error bars represent the standard deviations of three samples taken from the anodic chamber.

Results of sequential addition effect for octanoic acid and bacterial growth are shown in Figure 4.4. As displayed, after replenishment of the anodic chamber, the maximum value of biomass concentration achieved was around 104, 146 and 228 mg L^{-1} for initial concentrations of 100 (Figure 4.4 Panel A), 250 (Figure 4.4 Panel B) and 500 mg L^{-1} octanoic acid (Figure 4.4 Panel C), respectively. In contrast to trans-4MCHCA, these values were higher than those obtained during degradation of the first batch for all initial concentrations tested.

Regardless the initial concentration, shorter times were necessary to completely remove the second batch of octanoic acid. Complete removal of 100, 250 and 500 mg L^{-1} octanoic acid, occurred after 46, 74 and 172 h, respectively. Octanoic acid biodegradation rates, calculated using the slope of linear part of octanoic acid concentration profile during second batch, were 2.30, 3.15 and 2.99 mg L^{-1} h^{-1} for 100, 250 and 500 mg L^{-1}, respectively. As can be confirmed from this data, sequential addition led to higher degradation rates for all evaluated concentrations, which can be attributed to the biomass accumulated in the anodic chamber after being replenished. Similar to trans-4MCHCA, no lag phases were observed during the biodegradation of the second addition of octanoic acid.

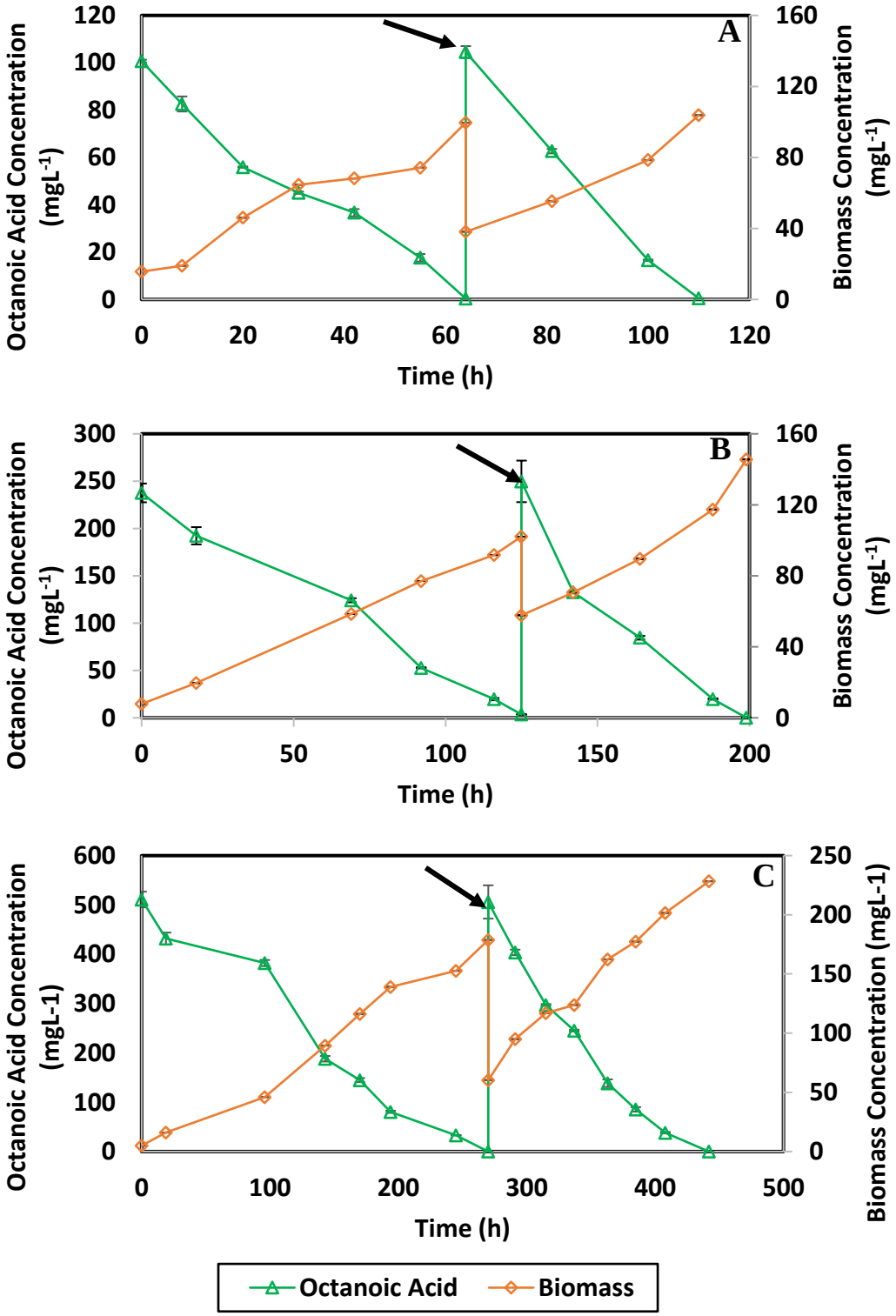

Figure 4.4 Profiles of octanoic acid and biomass concentrations during the sequential batch biodegradation. Panel (A) 100 mg L^{-1}, Panel (B) 250 mg L^{-1}, Panel (C) 500 mg L^{-1} in MFCs with single rod electrodes. Arrows indicate addition of octanoic acid. The error bars represent the standard deviations of three samples taken from the anodic chamber.

As mentioned earlier, circuit potential was monitored continuously. It was observed that open circuit potential (OCP) increased due to microbial growth, reaching its peak before biomass concentration started to decrease as a result of exhaustion of the substrate (trans-4MCHCA or octanoic acid). The maximum value of OCP during biodegradation of 100, 250 and 500 mg L^{-1} trans-4MCHCA and octanoic acid were 275, 483 and 407 mV, and 470, 545 and 558 mV, respectively. As seen there seems to be a correlation between biodegradation and potential whereby the potential observed during biodegradation of octanoic acid (more amenable to biodegradation) was higher than that of trans-4MCHCA. The OCP values obtained during the first addition of both model NAs were very close to those obtained during the sequential addition.

4.1.3 Co-biodegradation of mixture of naphthenic acids in batch operated MFCs

The results presented in the previous section have shown the ability of the microbial culture to degrade the linear (octanoic acid) and the cyclic (trans-4MCHCA) NAs, with the biodegradation of the linear compound occurring at a faster rate. Previous studies have indicated that recalcitrant organic compounds can be degraded more effectively when an easily biodegradable compound is present (Veeresh et al., 2005; D'Souza et al., 2014). Accordingly, co-biodegradation of mixtures of trans-4MCHCA (recalcitrant compound) and octanoic acid (amenable to biodegradation) in five combinations were evaluated in this study. The concentrations used for these experiments are presented in Table 4.2.

The concentration profiles for biomass and NAs observed during the co-biodegradation of NAs are shown in Figure 4.5.

A

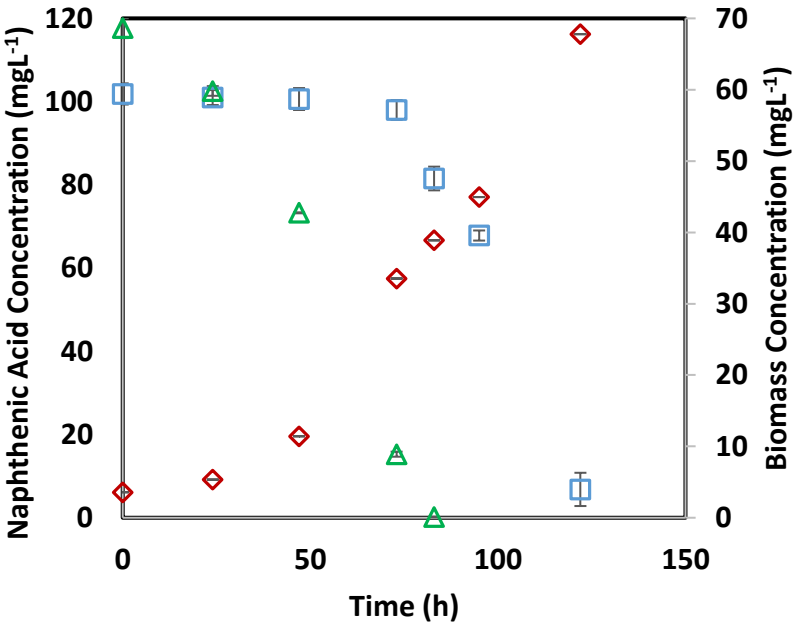
Naphthenic Acid Concentration (mgL-1)
Biomass Concentration (mgL-1)
Time (h)
0
20
40
60
80
100
120
0
10
20
30
40
50
60
70
0
50
100
150

B

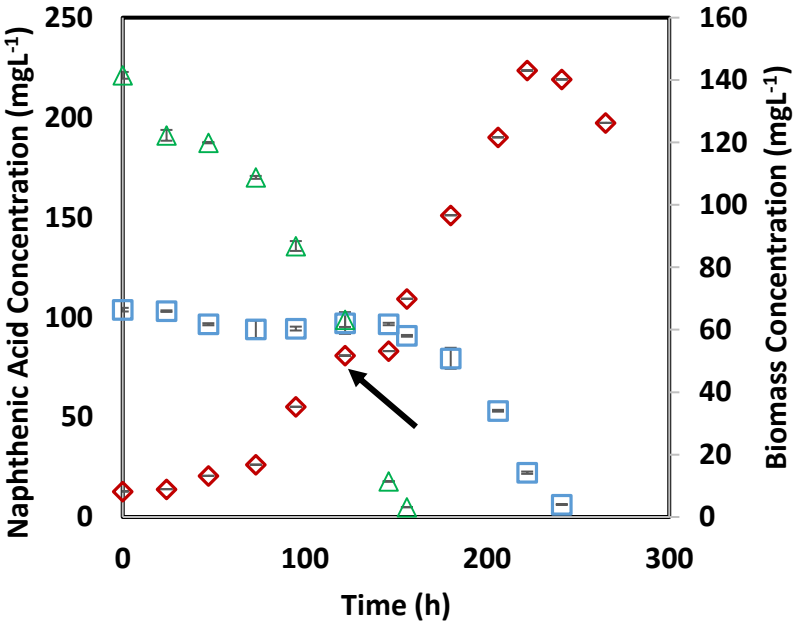
Naphthenic Acid Concentration (mgL-1)
Biomass Concentration (mgL-1)
Time (h)
0
50
100
150
200
250
0
20
40
60
80
100
120
140
160
0
100
200
300

C

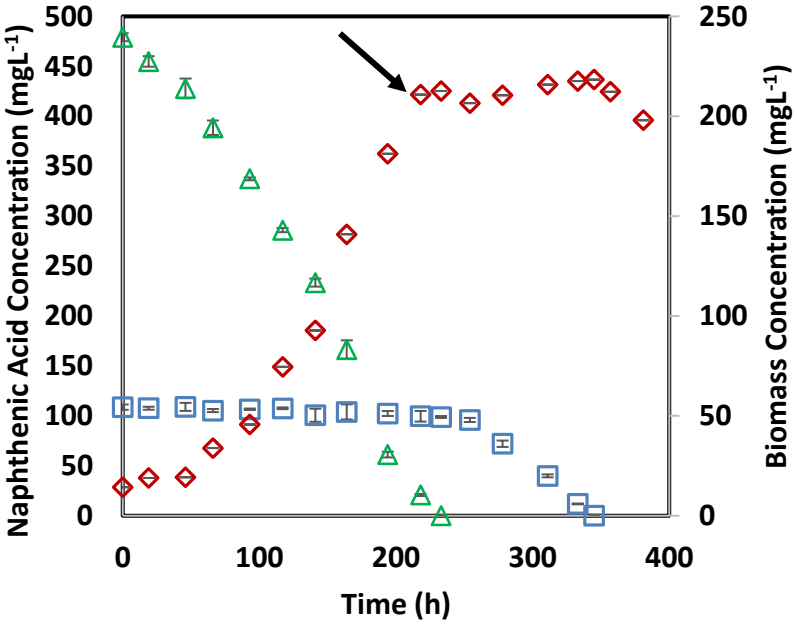
Naphthenic Acid Concentration (mgL-1)
Biomass Concentration (mgL-1)
Time (h)
0
50
100
150
200
250
300
350
400
450
500
0
50
100
150
200
250
0
100
200
300
400

D

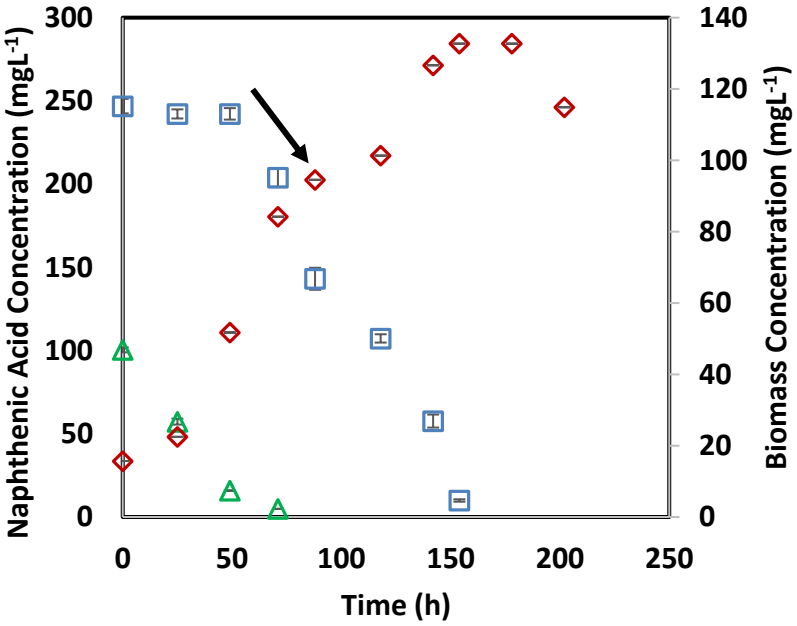
Naphthenic Acid Concentration (mgL-1)
Biomass Concentration (mgL-1)
Time (h)
0
50
100
150
200
250
300
0
20
40
60
80
100
120
140
0
50
100
150
200
250

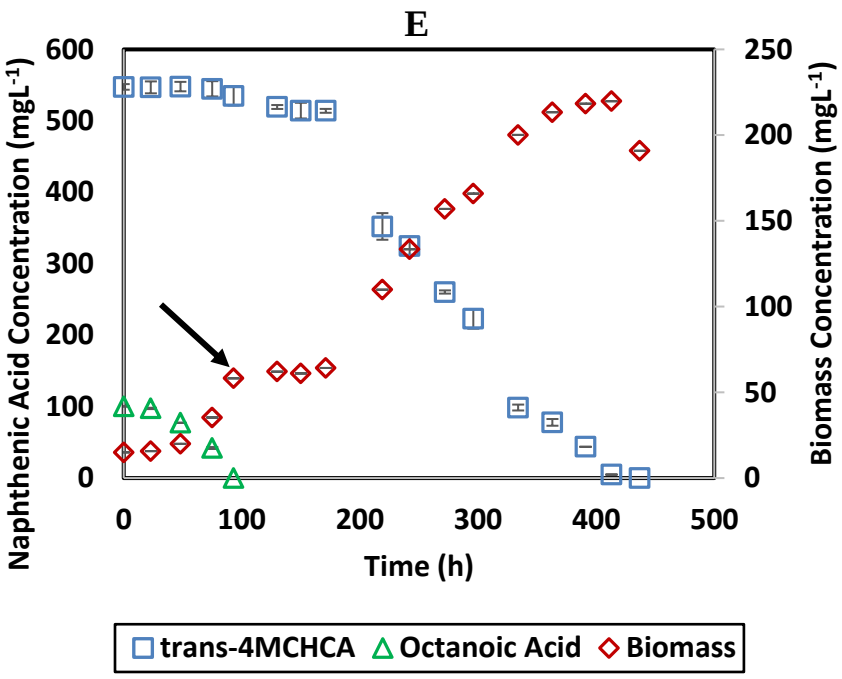

Figure 4.5 Co-biodegradation of mixture of NAs. Panel(A) 100 mg L^{-1} trans-4MCHCA & 100 mgL^{-1} octanoic acid, Panel (B) 100 mg L^{-1} trans-4MCHCA & 250 mg L^{-1} octanoic acid, Panel(C) 100 mgL^{-1} trans-4MCHCA & 500 mg L^{-1} octanoic acid, Panel (D) 250 mg L^{-1} trans-4MCHCA & 100 mg L^{-1} octanoic acid, and Panel (E) 500 mg L^{-1} trans-4MCHCA & 100 mg L^{-1} octanoic acid. Arrows indicates the second lag phase. The error bars represent the standard deviations of three samples taken from the anodic chamber.

Figure 4.5 illustrates that in the presence of a mixture of NAs, bacterial culture experienced diauxic growth. Diauxic growth is characterized by two exponential phases separated by a lag phase. To be more specific, in all evaluated mixtures, octanoic acid was used first as the preferred substrate and only after complete exhaustion of octanoic acid, degradation of trans-4MCHCA occurred. Thus, the first exponential phase in microbial growth, reflects the consumption of octanoic acid as the easier NA metabolized by bacteria, followed by a lag phase (indicated by an arrow), necessary for adaptation of bacteria to the use of trans-4MCHCA, and finally the second exponential phase coinciding with the degradation of trans-4MCHCA. It should be pointed out that the extent of this intermediate lag phase was dependent on the concentration of trans-4MCHCA. Specifically, lag phases of around 30 h and 78 h were observed in mixtures of 250 mg L^{-1} trans-4MCHCA and 100 mg L^{-1} octanoic acid (Figure 4.5 Panel D) and 500 mg L^{-1} trans-4MCHCA and 100 mg L^{-1} octanoic acid (Figure 4.5 Panel E), respectively.

Using the generated co-biodegradation data, removal rates of both NAs were calculated using the slopes of the linear parts of trans-4MCHCA and octanoic acid concentration profiles. Results are summarized in Table 4.2.

Table 4.2 Summary of biodegradation rates obtained during co-biodegradation of trans-4MCHCA and Octanoic Acid. Data for biodegradation of individual NAs are also included.

NAs mixture	**Concentration (mg L^{-1})**	**Removal Rate of Trans-4MCHCA (mg L^{-1} h^{-1})**	**Removal Rate of Octanoic Acid (mg L^{-1} h^{-1})**
trans-4MCHCA Octanoic Acid	100 100	1.49	 1.86
trans-4MCHCA Octanoic Acid	100 250	0.97	 1.36
trans-4MCHCA Octanoic Acid	100 500	0.81	 2.18
trans-4MCHCA Octanoic Acid	250 100	2.1	 1.39
trans-4MCHCA Octanoic Acid	500 100	1.74	 1.06
Individual NAs			
trans-4MCHCA	100 250 500	0.56 1.32 1.38	-
Octanoic Acid	100 250 500	-	1.46 1.85 1.93

A comparison between co-biodegradation rates (Table 4.2) and biodegradation rates obtained with individual NAs (Table 4.1), revealed that the octanoic acid removal rates at all evaluated concentrations were similar in the presence and absence of trans-4MCHCA, indicating that presence of a cyclic NA did not impact the degradation rates of linear NA. By contrast, in the presence of octanoic acid biodegradation rate of trans-4MCHCA was much higher, demonstrating that the presence of linear NA had a positive impact on removal rates of cyclic NA at all tested concentrations. This fact could be attributed to the higher level of biomass and enzymes that were produced during the metabolism of octanoic acid that subsequently contributed to faster degradation of trans-4MCHCA (D'Souza et al., 2014).

4.2 Biodegradation of naphthenic acids in MFC with granular electrodes

4.2.1 Batch mode of operation with individual naphthenic acids

Sequential batch biodegradation of NAs in MFCs with granular graphite electrodes was carried out with two main objectives: 1)- evaluate NAs biodegradation and associated rates in MFCs with granular electrodes and comparing these with the rates obtained in MFCs with single rod electrodes; 2)- promote biofilm formation, and therefore enhanced biomass hold-up in the MFC for subsequent use in continuous mode of operation.

Results of sequential biodegradation of 100 to 500 mg L^{-1} trans-4MCHCA are presented in Figure 4.6 (Panel A). Complete removal of 100 mg L^{-1} trans-4MCHCA in the first batch occurred after 14.5 h. Biodegradation of first batches of 250 and 500 mg L^{-1} required 33 and 91.5 h, respectively. Complete removal of the second addition of 100, 250 and 500 mg L^{-1} trans-4MCHCA took place after 13, 26.5 and 58 h, respectively. Average biodegradation rates at each initial concentration were calculated using the slope of trans-4MCHCA concentration profiles. Results obtained showed an increase of biodegradation rate from 8.93 $\pm$ 1.09 to 9.12 $\pm$ 0.01 mg $L^{-1}h^{-1}$ as initial concentration of trans-4MCHCA increased from 100 to 250 mg L^{-1}. Further increase in initial concentration to 500 mg L^{-1}, however, led to a decrease in biodegradation rate to 7.2 $\pm$ 2.30 mg L^{-1} h^{-1}.

Figure 4.6 (Panel B) shows results of sequential batch biodegradation of octanoic acid. Complete removal of the first and second batches of 100 mg L^{-1} octanoic acid occurred after 5.5 h (each addition). Biodegradation of the second batches of 250 and 500 mg L^{-1} octanoic acid took place faster as compared to the first batch. For instance at an initial concentration of 250 mg L^{-1} octanoic acid, the time required for removal of octanoic acid in the first and second batches was 13 h and 10.5 h, respectively. Similarly, 22.5 and 21 h were required to remove completely the first and second batch of 500 mg L^{-1} octanoic acid. Average biodegradation rates, calculated from the slope of octanoic acid concentration profiles, were 20.81 $\pm$ 1.06, 21.96 $\pm$ 1.16 and 22.78 $\pm$ 2.20 mg $L^{-1}h^{-1}$ for initial concentration of 100, 250 and 500 mg L^{-1}, respectively. These results indicate that biodegradation rates slightly increased as initial octanoic acid concentration increased in the range 100-500 mg L^{-1} which clearly was not the case with trans-4MCHCA.

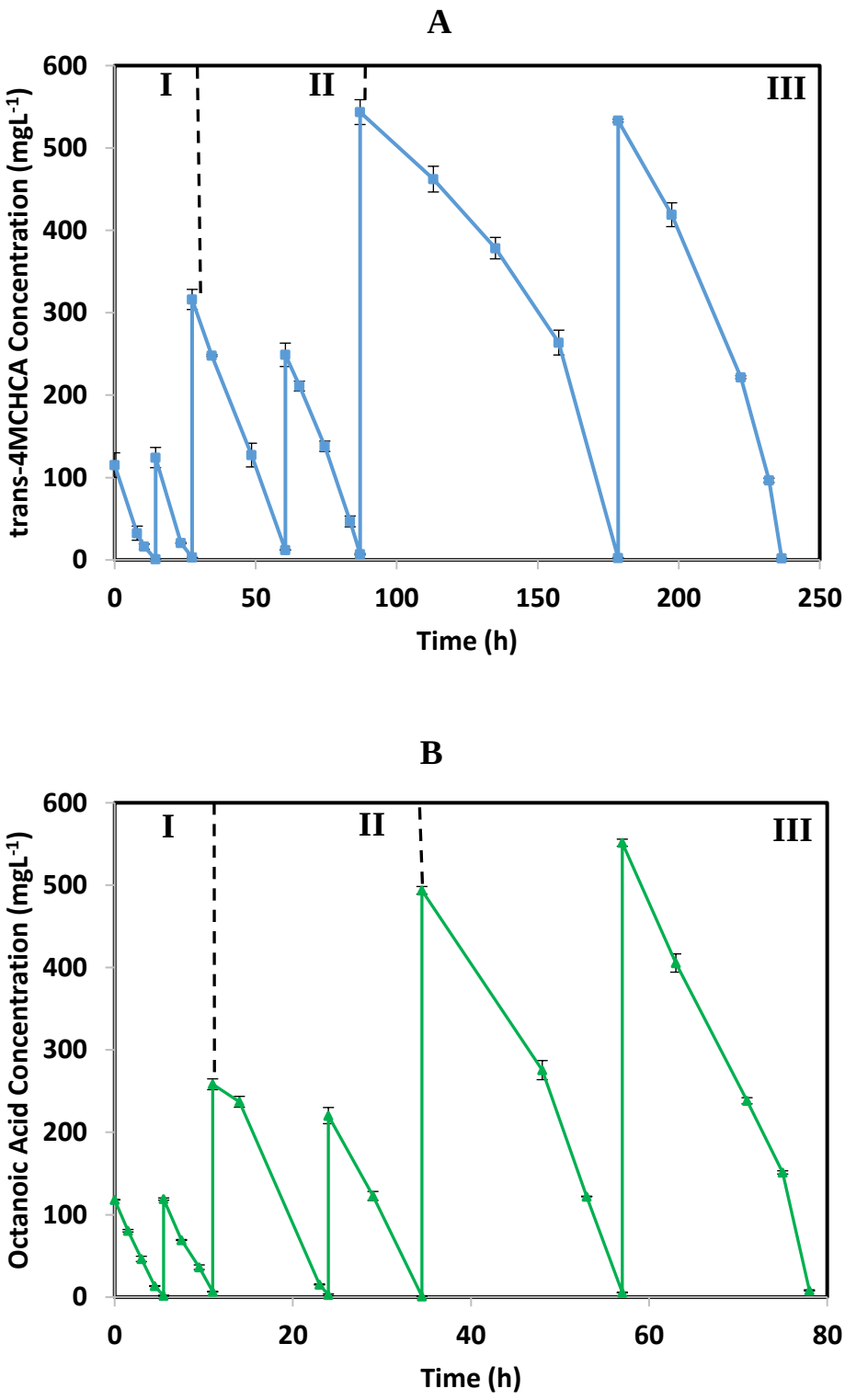

Figure 4.6 Sequential biodegradation of NAs in batch-wise operated MFCs with granular graphite electrodes. Panel (A): trans-4MCHCA, Panel (B): Octanoic Acid. Section I: 100 mg L^{-1}, Section II: 250 mg L^{-1}, Section III: 500 mg L^{-1}. The error bars represent the standard deviations of three samples taken from the anodic chamber.

4.2.2 Biodegradation of individual NAs in MFCs operated continuously

Biodegradation of trans-4MCHCA

The effects of trans-4MCHCA concentration and volumetric loading rate on its biodegradation rate and electrochemical outputs were evaluated in continuously operated MFCs with granular electrodes. As mentioned in the previous section, sequential batch operation led to biofilm formation in the anodic chamber after which the MFC system was fed continuously with McKinney's medium containing 100.4 $\pm$ 2.0 mg L^{-1} trans-4MCHCA at a flow rate of 1.3 mlh^{-1} (corresponding trans-4MCHCA loading rate: 1.0 mg L^{-1} h^{-1}; residence time: 103.8 h). Once steady conditions were achieved, flow rate was increased incrementally until decline in MFC performance in terms of biodegradation occurred. A total of 10 flow rates in the range indicated in Table 3.2 were tested. Figure 4.7 (Panel A) shows the relationship between the residual concentration and the trans-4MCHCA loading rate, indicating that application of loading rates as high as 5.9 mg L^{-1} h^{-1} led to complete removal of trans-4MCHCA. Further increase in loading rate caused an increase in residual concentrations of trans-4MCHCA, reaching a maximum value of 71.9 mg L^{-1} at a corresponding loading rate of 82.4 mg L^{-1} h^{-1}. This high residual concentration was obtained as a result of the inability of MFC system to handle a high loading rate of 82.4 mg L^{-1} h^{-1}, therefore no further increases in loading rate were carried out after this point.

Variation of trans-4MCHCA biodegradation rates and removal percentage as a function of its loading rate is presented in Figure 4.7 (Panel B). Complete removal of 100.4 $\pm$ 2.0 mg L^{-1} was observed for loading rates in the range of 1.0 – 5.9 mg L^{-1} h^{-1} (residence times: 103.8 – 16.9 h), with the highest biodegradation rate with 100% trans-4MCHCA removal being 5.9 mg L^{-1} h^{-1}. As seen, biodegradation rates increased with the application of higher loading rates and reached a maximum value of 30.8 mg L^{-1} h^{-1} at a loading rate of 64.4 mg L^{-1} h^{-1} with a corresponding removal percentage of 47.8%, after which the biodegradation rates decreased with further increases in loading rate. The lowest removal percentage of 30.2% was observed at the maximum loading rate applied of 82.4 mg L^{-1} h^{-1} (corresponding biodegradation rate: 24.9 mg L^{-1} h^{-1}).

Figure 4.7 (Panels C and D), shows polarization and power curves developed from the Linear sweep voltammetry (LSV) data conducted at loading rates of 3.2, 26.4, 64.4 and 82.4 mg L^{-1} h^{-1} (corresponding biodegradation rates: 3.2, 23.4, 30.8 and 24.9 mg L^{-1} h^{-1}, respectively). The value of potential corresponding to a zero current (OCP) at a loading rate of 3.2 mg L^{-1} h^{-1} was 174 mV. Corresponding OCP values for loading rates of 26.4, 64.4 and 82.4 mg L^{-1} h^{-1} were 323, 387 and 356 mV, respectively, indicating a correlation with biodegradation rate whereby higher OCPs were observed as biodegradation increased. The maximum power output (0.06 mW) was achieved at a loading rate of 64.4 mg L^{-1} h^{-1} with the corresponding current being 0.55 mA; using the working volume of 135 ml, these are translated to power and current densities of 444.4 mW m^{-3} and 4071.1 mA m^{-3}, respectively. The fact that the maximum power and current densities were observed at a loading rate of 64.4 mg L^{-1} h^{-1} whereby the biodegradation rate has the maximum value of 30.8 mg L^{-1} h^{-1} revealed a correlation between electrochemical outputs and biodegradation rates, indicating that higher biodegradation rates led to higher power and current outputs.

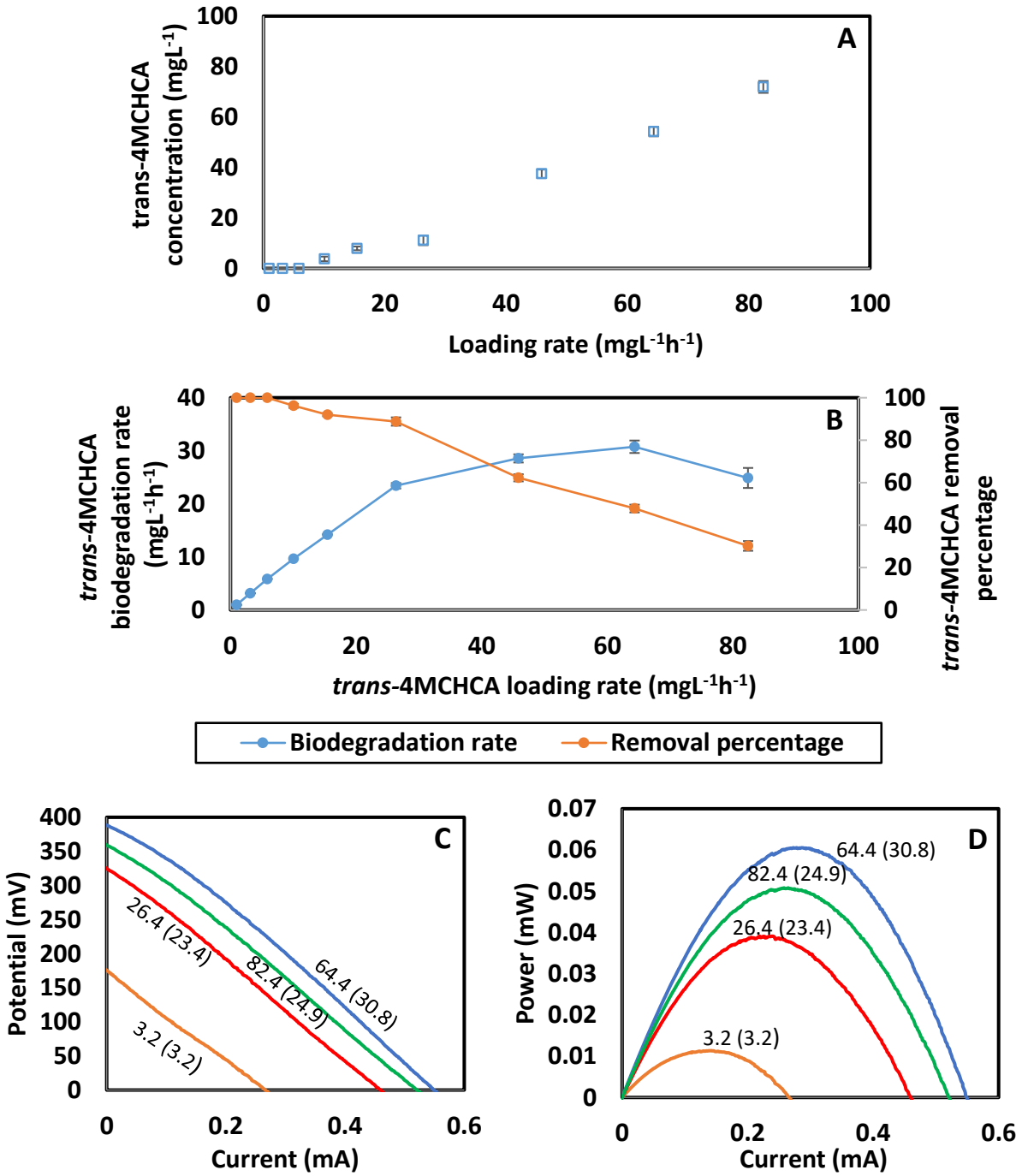

Figure 4.7 Biodegradation of 100.4 ± 2.0 mg L^{-1} trans-4MCHCA in continuously operated MFC with granular electrodes. Panel (A): Steady-state profiles of trans-4MCHCA residual concentration, Panel (B): Biodegradation rate and removal percentage as a function of loading rate. Panels (C) and (D): Polarization and Power curves for various loading rates. Labels on each curve represent applied loading rate, with the corresponding biodegradation rate given in the brackets. Presented results in Panels A and B are the average values of the data collected over three residence times after the establishment of steady state and error bars represent the standard deviations.

After completion of continuous biodegradation of 100.4 ± 2.0 mg L^{-1} trans-4MCHCA, experiments with a feed containing approximately 250 mg L^{-1} trans-4MCHCA (267.0 ± 19.4 mg L^{-1}) were carried out. Initial flow rate was set at 3.2 ml h^{-1} (residence time: 42.2 h; loading rate: 6.8 mg L^{-1} h^{-1}) and then three subsequent flow rates of 18.2, 26 and 34 ml h^{-1} (corresponding residence time: 7.4, 5.2 and 4 h; corresponding loading rates: 37.5, 50.2 and 61.2 mg L^{-1} h^{-1}) were tested. As Figure 4.8 (Panel A) indicates, no residual NA concentration was observed at a loading rate of 6.8 mg L^{-1} h^{-1}, while residual concentrations of 74.3 and 129 ml L^{-1} were observed at loading rates of 37.5 and 50.2 mg L^{-1} h^{-1}, respectively. A residual concentration of 153.4 mg L^{-1} was observed at the highest loading rate applied of 61.2 mg L^{-1} h^{-1} (approximately 65 percent of the feed concentration), thus no further increases in flow rate were carried out.

Figure 4.8 (Panel B) shows the variation of trans-4MCHCA biodegradation rates and its removal percentage as a function of loading rate in the continuously operated MFC. As seen, biodegradation rate increased when loading rate was increased from 6.8 to 37.5 mg L^{-1} h^{-1}, reaching the maximum value of 27.5 mg L^{-1} h^{-1} with a removal percentage of 73.3%. After this point, both biodegradation rate and removal percentage decreased until reaching the lowest removal percentage of 36.8% at the highest loading rate applied of 61.2 mg L^{-1} h^{-1} (biodegradation rate: 22.5 mg L^{-1} h^{-1}). Complete removal of 267.0 ± 19.4 mg L^{-1} trans-4MCHCA was only observed at the lowest tested loading rate of 6.8 mg L^{-1} h^{-1} (residence time: 42.2 h) with the corresponding biodegradation rate being 6.8 mg L^{-1} h^{-1}.

Polarization and power curves developed from Linear Sweep Voltammetry data at loading rates of 6.8, 37.5 and 61.2 mg L^{-1} h^{-1} (corresponding biodegradation rates: 6.8, 27.5 and 22.5 mg L^{-1} h^{-1}, respectively) are presented in Figure 4.8 (Panels C and D). The OCP values at these loading rates were 362, 392 and 390 mV, respectively. Similar to the electrochemical outputs during biodegradation of 100.4 ± 2.0 mg L^{-1} trans-4MCHCA, the highest biodegradation rate of 27.5 mg L^{-1} h^{-1} (loading rate: 37.5 mg L^{-1} h^{-1}) led to the maximum values of power and current densities, of 481.5 mW m^{-3} and 4296.3 mA m^{-3}, respectively.

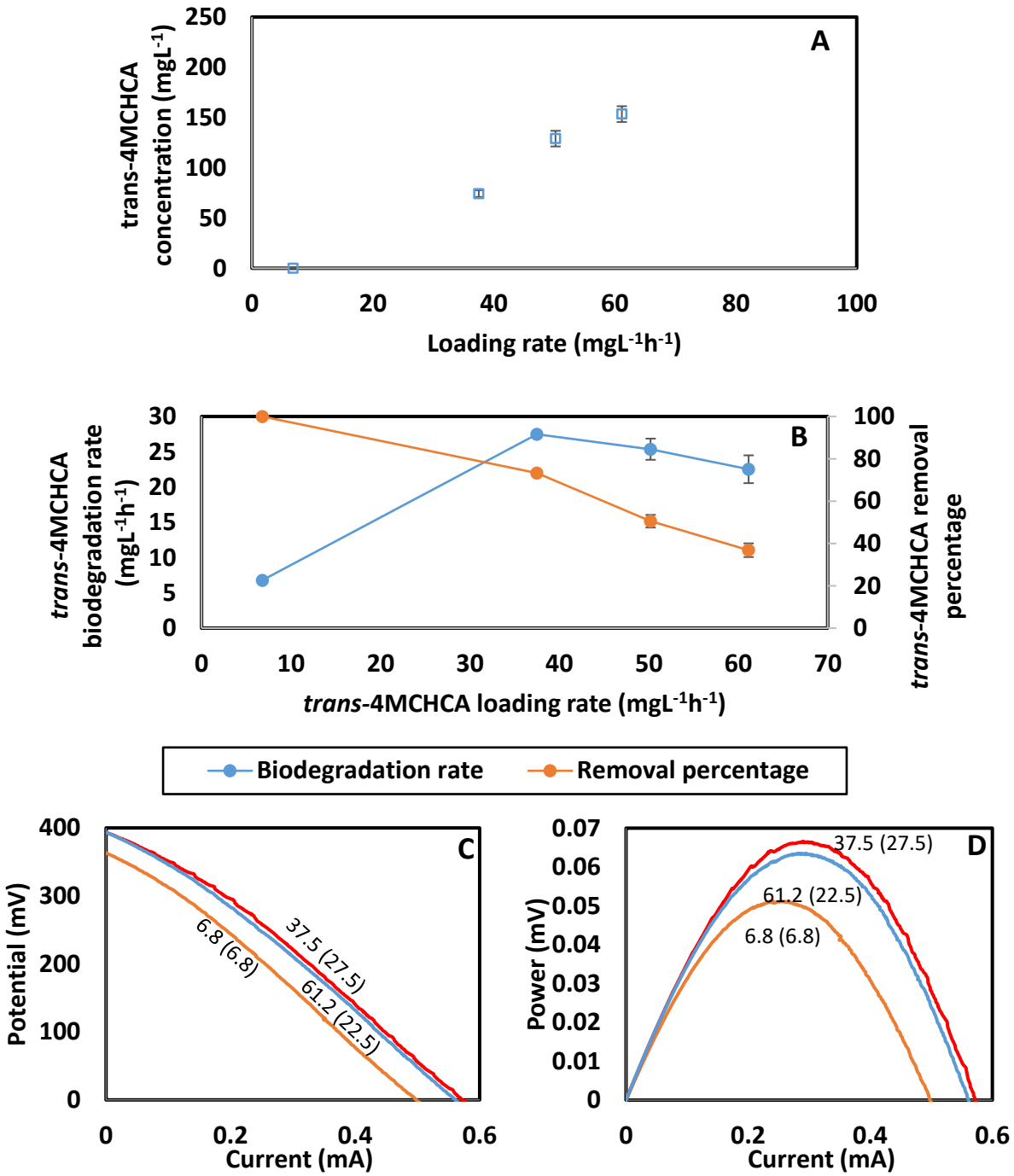

Figure 4.8 Biodegradation of 267.0 ± 19.4 mg L^{-1} trans-4MCHCA in continuously operated MFC with granular electrodes. Panel (A): Steady-state profiles of trans-4MCHCA residual concentration, Panel (B): Biodegradation rate and removal percentage as a function of loading rate. Panels (C) and (D): Polarization and Power curves for various loading rates. Labels on each curve represent applied loading rate, with the corresponding biodegradation rate given in the brackets. Presented results in Panels A and B are the average values of the data collected over three residence times after the establishment of steady state and error bars represent the standard deviations.

The last set of experiments in continuously operated MFC was with a feed containing 506.20 $\pm$ 4.6 mg L^{-1} trans-4MCHCA. Figure 4.9 (Panel A) shows the increase of trans-4MCHCA residual concentration as the loading rate applied increased. As can be observed, residual concentrations remained below 84 mg L^{-1} in a loading rate range from 13.3 to 38.9 mg L^{-1} h^{-1}. The highest trans-4MCHCA residual concentration of 348.3 mg L^{-1} was achieved at a loading rate of 97.4 mg L^{-1} h^{-1} (residence time: 5.2 h.).

The dependency of removal rate and removal percentage on trans-4MCHCA loading rate is shown in Figure 4.9 (Panel B). Initial increases in loading rate up to 68.3 mg L^{-1} h^{-1} (residence time: 7.5 h) led to higher biodegradation rates. The maximum value of biodegradation rate achieved at this loading rate was 36.5 mg L^{-1} h^{-1} (removal percentage: 53.4%). After this point, the loading rate was set at 97.4 mg L^{-1} h^{-1} resulting in a decline of biodegradation rate to 30.3 mg L^{-1} h^{-1} (removal percentage: 31.1%).

Figure 4.9 (Panels C and D) shows polarization and power curves obtained during the continuous operation of MFC at three different loading rates of 13.3, 68.3 and 97.4 mg L^{-1} h^{-1}. Similar to previous experiments, the maximum electrochemical outputs were obtained when the biodegradation rate was at the highest level. Accordingly, the maximum power density (481.5 mW m^{-3}), and maximum current density (4296.3 mA m^{-3}), were obtained at a loading rate of 68.3 mg L^{-1} h^{-1} that corresponded to maximum biodegradation rate of 36.5 mg L^{-1} h^{-1}.

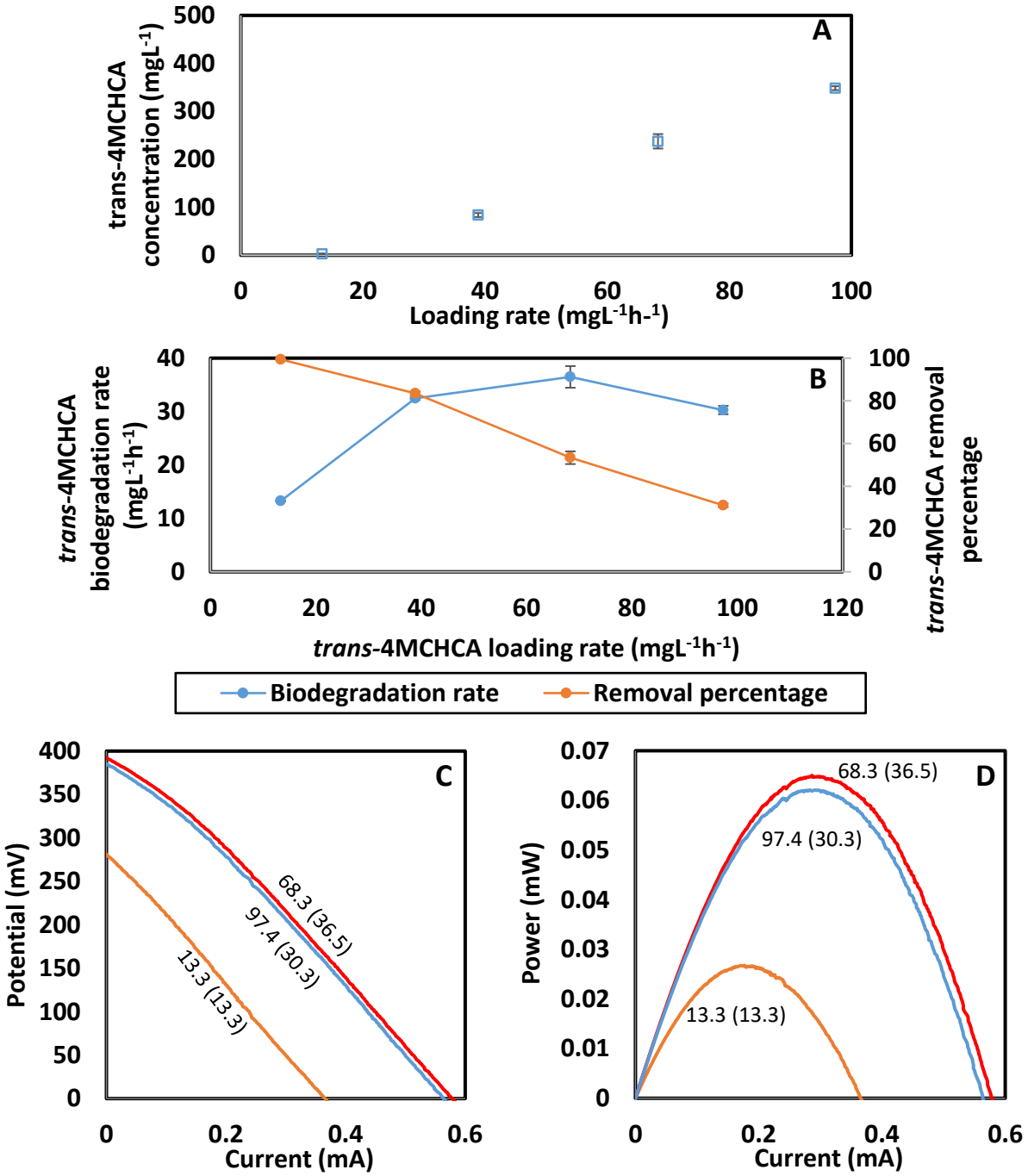

Figure 4.9 Biodegradation of 506.2 ± 4.6 mg L^{-1} trans-4MCHCA in continuously operated MFC with granular electrodes. Panel (A): Steady-state profiles of trans-4MCHCA residual concentration, Panel (B): Biodegradation rate and removal percentage as a function of loading rate. Panels (C) and (D): Polarization and Power curves for various loading rates. Labels on each curve represent applied loading rate, with the corresponding biodegradation rate given in the brackets. Presented results in Panels A and B are the average values of the data collected over three residence times after the establishment of steady state and error bars represent the standard deviations.

To assess the effect of trans-4MCHCA concentration, the data obtained at various concentrations are compiled in Figure 4.10 and 4.11. Figure 4.10 exhibits that trans-4MCHCA removal percentages remained high at low loading rates and then started to drop as the loading rate was increased. With a feed of 100.4 $\pm$ 2.0 mg L^{-1} trans-4MCHCA, removal rates remained high (>96%) up to a loading rate of 10.1 mg L^{-1} h^{-1} (residence time: 9.8 h) and then started to decrease until a removal percentage of 30.2% was reached at a loading rate of 82.4 mg L^{-1} h^{-1} (residence time: 1.3 h.). With a feed of 267.0 $\pm$ 19.4 mg L^{-1} trans-4MCHCA, the removal percentages remained above 70% in the loading rate ranging from 6.8 to 37.5 mg L^{-1} h^{-1} (residence time: 42.2 to 7.4 h) and then dropped to the lowest level of 36.8% at a loading rate of 61.2 mg L^{-1} h^{-1} (residence time: 4.0 h). It was expected that at this trans-4MCHCA concentration removal percentages and rates to remain high for a loading rate range similar than the one observed for 100.4 $\pm$ 2.0 mg L^{-1} trans-4MCHCA. However, both parameters started to decline at a loading rate of 50.2 mg L^{-1} h^{-1} (biodegradation rate and percentage: 25.4 mg L^{-1} h^{-1}, 50.5%). This fast decrease may be attributed to the fact that bacteria were not adapted to high trans-4MCHCA concentrations at this point. This was evident during the experiments with 506.2 $\pm$ 4.6 mg L^{-1} trans-4MCHCA where removal rates and percentages stayed high at higher loading rates which allowed application of loading rates as high as the maximum value of 97.4 mg L^{-1} h^{-1} (removal percentage: 31.1%), resulting in the widest loading rate range applied from all trans-4MCHCA concentrations evaluated. This trend confirms that the experiments with 267.0 $\pm$ 19.4 mg L^{-1} trans-4MCHCA may have promoted bacterial adaptation to environments with high trans-4MCHCA concentrations and consequently a better performance of MFC operated at higher loading rates.

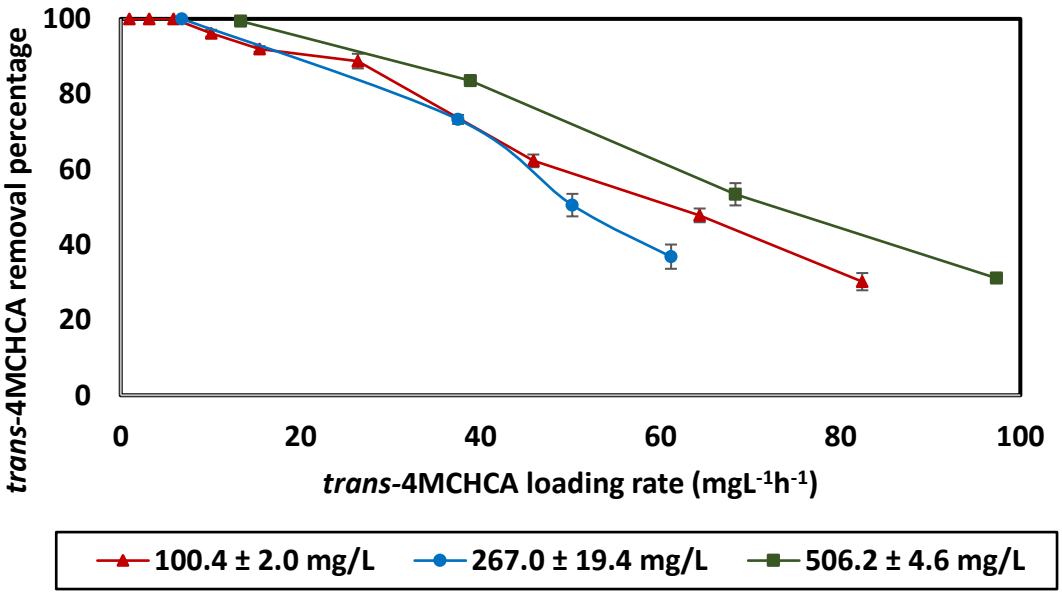

Figure 4.10 Removal percentages of trans-4MCHCA at various initial concentrations in continuously operated MFC with granular electrodes. Presented results are the average values of the data collected over three residence times after the establishment of steady state and error bars represent the standard deviations.

As can be observed in Figure 4.11, biodegradation rates followed the same pattern regardless the trans-4MCHCA concentration tested. In all cases, removal rates kept increasing with initial increases in their loading rate until they reached their maximum values and then started to decline with further increases of the trans-4MCHCA loading rates. It is worthwhile to note that the highest concentration tested of 506.20 $\pm$ 4.6 mg L^{-1} trans-4MCHCA led to the highest value of biodegradation rate, with the maximum value of biodegradation rate being 36.5 mg L^{-1} h^{-1} at a loading rate of 68.3 mg L^{-1} h^{-1}.

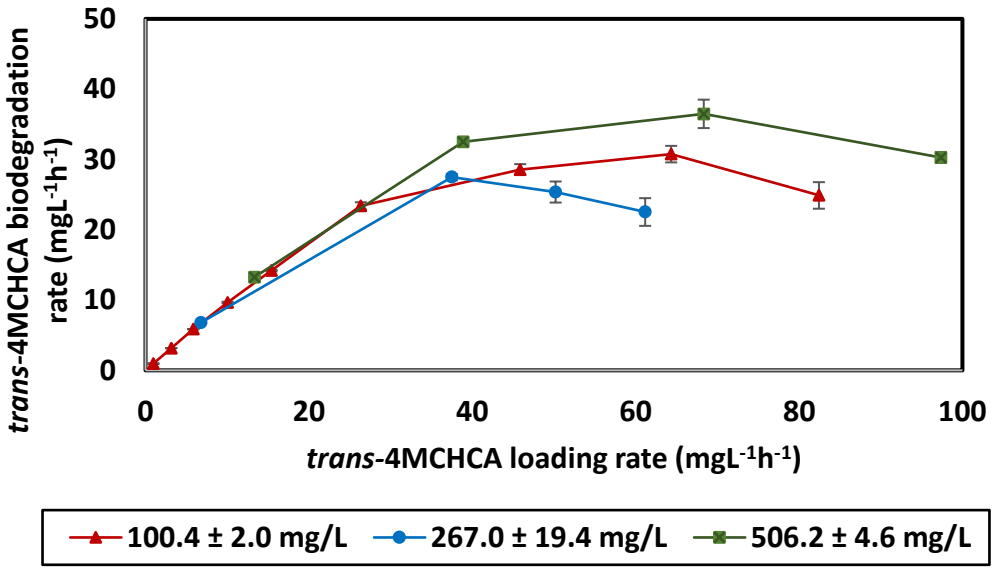

Figure 4.11 Biodegradation rates of various concentrations of trans-4MCHCA as a function of its loading rate in continuously operated MFC with granular electrodes. Presented results are the average values of the data collected over three residence times after the establishment of steady state and error bars represent the standard deviations.

Biodegradation of octanoic acid

Initially, McKinney's medium containing 101.3 $\pm$ 4.4 mg L^{-1} octanoic acid was fed into the anodic chamber at a flow rate of 1.5 ml h^{-1} (loading rate: 1.1 mg L^{-1} h^{-1}; residence time: 90 h). When a removal of 100% was achieved at steady state conditions, the flow rate was increased stepwise. The evaluated flow rates were 9, 14, 20, 27, 31, 60, 80, 114 and 150 ml h^{-1} with the corresponding residence times in the range of 90 to 0.9 hours and loading rates of 1.1 to 114 mg L^{-1} h^{-1}. Figure 4.12 (Panel A) illustrates the residual octanoic acid concentration as a function of its loading rate. As can be seen, complete removal of octanoic acid was achieved for loading rates up to 10.4 mg L^{-1} h^{-1} but further increases in loading rate led to accumulation of octanoic acid. A residual concentration of 66 mg L^{-1} octanoic acid was observed at the highest applied loading rate of 114 mg L^{-1} h-1, and this was considered sufficient deterioration in MFC performance to stop the experiment (i.e. residual octanoic acid concentration was close to the feed concentration).

Figure 4.12 (Panel B) presents biodegradation rates and removal percentages obtained with 101.3 $\pm$ 4.4 mg L^{-1} octanoic acid as a function of its loading rate. As was the case with trans-4MCHCA biodegradation rates increased almost linearly with initial increases in loading rates, reached a maximum value and then declined. The highest biodegradation rate with complete removal of octanoic acid was 10.4 mg L^{-1} h^{-1}. The maximum biodegradation rate was 45.0 mg L^{-1} h^{-1} and obtained at a loading rate of 88.9 mg L^{-1} h^{-1} (removal percentage: 50.7 %). Further increase in loading rate to 114 mg L^{-1} h^{-1} resulted in a biodegradation rate of 40.71 mg L^{-1} h^{-1} and a removal percentage of 35%.

Linear Sweep Voltammetry was carried out at three different loading rates of 23.6, 88.9 and 106.1 mg L^{-1} h^{-1} (corresponding biodegradation rates: 19.5, 45.0 and 37.9 mg L^{-1} h^{-1}) and the data generated was used to develop polarization and power curves presented in Figure 4.12 (Panels C and D). Open circuit potentials observed at these loading rates were 496, 619 and 605 mW, respectively. Similar to the trend seen with trans-4MCHCA as substrate, the maximum power and current densities (940.7 mW m^{-3} and 5929.9 mA m^{-3}) were obtained when the biodegradation rate was at the highest value of 45 mg L^{-1} h^{-1}.

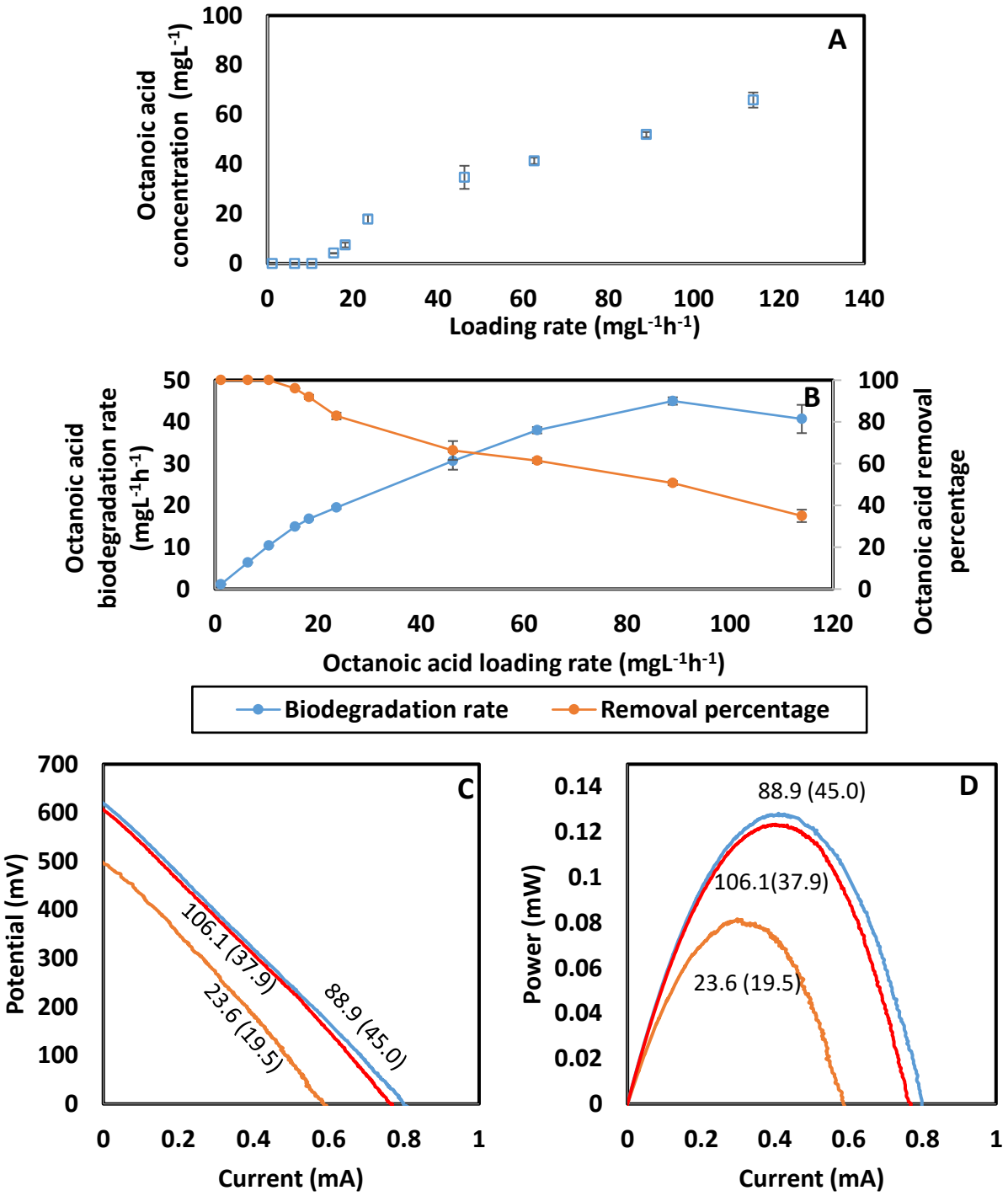

Figure 4.12 Biodegradation of 101.3 ± 4.4 mg L^{-1} octanoic acid in continuously operated MFC with granular electrodes. Panel (A): Steady-state profiles of octanoic acid residual concentration, Panel (B): Biodegradation rate and removal percentage as a function of loading rate. Panels (C) and (D): Polarization and Power curves for various loading rates. Labels on each curve represent applied loading rate, with the corresponding biodegradation rate given in the brackets. Presented results in Panels A and B are the average values of the data collected over three residence times after the establishment of steady state and error bars represent the standard deviations.

Following completion of experiments with 101.3 ± 4.4 mg L^{-1} octanoic acid, the anodic chamber was fed with medium containing 257.0 ± 13.8 mg L^{-1} octanoic acid. Four different flow rates of 4, 24, 32 and 54 ml h^{-1} were evaluated (loading rates: 7.5, 47.9, 60.2 and 95.5 mg h^{-1} L^{-1}; residence times: 35.5, 5.6, 4.2 and 2.5 h, respectively). Figure 4.13 (Panel A) shows that steady state residual concentrations increased from 0 to 145.2 mg L^{-1} as the loading rate increased from 7.5 to 95.5 mg L^{-1} h^{-1}.

As demonstrated in Figure 4.13 (Panel B) the increases in loading rate from 7.5 to 60.2 mg L^{-1} h^{-1} led to increases in biodegradation rate from 7.5 to 39.5 mg L^{-1} h^{-1}; further increase of loading rate to 95.5 mg L^{-1} h^{-1} caused a drop in removal rate to 37.4 mg L^{-1} h^{-1}. When the maximum biodegradation rate of 39.5 mg L^{-1} h^{-1} was achieved, the removal percentage of octanoic acid was 65.5%. A complete removal of octanoic acid was observed at the lowest applied loading rate and the octanoic acid removal percentage was 39.2% at the highest loading rate applied of 95.5 mgL^{-1} h^{-1}.

Linear Sweep Voltammetry data obtained at loading rates of 7.5, 47.9, 60.2 and 95.5 mg h^{-1} L^{-1} (corresponding degradation rates: 7.5, 33.4, 39.5 and 37.4 mg L^{-1} h^{-1}) were employed to develop polarization and power curves shown in Figure 4.13 (Panels C and D). OCP values at these loading rates were 326, 563, 619 and 620 mV, respectively. As expected the maximum power and current outputs of 740.7 mW m^{-3} and 4963.0 mA m^{-3} were again coincided with the highest biodegradation rate of 39.5 mg L^{-1} h^{-1}. It should be noted that similar biodegradation rates led to similar power and current outputs. For instance with biodegradation rates of 39.5 and 37.5 mg L^{-1} h^{-1}, the OCP and maximum power outputs were 619 and 620 mv, 0.10 and 0.98 mW, and 0.66 and 0.61 mA, respectively.

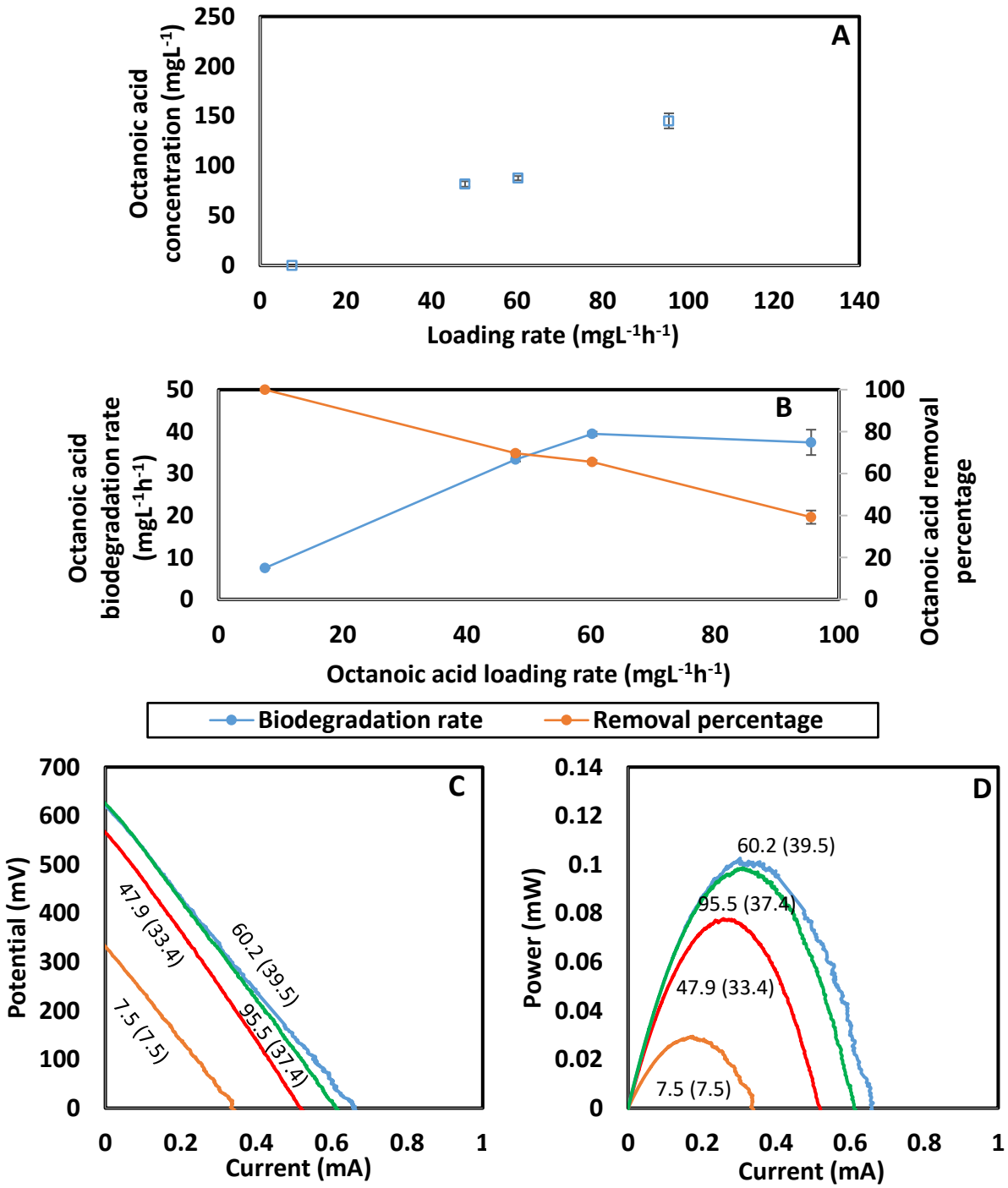

Figure 4.13 Biodegradation of 257.0 ± 13.8 mg L^{-1} octanoic acid in continuously operated MFC with granular electrodes. Panel (A): Steady-state profiles of octanoic acid residual concentration, Panel (B): Biodegradation rate and removal percentage as a function of loading rate. Panels (C) and (D): Polarization and Power curves for various loading rates. Labels on each curve represent applied loading rate, with the corresponding biodegradation rate given in the brackets. Presented results in Panels A and B are the average values of the data collected over three residence times after the establishment of steady state and error bars represent the standard deviations.

The last octanoic acid concentration evaluated in continuously operated MFC was 493.7 $\pm$ 11.4 mg L^{-1}. The feed flow rate was initially set at 3.8 ml h^{-1} (residence time: 35.5 h) and then increased gradually up to 39 m h^{-1} (residence time: 3.5 h), resulting in loading rates in the range of 14.2 – 142.2 mg L^{-1} h^{-1}. Figure 4.14 (Panel A) illustrates the increasing in residual octanoic acid concentration as the applied loading rate increased. No residual concentration was observed at a loading rate of 14.2 mg L^{-1} h^{-1}; further increases in loading rate resulted in accumulation of octanoic acid. The highest residual concentration of 338 mg L^{-1} octanoic acid was observed at a loading rate of 142.2 mg L^{-1} h^{-1}. The MFC performance was considered deteriorated at this point, and no further increases in loading rate were carried out.

Biodegradation rates and removal percentage with 493.7 $\pm$ 11.4 mg L^{-1} octanoic acid as a function of volumetric loading rate are presented in Figure 4.14 (Panel B). Complete removal of octanoic acid was achieved at the lowest applied loading rate of 14.2 mg L^{-1} h^{-1}. Biodegradation rates kept increasing with increases in loading rates up to the maximum value of 49.9 mg L^{-1} h^{-1} at a loading rate of 88.8 mg L^{-1} h^{-1}; removal percentage: 56.1%). After this point the removal rate declined to 44.6 mg L^{-1} h^{-1} (removal percentage: 31.3%) due to further increasing in loading rate to 142.2 mg L^{-1} h^{-1}.

The polarization and power curves were developed at three different loading rates of 14.2, 88.8 and 142.2 mg L^{-1} h^{-1} (corresponding removal rates: 14.2, 49.9 and 44.6). The OCP values obtained at these loading rates were 441, 608 and 599 mV, respectively (Figure 4.14 Panel C). In accordance with the results obtained from the previous octanoic acid concentrations, the power outputs exhibited higher values when the loading rate with the highest removal rate was applied. Maximum power and current densities were 963 mW m^{-3} and 6000 mA m^{-3} at a loading rate of 88.8 mg L^{-1} h^{-1} (biodegradation rate: 49.9 mg L^{-1} h^{-1}).

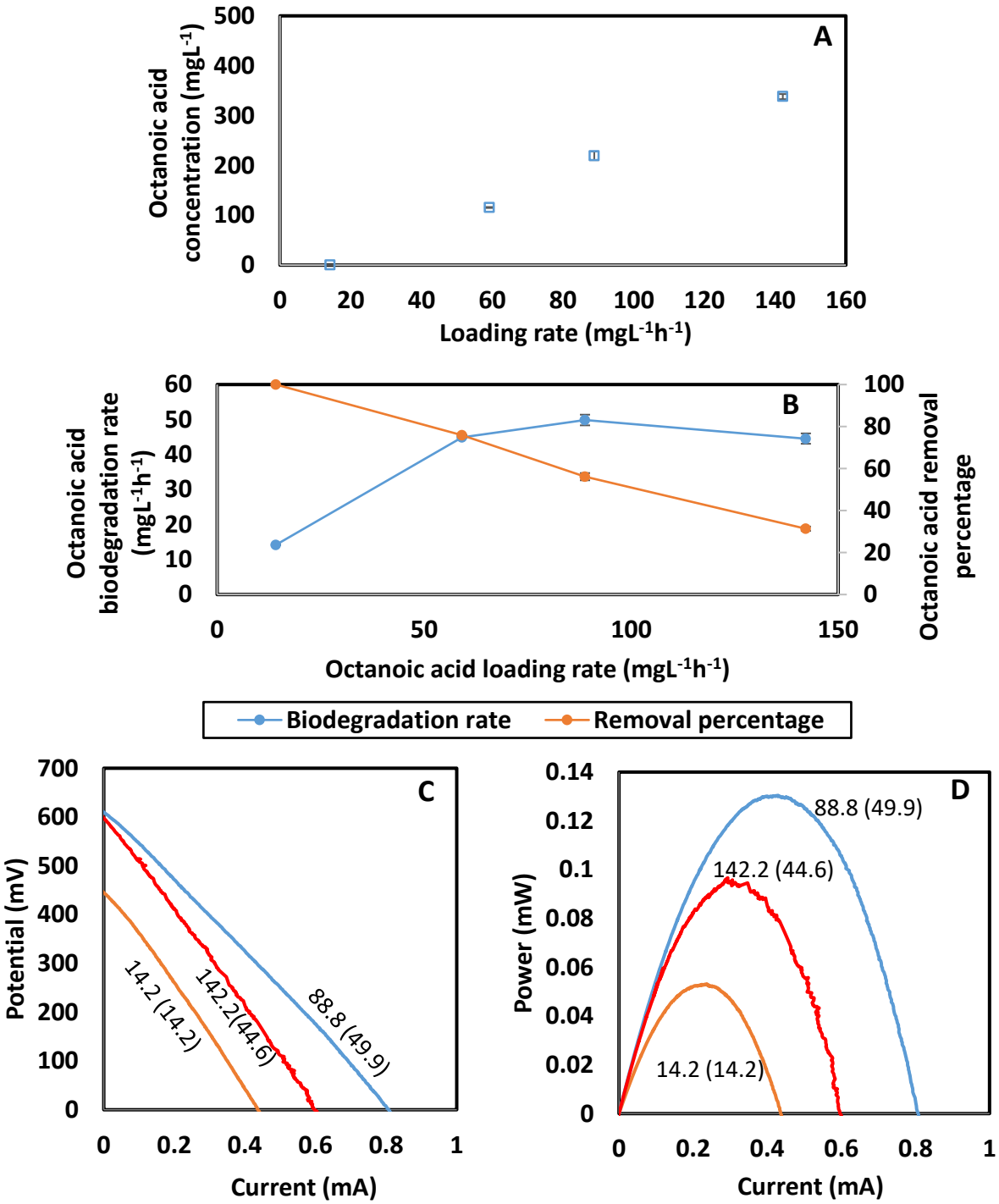

Figure 4.14 Biodegradation of 493.7 ± 11.4 mg L^{-1} octanoic acid in continuously operated MFC with granular electrodes. Panel (A): Steady-state profiles of octanoic acid residual concentration, Panel (B): Biodegradation rate and removal percentage as a function of loading rate. Panels (C) and (D): Polarization and Power curves for various loading rates. Labels on each curve represent applied loading rate, with the corresponding biodegradation rate given in the brackets. Presented results in Panels A and B are the average values of the data collected over three residence times after the establishment of steady state and error bars represent the standard deviations.

Figures 4.15 and 4.16 compare all the results obtained with various octanoic acid concentrations. Removal percentage profiles for different octanoic acid concentrations are displayed in Figure 4.15. As observed, removal percentages higher than 65% were achieved at loading rates in the range from 1.1 to 50 mg L^{-1} h^{-1} for all octanoic acid concentrations evaluated. Interestingly, with a feed containing 257.0 $\pm$ 13.8 mg L^{-1} octanoic acid the removal percentages started to decline faster, resulting in the shortest range of applied loading rates (7.5 – 95.5 mg L^{-1} h^{-1}). In other words, the performance of the MFC at this octanoic acid concentration was deteriorated (low removal rates and percentages) at low loading rates when compared with the other two octanoic acid concentrations evaluated. This fact may be attributed to the lack of acclimation of bacteria to high octanoic acid concentration at the time that experiments with an octanoic acid concentration of 257.0 $\pm$ 13.8 mg L^{-1} were carried out. By contrast, the widest range of loading rates achieved (14.2 – 142.2 mg L^{-1} h^{-1}) was observed at the highest octanoic acid concentration tested (493.7 $\pm$ 11.4 mg L^{-1}), indicating that bacterial consortium might have been better adapted to high octanoic acid concentration during previous experiments with 257.0 $\pm$ 13.8 mg L^{-1} in the feed.

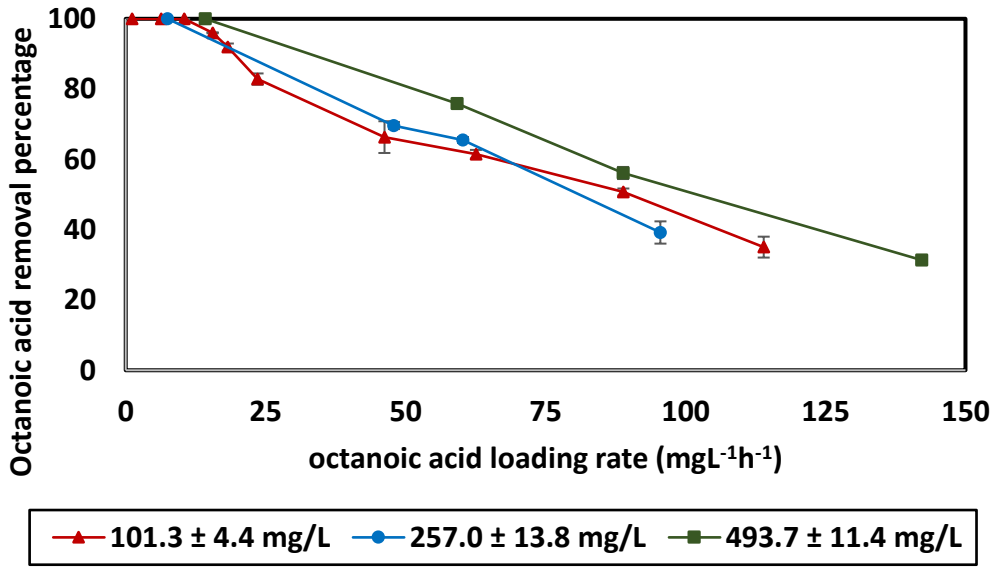

Figure 4.15 Removal rates of octanoic acid various concentrations as a function of its loading rate in continuously operated MFC with granular electrodes. Presented results are the average values of the data collected over three residence times after the establishment of steady state and error bars represent the standard deviations.

As shown in Figure 4.16 biodegradation rates followed the same pattern with all octanoic acid concentrations, increasing linearly with initial increases in loading rates, reaching to the peak value and then started to decline with further increases in loading rates. It is important to note that the highest value of biodegradation rate observed from all evaluated concentrations was 49.9 mg L^{-1} h^{-1} (loading rate: 88.8 mg L^{-1} h^{-1}; removal percentage: 56.1%) and was achieved when the MFC was fed with medium containing 493.7 $\pm$ 11.4 mg L^{-1} octanoic acid. A close biodegration rate of 45.01 mg L^{-1} h^{-1} (loading rate: 88.9 mg L^{-1} h^{-1}; removal percentage: 50.7%) was achieved with a feed containing 101.3 $\pm$ 4.4 mg L^{-1} octanoic acid. Although these removal rates were observed at similar loading rates, the flow rate employed for a concentration of 101.3 $\pm$ 4.4 mg L^{-1} was significantly higher than that employed at a concentration of 493.7 $\pm$ 11.4 mg L^{-1} octanoic acid and residence time was substantially shorter (114 ml h^{-1} vs 24 ml h^{-1}, and 1.2 vs 5.6 h., respectively).

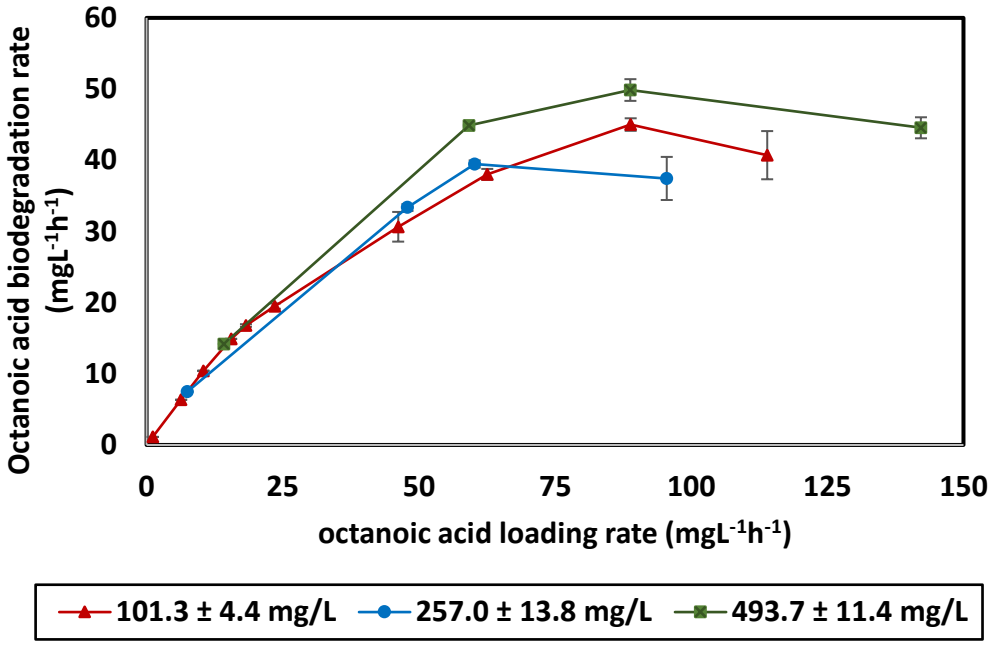

Figure 4.16 Biodegradation rates of octanoic acid at various concentrations as a function of its loading rate in continuously operated MFC with granular electrodes. Presented results are the average values of the data collected over three residence times after the establishment of steady state and error bars represent the standard deviations.

4.2.3 Continuous co-biodegradation of octanoic acid and trans-4MCHCA

As explained in section 3.5, two separate MFC set-ups with granular electrodes were used in this study, one was fed with trans-4MCHCA and the other with octanoic acid, resulting in the development of biofilm adapted to a cyclic or a linear NA, respectively. After completion of batch and continuous experiments, these MFCs were both fed with a medium containing approximately 50 mg L^{-1} trans-4MCHCA and 50 mg L^{-1} to evaluate the co-biodegradation of this mixture. Biodegradation profiles and electrochemical outputs for both MFCs are presented in the next sections.

Figure 4.17 presents biodegradation rates and percentages achieved during removal of a mixture of 45.8 $\pm$ 4.5 mg L^{-1} trans-4MCHCA and 49.9 $\pm$ 6.1 mg L^{-1} octanoic acid as a function of their respective loading rates in MFC with biofilm acclimated to the removal of trans-4MCHCA. Initially, the MFC was operated at a flow rate of 9 ml h^{-1} and then the flow rate was gradually increased to 18, 28, 44, 80 and 100 ml h^{-1}. As can be observed in Figure 4.17 (Panel A), removal rates for both NAs kept increasing with initial increases in the loading rate until they reached their maximum value and then started to decline with further increases in loading rates. As expected, higher biodegradation rates were achieved for octanoic acid for the entire range of applied loading rates, with the maximum biodegradation rate being 14 mg L^{-1} h^{-1} at a loading rate of 25.8 mg L^{-1} h^{-1} (removal percentage: 54.4%). The maximum trans-4MCHCA degradation rate was 9.1 mg L^{-1} h^{-1} and occurred at a loading rate of 25.3 mg L^{-1} h^{-1} (removal percentage: 35.9%). As seen in Figure 4.17 (Panel B), complete removal of both NAs was only observed at the lowest applied loading rate of 3.4 mg L^{-1} h^{-1} and further increases in loading rate led to lower removal percentages of both compounds. At the highest applied loading rate of approximately of 32.6 mg L^{-1} h^{-1}, the removal percentage was 37.4 and 31.8 % for octanoic acid and trans-4MCHCA, respectively. These results clearly indicate that when a linear and a cyclic compound are presented in a mixture, bacterial consortium will preferably consume the linear compound, resulting in higher removal rates and percentages for octanoic acid.

Overall biodegradation rates and removal percentages as a function of the overall loading rate are presented in Figure 4.18 (Panel A). In this case, all parameters were calculated by adding together initial and residual concentrations of both NAs, resulting in a loading rate range from 6.9 to 65.2 mg L^{-1} h^{-1}. A biodegradation rate of 6.9 mg L^{-1} h^{-1} was observed when the removal of both

NAs was complete, and the highest biodegradation rate achieved in the system was 23.1 $mgL^{-1}h^{-1}$ (removal percentage: 45.3%).

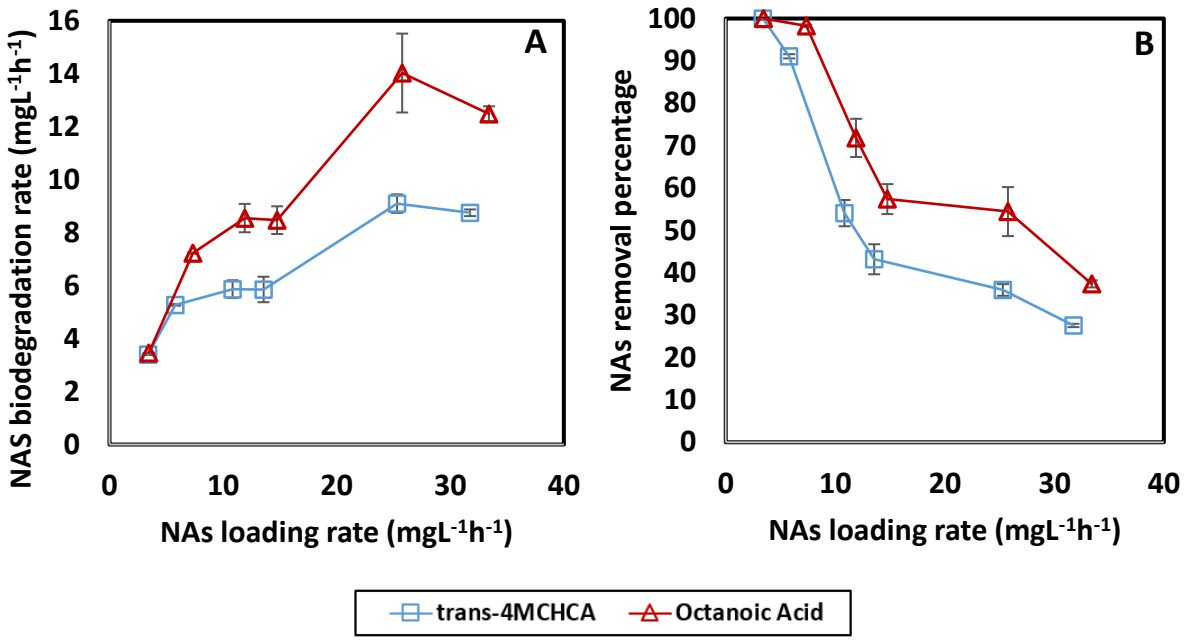

Figure 4.17 Continuous co-biodegradation of 45.8 + 4.5 mg L-1 trans-4MCHCA and 49.9 + 6.1 mg L-1 octanoic acid in MFC with biofilm acclimated to removal of trans-4MCHCA. Panel (A) Biodegradation rate. Panel (B) Removal percentage. Presented results are the average values of the data collected over three residence times after the establishment of steady state and error bars

Polarization and power curves were developed from the LSV data collected at four different loading rates and are presented in Figure 4.18 (Panels B and C). The values of OCP were 196.1, 291.6, 376.8 and 366.7 mV for loading rates of 6.9, 22.8, 51.1 and 65.2 mg L^{-1} h^{-1} (corresponding biodegradation rates: 6.9, 14.4, 23.1 and 21.2 mg L^{-1} h^{-1}, respectively). The highest power and current densities were observed at the highest biodegradation rate of 23.1 mg L^{-1} h^{-1} (loading rate 51.1 : mg L^{-1} h^{-1}), with the values being 422.2 mW m^{-3} and 4000 mA m^{-3}, respectively. As seen, the pattern observed when the MFC was fed with a mixture of NAs was the same as that observed when the system was fed with individual NAs, whereby the highest biodegradation rates led to the highest power and current outputs.

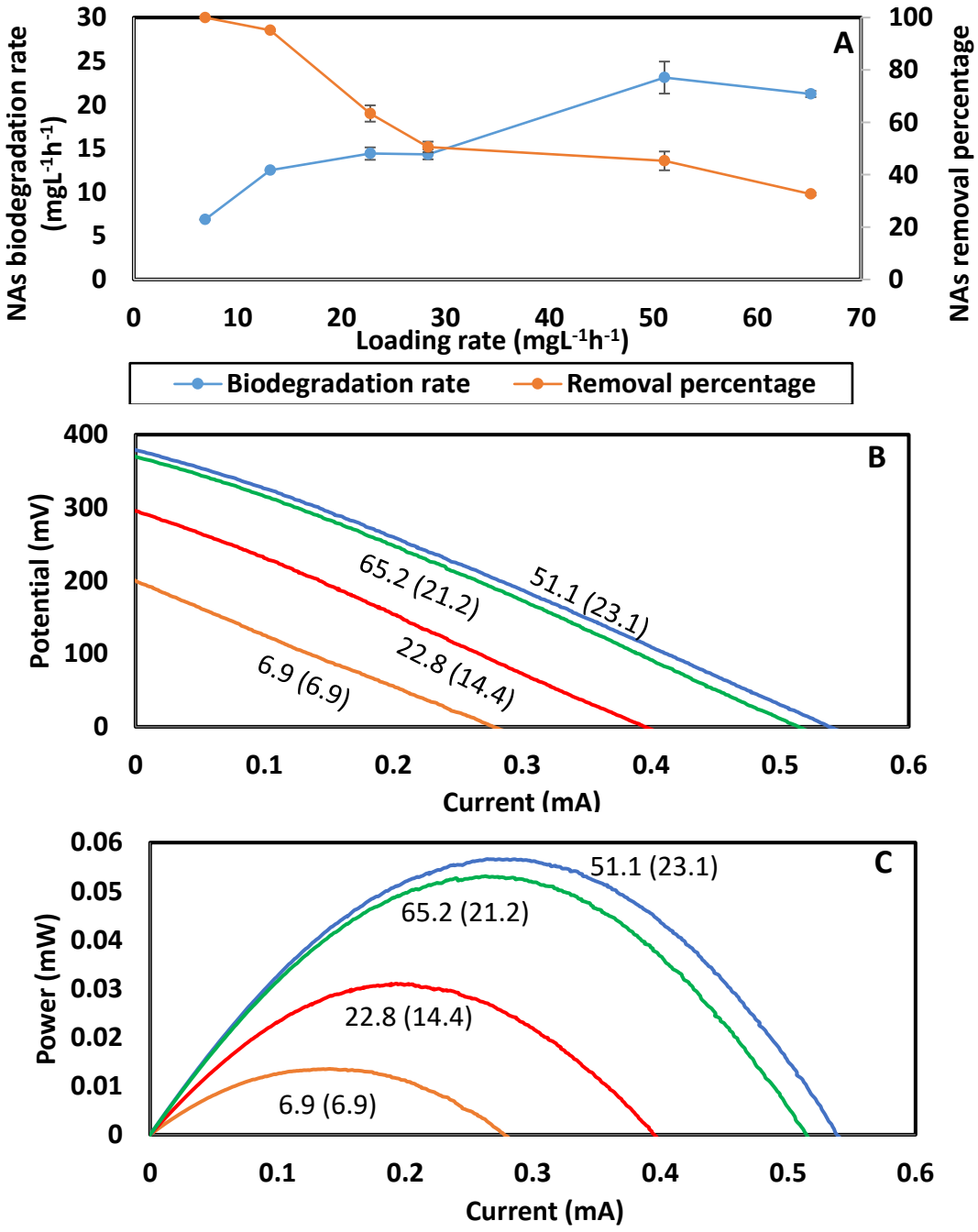

Figure 4.18 Continuous co-biodegradation of 45.8 ± 4.5 mg L^{-1} trans-4MCHCA and 49.9 ± 6.1 mg L^{-1} octanoic acid in MFC with biofilm acclimated to removal of trans-4MCHCA. Panel (A): Overall biodegradation rate and removal percentage as a function of overall loading rate. Panels (B) and (C): Polarization and Power curves for various loading rates. Labels on each curve represent applied overall loading rate, with the corresponding overall biodegradation rate given in the brackets. Presented results in Panel A are the average values of the data collected over three residence times after the establishment of steady state and error bars represent the standard deviations.

Removal profiles of 45.8 ± 4.5 mg L^{-1} trans-4MCHCA and 49.9 ± 6.1 mg L^{-1} octanoic acid in the MFC with biofilm acclimated to the removal of octanoic acid are presented in Figure 4.19. The MFC was operated at four different flow rates (12 to 88 ml h^{-1}). No further increases in flow rate were carried out since the MFC performance was deteriorated at the maximum flow rate of 88 ml h^{-1} (low removal rates and percentages). Similar to the pattern observed in MFC with biofilm developed with trans-4MCHCA as the substrate, the removal rates for octanoic acid were higher than those achieved for trans-4MCHCA (Figure 4.19 Panel A). The maximum degradation rates were 13.3 mg L^{-1} h^{-1} (loading rate: 22.8 mg l^{-1} h^{-1}; removal percentage: 58.2%) and 6.7 mg L^{-1} h^{-1} (loading rate: 10.0 mg l^{-1} h^{-1}; removal percentage: 66.9%) for octanoic acid and trans-4MCHCA, respectively. As seen in Figure 4.21 (Panel B), complete removal of both NAs was not achieved at any loading rate applied and the lowest removal percentages at the highest loading rate were 32.0 and 11.8 % for octanoic acid and trans-4MCHCA, respectively.

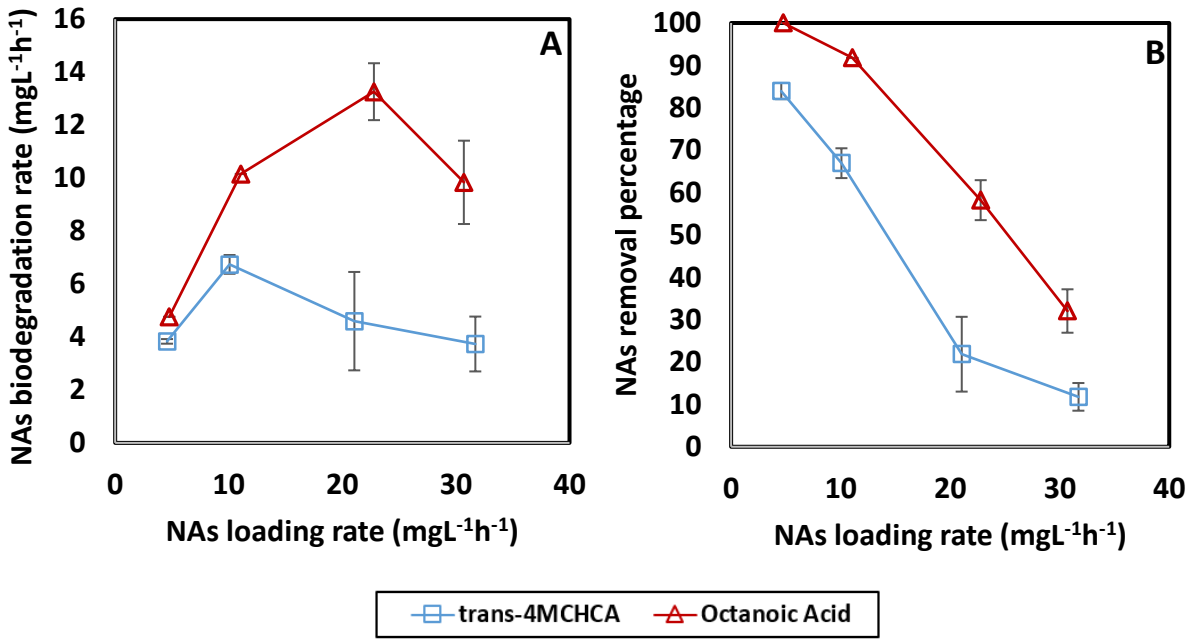

Figure 4.19 Continuous co-biodegradation of 45.8 + 4.5 mg L-1 trans-4MCHCA and 49.9 + 6.1 mg L-1 octanoic acid in MFC with biofilm acclimated to removal of octanoic acid. Panel (A) Biodegradation rate Panel (B) Removal percentage. Presented results are the average values of the data collected over three residence times after the establishment of steady state and error bars represent the standard deviations.

Figure 4.20 (Panel A) presents overall biodegradation rates and percentages as a function of the overall loading rate. When octanoic acid and trans-4MCHCA initial and residual concentrations were added together, the loading rate range achieved was 9.3 - 62.4 mg L^{-1} h^{-1}. The maximum biodegradation rate was 17.9 and occurred at a loading rate of 43.8 mg L^{-1} h^{-1} (removal percentage: 40.7%). LSV was performed at three different loading rates and the polarization and power curves obtained are shown in Figure 4.20 (Panels B and C), respectively. As can be seen, maximum power and current densities of 311.1 mW m^{-3} and 3851.9 mA m^{-3} were obtained when the biodegradation rate was at the maximum level of 17.9 mg L^{-1} h^{-1} (loading rate:43.8 mg$L^{-1}h^{-1}$).

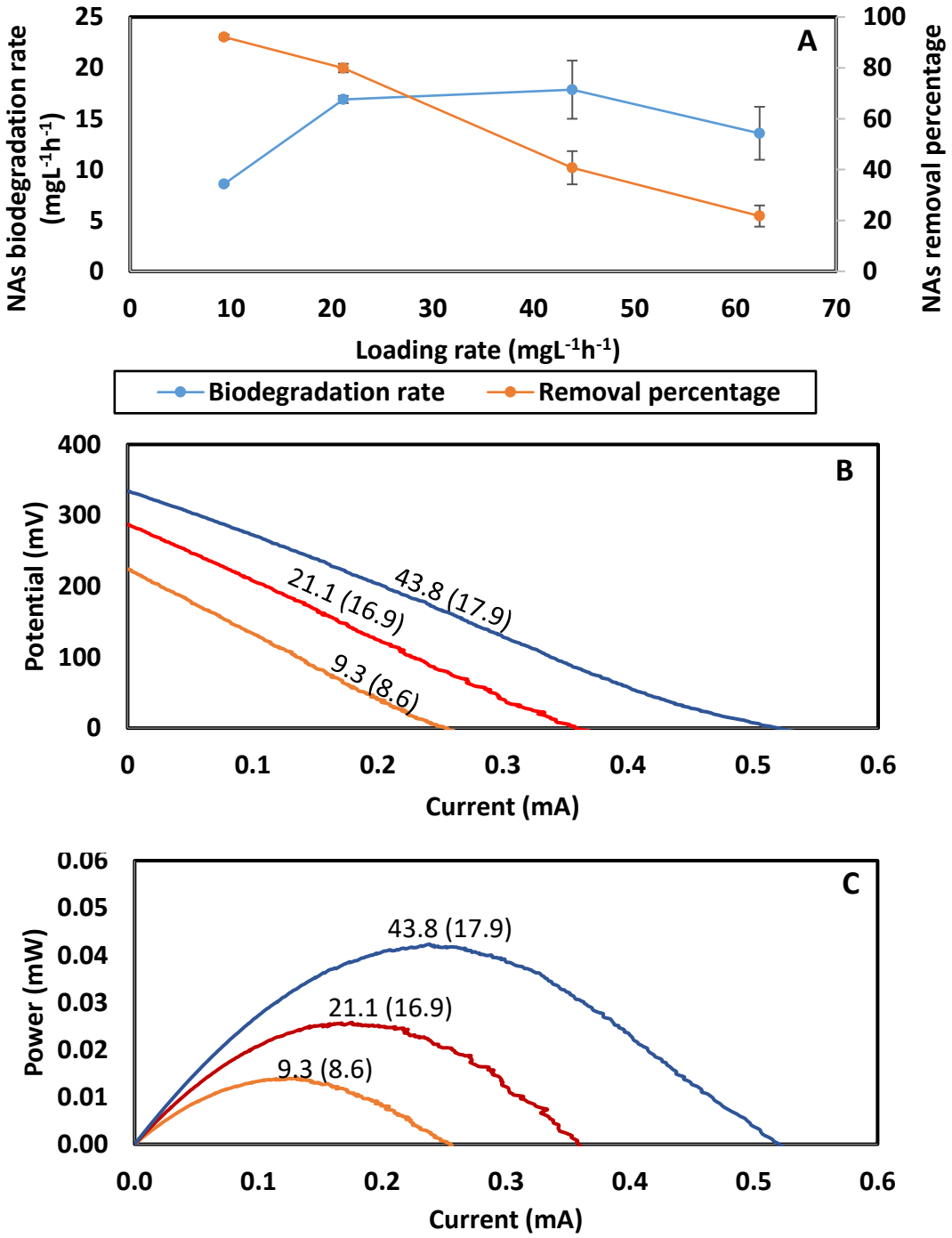

Figure 4.20 Continuous co-biodegradation of 49.7 ± 2.2 mg L^{-1} trans-4MCHCA and 52.1 ± 4.3 mg L^{-1} octanoic acid in MFC with biofilm acclimated to removal of octanoic acid. Panel (A): Biodegradation rate and removal percentage as a function of loading rate. Panels (B) and (C): Polarization and Power curves for various loading rates. Labels on each curve represent applied loading rate, with the corresponding biodegradation rate in the brackets. Presented results in Panel A are the average values of the data collected over three residence times after the establishment of steady state and error bars represent the standard deviations.

Bacterial communities identified in MFC with biofilm acclimated to the removal of octanoic acid or trans-4MCHCA

As indicated earlier in order to identify the dominant bacterial communities in MFCs with biofilm developed with a linear or a cyclic NA, samples from the biofilm developed in the anodic chamber of each MFC were sent to an external laboratory for compositional analysis. The bacterial diversity at phylum and class levels are presented in Figure 4.21 and 4.22, respectively.

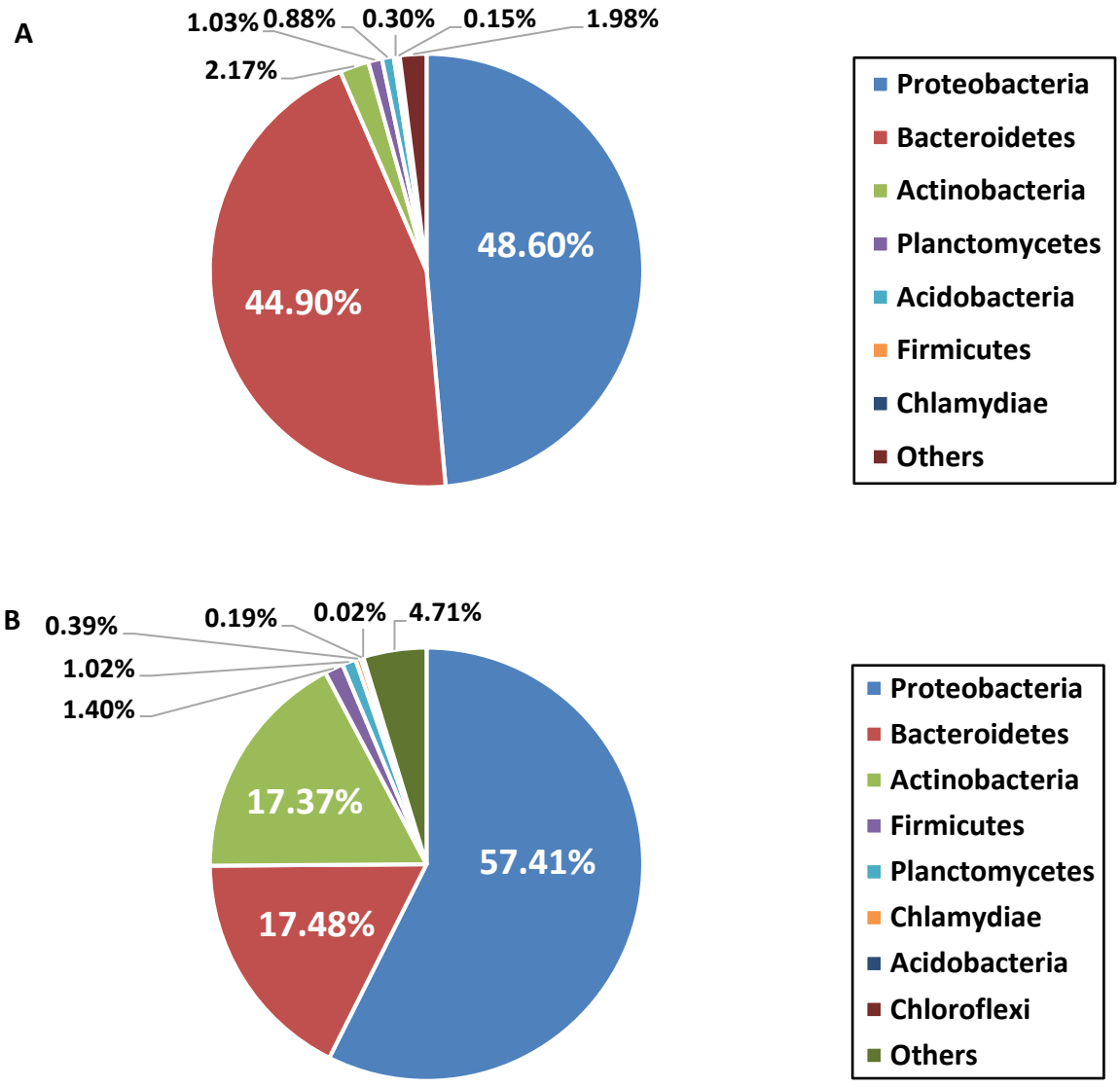

Figure 4.21 Taxonomic classification at the phylum level. Panel (A): Biofilm developed with trans-4MCHCA. Panel (B): Biofilm developed with octanoic acid. Phyla that are less than 1% of total composition or not identified are classified as others.

As can be seen in Figure 4.21 (Panel A), in the MFC with biofilm acclimated to the removal of trans-4MCHCA the most abundant phyla were *Proteobacteria* (48.60%) and *Bacteroidetes* (44.90%). These phyla were also the most abundant in the biofilm acclimated to the removal of octanoic acid (Figure 4.21 Panel B), with abundances of 57.41 and 17.48%, respectively. Another abundant phylum found in this biofilm was *Actinobacteria* (17.37%). These bacterial phyla have been previously reported in studies of OSPW treatment in a single chamber MFC (Choi and Liu 2014).

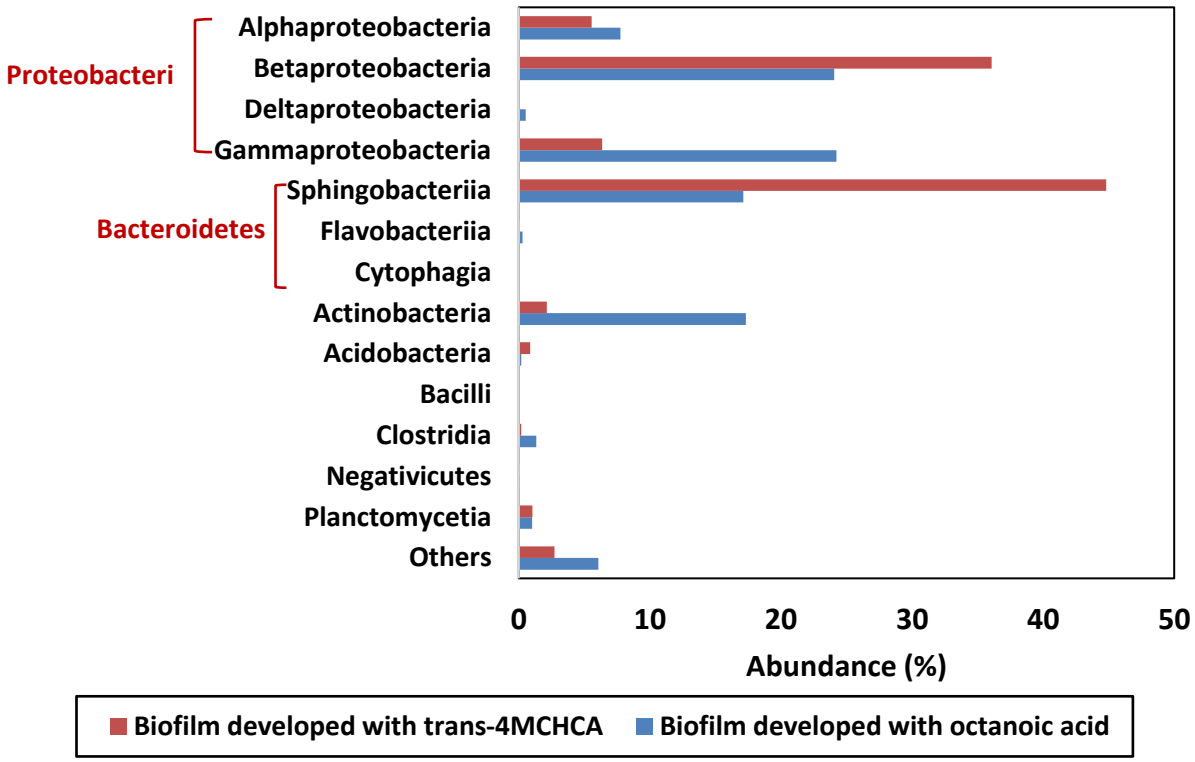

Figure 4.22 Taxonomic classification at the class level. Classes that are less than 1% of total composition or not identified are classified as others.

The taxonomic classification at the class level is shown in Figure 4.22. The dominant classes in MFC with biofilm acclimated to degradation of trans-4MCHCA were *Sphingobacteriia* (44.80%) and *Betaproteobacteria* (36.10 %), while in biofilm developed with octanoic acid the dominant classes were *Gammaproteobacteria* (24.05%), *Betaproteobacteria* (17.33%), *Actinobacteria* (17.33%) and *Sphingobacteriia* (17.12%). These results confirm the predominance of the *Proteobacteria* and *Bacteriodetes* phyla in both MFCs.

4.3 Comparison of individual NAs biodegradation in batch-wise operated MFC with single rod and granular electrodes

This section compares the performances of batch operated MFCs with single rod and granular electrodes. Figure 4.23 (Panel A) contrasts biodegradation rates achieved during removal of three different concentrations of trans-4MCHCA. As seen, regardless the initial concentration, biodegradation rates in MFCs with granular electrodes were significantly higher than those obtained with single rod electrodes. To be more specific, the removal rates in the MFC with granular electrodes were 11, 6.3 and 4.6 times higher than those observed for single rod electrodes MFC at concentrations of 100, 250 and 500 mg L^{-1} trans-4MCHCA, respectively. This significantly improved MFC performance can be attributed to the larger surface area provided by granular electrodes that would facilitate the transfer of electrons (187 m^2 of granular electrodes compared to $1.97x10^{-3}m^2$ of single rod electrodes). Additionally, biofilm formation in the anodic chamber could be another contributing factor since the granular electrodes provide a suitable matrix for cell immobilization and promote high biomass hold up in the system.

Figure 4.23 (Panel B) compares the degradation rates achieved with 100, 250 and 500 mg L^{-1} octanoic acid in MFCs with single rod and granular graphite electrodes. Similar to the pattern observed during biodegradation of trans-4MCHCA, the use of granular electrodes led to a superior performance of the MFC. This can be seen as higher removal rates in granular electrode MFC, with the rates achieved being 20.81, 21.96 and 22.78 mg L^{-1} h^{-1} for initial concentrations of 100, 250 and 500 mg L^{-1} octanoic acid, respectively. When compared with the rates obtained in MFC with single rods, these values are 11.1, 8.8 and 9.3 times greater than their corresponding values in single rod electrode MFCs.

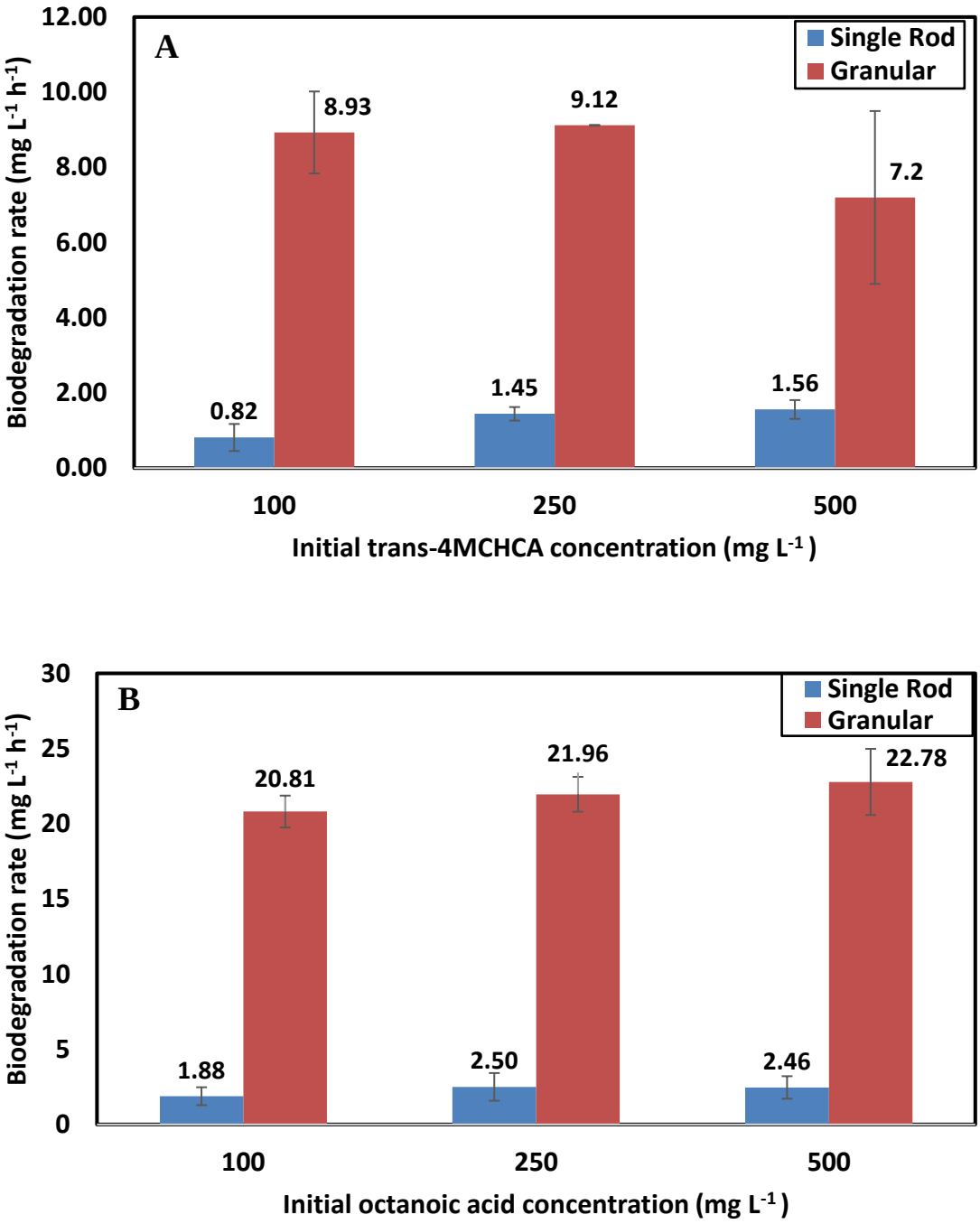

Figure 4.23 Biodegradation rates of NAs at different concentrations in batch-wise operated MFCs with single rod and granular graphite electrodes. Panel (A): Trans-4MCHCA Panel (B): Octanoic acid. Values reported are the average of biodegradation rates observed during the first and second sequential batches. Error bars represent the standard deviations and might not be visible in some cases.

4.4 Comparison of continuous biodegradation of trans-4MCHCA and octanoic acid in granular electrodes MFCs

Table 4.4 provides a summary of the maximum biodegradation rates and corresponding power outputs achieved during continuous biodegradation of both model NAs in granular MFC. As can be seen, maximum values of biodegradation rates for both individual NAs were achieved at a concentration of 500 mg L^{-1}. Similarly, power and current densities reached their maximum values at this concentration.

When the MFC was operated with a feed containing trans-4MCHCA, it was observed that regardless the initial concentration the power outputs reached the maximum value of 481.5 mW m^{-3} (4296.3 mA m^{-3}) and then remained constant even with further increases in the removal rates. This fact can be confirmed with concentrations of 250 and 500 mg L^{-1} trans-4MCHCA, where the corresponding removal rates of 27.5 and 36.5 mg L^{-1} h^{-1} led to same values of power and current densities. In contrast, the trend observed with a feed containing octanoic acid was that higher removal rates led to higher current and power outputs.

Table 4.3 also reveals that MFC performance was superior in terms of biodegradation rates and power outputs during the removal of octanoic acid. This enhanced performance can be attributed to the linear structure of octanoic acid, which makes it more amenable to biodegradation processes.

Table 4.3 Summary of biodegradation results for individual NAs in continuously operated MFC with granular graphite electrodes.

Concentration (mg L^{-1})	***trans*-4MCHCA**			**Octanoic acid**		
	Maximum removal rate ($mgL^{-1}h^{-1}$)	Maximum power density (mW m^{-3})	Maximum current density (mA m^{-3})	Maximum removal rate ($mgL^{-1}h^{-1}$)	Maximum power density (mW m^{-3})	Maximum current density (mA m^{-3})
100	30.8	444.4	4071.1	45.0	940.7	5929.9
250	27.5	481.5	4296.3	39.5	740.7	4963.0
500	36.5	481.5	4296.3	49.9	963.0	6000.0

4.5 Comparison of co-biodegradation of octanoic acid and trans-4MCHCA in batch operated MFCs with single rod electrodes and in continuously operated MFCs with granular electrodes.

Co-biodegradation of octanoic acid and trans-4MCHCA in batch MFCs with single rod electrode revealed that in a mixture of NAs, bacterial culture preferably degraded the linear NA, and degradation of the cyclic compound occurred once the linear compound was completely depleted. These results differ substantially from those obtained in continuously operated MFCs with granular electrodes, in which biodegradation of both compounds occurred simultaneously.

In both MFCs configurations and modes of operation, the biodegradation of octanoic acid proceeded at faster rates, which confirms the fact that linear NAs are more amenable to biodegradation compared to a cyclic structure.

4.6 Comparison of continuous co-biodegradation of octanoic acid and trans-4MCHCA in MFCs with granular electrodes and biofilm developed with a linear or cyclic NA.

Comparing the performances of MFCs acclimated to a linear and a cyclic NAs, revealed that the MFC in which biofilm was developed with trans-4MCHCA as the carbon source was more effective in degradation of both NAs. In other words octanoic acid and trans-4MCHCA biodegradation rates were higher in the MFC originally operated with trans-4MCHCA and these higher rates were also achieved at higher loading rates or shorter residence times. By contrast, in the MFC with biofilm acclimated to octanoic acid the removal rates and percentages for trans-4MCHCA dramatically decreased for loading rates of 10 mg L^{-1} and higher, while in the MFC with biofilm acclimated to trans-4MCHCA these remained high for loading rates as high as 25.3 mg L^{-1} h^{-1}.

The power and current outputs also confirmed the superior performance of MFC with biofilm developed with a cyclic NA. In other words, the higher overall biodegradation rates achieved in this system led to higher power and current densities. Performances of two MFCs employed for continuous biodegradation of NAs are compared in Table 4.4.

Table 4.4 Performances of MFCs with biofilm acclimated to linear and cyclic NAs during continuous co-biodegradation of approximately 50 mg L^{-1} trans-4MCHCA and 50 mg L^{-1} octanoic acid.

	MFC with biofilm acclimated to *trans*-4MCHCA	**MFC with biofilm acclimated to octanoic acid**
Overall maximum biodegradation rate (mg L^{-1} h^{-1})	23.1	17.9
Maximum octanoic acid biodegradation rate (mg l^{-1} h^{-1})	14.0	13.3
Maximum trans-4MCHCA biodegradation rate (mg L^{-1} h^{-1})	9.1	6.7
Power density (mW m^{-3})	422.2	311.1
Current density (mA m^{-3})	4000.0	3851.9

4.7 Comparison of batch biodegradation of trans-4MCHCA in MFCs and anaerobic conventional bioreactors

Table 4.5 compares the batch anoxic biodegradation rates of trans-4MCHCA at different concentrations obtained in conventional bioreactors with two different electron acceptors (nitrate and nitrite) and in MFCs (present work). As seen, biodegradation rates with nitrate as electron acceptor were up to 3.7 higher than those obtained in batchwise operated MFCs. When nitrite was used as the terminal electron acceptor, it was observed that biodegradation rates were similar that those obtained in MFCs.

It should be pointed out that in a MFC, the anode is the final electron acceptor and its potential limits the energy gain for the bacteria to grow (Logan et al., 2006). Thus, the energy available for bacterial growth is limited which results in lower biomass concentrations and biodegradation rates when compared to a conventional bioreactor.

Table 4.5 Comparison of biodegradation rates of trans-4MCHCA obtained at various initial concentrations in anaerobic conventional reactors and MFCs.

trans-4MCHCA Concentration (mgL^{-1})	**Biodegradation rate of trans-4MCHCA ($mg\ L^{-1}\ h^{-1}$)**		
	Nitrate (Gunawan et al., 2013)	**Nitrite (Dong and Nemati, 2016)**	**Present Work**
100	1.25	0.8	0.56
250	5.22	0.8	1.32
500	5.48	-	1.38

4.8 Overview of the works focusing on treatment of aromatic compounds, NAs or OSPW in MFC systems

Table 4.6 contrasts the performances of dual-chambered MFCs utilized in biodegration of phenol, NAs or OSPW. As seen, the lowest treatment efficiency was observed with OSPW as the substrate, while the highest removal percentage was achieved with phenol as the carbon source. Additionally, maximum power outputs obtained with different substrates were in the range of 444 to 613 mW/m^3.

Interestingly, the highest power output was achieved in the MFC operated with octanoic acid, which can be attributed to the fact that its linear structure is more amenable to biodegradation compared to the structures of the other substrates evaluated.

Table 4.6 Overview of earlier works on biodegradation of aromatic compounds, NAs or OSPW in MFC systems

Reference	Substrate	Removal Percentage	Maximum Biodegradation Rate ($mgL^{-1}h^{-1}$)	Maximum Power Output ($mW\ m^{-3}$)
Moreno et al. (2017)	Phenol	53% Phenol	11.5	777.8
Present work	trans-4MCHCA	48% trans-4MCHCA	30.8	444.4
Present Work	Octanoic acid	51% Octanoic Acid	45.0	940.7
Jiang et al. (2013)	OSPW	27.8% COD 32.9% AEO	-	612.5

CHAPTER 5
CONCLUSIONS AND RECOMMENDATIONS FOR FUTURE WORK

5.1 Conclusions

In the present study, anoxic biodegradation of a linear (octanoic acid) and a cyclic (trans-4MCHCA) NAs were carried out in an unconventional bioreactor: Microbial Fuel Cells. The study encompass the use of different types of graphite electrodes (single rod and granular), different modes of operation (batch and continuous), and the variation of the initial concentration of individual NAs or combination of NAs (co-biodegradation), as well as their loading rates.

Batch biodegradation of 100, 250 and 500 mg L^{-1} of both model NAs in MFCs with single rod electrodes and freely suspended cells, demonstrated that the biodegradation of the linear NA occurred at a faster rate than the cyclic NA. It was also found that for both NAs evaluated, the increase in initial concentration of NA led to higher biodegradation rates. With trans-4MCHCA as substrate (cyclic NA), the biodegradation rate increased from 0.56 to 1.38 mg L^{-1} h^{-1} as the initial concentration was increased from 100 to 500 mg L^{-1}. The same pattern was observed with octanoic acid, where biodegradation rates increased from 1.46 to 1.93 mg L^{-1} h^{-1} when the initial concentration increased from 100 to 500 mg L^{-1}.

Sequential addition of both individual NAs was carried out in batch operated MFCs (with single rod and granular electrodes) and the results indicated that consecutives batches could lead to higher biodegradation rates.

During the co-biodegradation of the linear and the cyclic NAs, the biodegradation of octanoic acid (linear) proceeded first, and biodegradation of trans-4MCHCA took place after complete exhaustion of octanoic acid. This fact indicated that bacterial culture preferably consumed the linear compound. In respect of the interaction of a linear and cyclic NAs, biodegradation of octanoic acid was not influenced by the presence of trans-4MCHCA. By contrast, biodegradation of trans-4MCHCA was improved in the presence of octanoic acid.

During continuous biodegradation of individual NAs in MFCs with granular electrodes, two important facts were revealed. The first finding was that the use of graphite electrodes and the subsequent biofilm formation in the anodic chamber led to marked improvement of MFC performance in terms of biodegradation and electrochemical outputs. This can be attributed to the extended surface area provided by the granular electrodes, which not only promote formation of biofilm and enhanced the biomass hold up in the system, but also facilitate the electron transfer. The second observation was that the maximum biodegradation rates of both individuals NAs were achieved during with the highest initial concentration evaluated (500 mg L^{-1}). The maximum biodegradation rates were 36.5 mg L^{-1} h^{-1} (loading rate: 68.3 mg L^{-1} h^{-1}; removal percentage: 53.4%) and 49.9 mg L^{-1} h^{-1} (loading rate: 88.8 mg L^{-1} h^{-1}; removal percentage: 56.1%) for trans-4MCHCA and octanoic acid, respectively. Interestingly, the highest electrochemical outputs were achieved at this maximum biodegradation rates, with the values being 481.5 mW m^{-3} and 4296.3 mA m^{-3} with trans-4MCHCA as the substrate and 963 mW m^{-3} and 6000 mA m^{-3} with a feed containing octanoic acid. This fact indicated that higher biodegradation rates led to higher power generation.

In the continuously operated MFC with granular electrodes simultaneous biodegradation of both NAs was observed which was different from that observed during batch operation of MFC with rod electrodes. Consistent with the results in MFC with single rod electrodes, biodegradation of octanoic acid occurred at much faster rate than trans-4MCHCA. Furthermore, MFC with biofilm acclimated to trans-4MCHCA degradation was more effective in degradation of NA mixtures, which was evident from the higher biodegradation rates and electrochemical outputs achieved.

5.2 Recommendations for future work

Successfully degradation of a linear and a cyclic naphthenic acids in H-type microbial fuel cell bioreactors with concomitant generation of energy was achieved in the present work. In order to decrease the internal loses in the MFC system, it is recommended to evaluate the performance of different MFC configurations such as single-chamber MFC in which the elimination of an ion exchange membrane may lead to reduction of ohmic resistance.

Additional research needs to be carried out using NAs with more complex molecular structure (high number of carbon rings and/or different alkyl positions), such as those directly extracted from the oil sand process water. Furthermore, biodegradation of NAs in MFCs at different temperatures should be assessed, especially at low temperatures which would allow to know the electricity generation capacity of the system without extra supply of energy.

Finally, biodegradation modelling should be carried out for continuously operated MFC in order to compare the biokinetics coefficients with those obtained from the continuous operation of conventional bioreactors.

REFERENCES

Aelterman, P., Rabaey, K., Verstraete, W., 2006. Continuous Electricity Generation at High Voltages and Currents Using Stacked Microbial Fuel Cells. Commun. Agric. Appl. Biol. Sci. 40, 3388–3394. doi:10.1021/es0525511

Allen, E.W., 2008a. Process water treatment in Canada's oil sands industry: I. Target pollutants and treatment objectives. J. Environ. Eng. Sci. 7, 123–138. doi:10.1139/S07-038

Allen, E.W., 2008b. Process water treatment in Canada's oil sands industry: II. A review of emerging technologies. J. Environ. Eng. Sci. 7, 499–524. doi:10.1139/S08-020

An, D., Brown, D., Chatterjee, I., Dong, X., Ramos-Padron, E., Wilson, S., ... & Voordouw, G., 2013. Microbial community and potential functional gene diversity involved in anaerobic hydrocarbon degradation and methanogenesis in an oil sands tailings pond 1. Genome, 56(10), 612-618. doi:10.1139/gen-2013-0083

Brient, J.A., Wessner, P.J., Doyle, M.N., 2000. Naphthenic acids, in: John Wiley & Sons Inc. (Ed.), Kirk-Othmer Encyclopedia of Chemical Technology. New York, pp. 1–10. doi:10.1002/0471238961.1401160802180905.a01

Brown, L.D., Ulrich, A.C., 2015. Oil sands naphthenic acids: A review of properties, measurement, and treatment. Chemosphere 127, 276–290. doi:10.1016/j.chemosphere.2015.02.003

Buitrón, G., Moreno-Andrade, I., 2014. Performance of a Single-Chamber Microbial Fuel Cell Degrading Phenol: Effect of Phenol Concentration and External Resistance. Appl. Biochem. Biotechnol. 174, 2471–2481. doi:10.1007/s12010-014-1195-5

Canadian Association of Petroleum Producers (CAPP) [WWW Document], 2015. Facts Oil Sands. URL http://www.capp.ca/Publications and Statistics/Publications/270274 (accessed 11.23.16).

Choi, J., Liu, Y., 2014. Power generation and oil sands process-affected water treatment in microbial fuel cells. Bioresour. Technol. 169, 581–587. doi:10.1016/j.biortech.2014.07.029

Clark, K.A., Pasternack, D.S., 1932. Hot Water Seperation of Bitumen from Alberta Bituminous Sand. Ind. Eng. Chem. 24, 1410–1416. doi:10.1021/ie50276a016

Clemente, J.S., Fedorak, P.M., 2005. A review of the occurrence, analyses, toxicity, and biodegradation of naphthenic acids. Chemosphere 60, 585–600. doi:10.1016/j.chemosphere.2005.02.065

Clemente, J.S., MacKinnon, M.D., Fedorak, P.M., 2004. Aerobic biodegradation of two commercial naphthenic acids preparations. Environ. Sci. Technol. 38, 1009–1016. doi:10.1021/es030543i

Clothier, L.N., Gieg, L.M., 2016. Anaerobic biodegradation of surrogate naphthenic acids. Water Res. 90, 156–166. doi:10.1016/j.watres.2015.12.019

D'Souza, L., Sami, Y., Nemati, M., Headley, J., 2014. Continuous Co-biodegradation of linear and cyclic naphthenic acids in circulating packed-bed bioreactors. Environ. Prog. Sustain. Energy 33, 835–843. doi:10.1002/ep.11856

Del Rio, L.F., Hadwin, A.K.M., Pinto, L.J., MacKinnon, M.D., Moore, M.M., 2006. Degradation of naphthenic acids by sediment micro-organisms. J. Appl. Microbiol. 101, 1049–1061. doi:10.1111/j.1365-2672.2006.03005.x

Dong, F., 2014. Anoxic Biodegradation of Naphthenic Acid Using Nitrite as an Electron Acceptor. M.Sc. Thesis, University of Saskatchewan, Saskatoon, Canada.

Dong, F., Nemati, M., 2016. Anoxic biodegradation of a surrogate naphthenic acid coupled to reduction of nitrite. Biochem. Eng. J. 110, 84–94. doi:10.1016/j.bej.2016.02.013

Du, Z., Li, H., Gu, T., 2007. A state of the art review on microbial fuel cells: A promising technology for wastewater treatment and bioenergy. Biotechnol. Adv. 25, 464–482. doi:10.1016/j.biotechadv.2007.05.004

ElMekawy, A., Srikanth, S., Bajracharya, S., Hegab, H. M., Nigam, P. S., Singh, A., ... & Pant, D., 2015. Food and agricultural wastes as substrates for bioelectrochemical system (BES): the synchronized recovery of sustainable energy and waste treatment. Food Research International, 73, 213-225. doi:10.1016/j.foodres.2014.11.045

Folwell, B.D., McGenity, T.J., Price, A., Johnson, R.J., Whitby, C., 2016. Exploring the capacity for anaerobic biodegradation of polycyclic aromatic hydrocarbons and naphthenic acids by microbes from oil-sands-process-affected waters. Int. Biodeterior. Biodegrad. 108, 214–221. doi:10.1016/j.ibiod.2014.12.016

Golby, S., Ceri, H., Gieg, L.M., Chatterjee, I., Marques, L.L.R., Turner, R.J., 2012. Evaluation of microbial biofilm communities from an Alberta oil sands tailings pond. FEMS Microbiol. Ecol. 79, 240–250. doi:10.1111/j.1574-6941.2011.01212.x

Gorby, Y. A., Yanina, S., McLean, J. S., Rosso, K. M., Moyles, D., Dohnalkova, A., ... & Culley, D. E., 2006. Electrically conductive bacterial nanowires produced by Shewanella oneidensis strain MR-1 and other microorganisms. Proceedings of the National Academy of Sciences, 103, 11358-11363.

Government of Alberta [WWW Document], 2015. . Oil Sands. URL http://www.energy.alberta.ca/OilSands/pdfs/FactSheet_OilSands.pdf (accessed 11.25.16).

Grewer, D.M., Young, R.F., Whittal, R.M., Fedorak, P.M., 2010. Naphthenic acids and other acid-extractables in water samples from Alberta: What is being measured? Sci. Total Environ. 408, 5997–6010. doi:10.1016/j.scitotenv.2010.08.013

Gunawan, Y., Nemati, M., Dalai, A., 2014. Biodegradation of a surrogate naphthenic acid under denitrifying conditions. Water Res. 51, 11–24. doi:10.1016/j.watres.2013.12.016

Guo, X., Zhan, Y., Chen, C., Cai, B., Wang, Y., Guo, S., 2016. Influence of packing material characteristics on the performance of microbial fuel cells using petroleum refinery wastewater as fuel. Renew. Energy 87, 437–444. doi:10.1016/j.renene.2015.10.041

Guo, X., Zhan, Y., Chen, C., Sun, S., Zhao, L., Guo, S., 2015. Simultaneous bioelectricity

generation and biodegradability improvement of refinery wastewater using microbial fuel cell technology. Desalin. Water Treat. 53, 2740–2745. doi:10.1080/19443994.2014.931535

Han, X., Scott, A.C., Fedorak, P.M., Bataineh, M., Martin, J.W., 2008. Influence of molecular structure on the biodegradability of naphthenic acids. Environ. Sci. Technol. 42, 1290–1295. doi:10.1021/es702220c

Headley, J. V, Du, J.L., Peru, K.M., Gurprasad, N., McMartin, D.W., 2008. Evaluation of algal phytodegradation of petroleum naphthenic acids. J. Environ. Sci. Health. A. Tox. Hazard. Subst. Environ. Eng. 43, 227–232. doi:10.1080/10934520701792670

Headley, J. V, McMartin, D.W., 2004. A review of the occurrence and fate of naphthenic acids in aquatic environments. J. Environ. Sci. Health. A. Tox. Hazard. Subst. Environ. Eng. 39, 1989–2010. doi:10.1081/ESE-120039370

Headley, J. V., Peru, K. M., Mohamed, M. H., Frank, R. A., Martin, J. W., Hazewinkel, R. R. O., ... & Lindeman, D., 2013. Chemical fingerprinting of naphthenic acids and oil sands process waters—A review of analytical methods for environmental samples. Journal of Environmental Science and Health, Part A, 48, 1145-1163. doi:10.1080/10934529.2013.776332

Herman, D.C., Fedorak, P.M., MacKinnon, M.D., Costerton, J.W., 1994. Biodegradation of naphthenic acids by microbial populations indigenous to oil sands tailings. Can. J. Microbiol. 40, 467–477. doi:10.1139/m94-076

Holowenko, F.M., MacKinnon, M.D., Fedorak, P.M., 2001. Naphthenic acids and surrogate naphthenic acids in methanogenic microcosms. Water Res. 35, 2595–2606. doi:10.1016/S0043-1354(00)00558-3

Huang, L. Y., 2011. Bioremediation of Naphthenic Acids in a Circulating Packed Bed Bioreactor. M.Sc. Thesis, Univ. of Saskatchewan, Saskatoon, Canada.

Huang, J., Nemati, M., Hill, G., Headley, J., 2012. Batch and continuous biodegradation of three model naphthenic acids in a circulating packed-bed bioreactor. J. Hazard. Mater. 201–202, 132–140. doi:10.1016/j.jhazmat.2011.11.052

Hwang, G., Dong, T., Islam, M.S., Sheng, Z., Pérez-Estrada, L.A., Liu, Y., Gamal El-Din, M., 2013. The impacts of ozonation on oil sands process-affected water biodegradability and biofilm formation characteristics in bioreactors. Bioresour. Technol. 130, 269–277. doi:10.1016/j.biortech.2012.12.005

Islam, M.S., Zhang, Y., McPhedran, K.N., Liu, Y., Gamal El-Din, M., 2016. Mechanistic investigation of industrial wastewater naphthenic acids removal using granular activated carbon (GAC) biofilm based processes. Sci. Total Environ. 541, 238–246. doi:10.1016/j.scitotenv.2015.09.091

Jiang, Y., Ulrich, A.C., Liu, Y., 2013. Coupling bioelectricity generation and oil sands tailings treatment using microbial fuel cells. Bioresour. Technol. 139, 349–354. doi:10.1016/j.biortech.2013.04.050

Kannel, P.R., Gan, T.Y., 2012. Naphthenic acids degradation and toxicity mitigation in tailings wastewater systems and aquatic environments: a review. J. Environ. Sci. Health. A. Tox. Hazard. Subst. Environ. Eng. 47, 1–21. doi:10.1080/10934529.2012.629574

Lai, J. W., Pinto, L. J., Bendell-Young, L. I., Moore, M. M., & Kiehlmann, E., 1996. Factors that affect the degradation of naphthenic acids in oil sands wastewater by indigenous microbial communities. Environmental Toxicology and Chemistry, 15, 1482-1491. doi:Doi 10.1897/1551-5028(1996)015<1482:Ftatdo>2.3.Co;2

Liu, H., Logan, B.E., 2004. Electricity generation using an air-cathode single chamber microbial fuel cell in the presence and absence of a proton exchange membrane. Environ. Sci. Technol. 38, 4040–4046. doi:10.1021/es0499344

Logan, B.E., 2008. Microbial Fuel Cells, Microbial Fuel Cells. doi:10.1002/9780470258590

Logan, B. E., Hamelers, B., Rozendal, R., Schröder, U., Keller, J., Freguia, S., ... & Rabaey, K., 2006. Microbial fuel cells: methodology and technology. Environmental science & technology, 40(17), 5181-5192. doi:10.1021/es0605016

MacKinnon, M. D., & Boerger, H., 1986. Description of two treatment methods for detoxifying oil sands tailings pond water. Water quality research journal of Canada, 21(4), 496-512.

Majumder, D., Maity, J. P., Tseng, M. J., Nimje, V. R., Chen, H. R., Chen, C. C., ... & Chen, C. Y., 2014. Electricity generation and wastewater treatment of oil refinery in microbial fuel cells using Pseudomonas putida. International journal of molecular sciences, 15, 16772-16786. doi:10.3390/ijms150916772

Marsili, E., Rollefson, J. B., Baron, D. B., Hozalski, R. M., & Bond, D. R. (2008). Microbial biofilm voltammetry: direct electrochemical characterization of catalytic electrode-attached biofilms. Applied and environmental microbiology, 74(23), 7329-7337.

Martin, J. W., Barri, T., Han, X., Fedorak, P. M., El-Din, M. G., Perez, L., ... & Jiang, J. T., 2010. Ozonation of oil sands process-affected water accelerates microbial bioremediation. Environmental science & technology, 44, 8350-8356. doi:10.1021/es101556z

Moreno, L., Nemati, M., Predicala, B., 2015. Biokinetic evaluation of fatty acids degradation in microbial fuel cell type bioreactors. Bioprocess Biosyst. Eng. 38, 25–38. doi:10.1007/s00449-014-1240-3

Moreno, L., Nemati, M., Predicala, B., 2017. Biodegradation of phenol in batch and continuous flow microbial fuel cells with rod and granular graphite electrodes. Environ. Technol. 1–13. doi:10.1080/09593330.2017.1296895

Oh, S.E., Logan, B.E., 2006. Proton exchange membrane and electrode surface areas as factors that affect power generation in microbial fuel cells. Appl. Microbiol. Biotechnol. 70, 162–169. doi:10.1007/s00253-005-0066-y

Pandey, P., Shinde, V.N., Deopurkar, R.L., Kale, S.P., Patil, S.A., Pant, D., 2016. Recent advances in the use of different substrates in microbial fuel cells toward wastewater treatment and simultaneous energy recovery. Appl. Energy 168, 706–723. doi:10.1016/j.apenergy.2016.01.056

Paslawski, J.C., Headley, J. V., Hill, G.A., Nemati, M., 2009. Biodegradation kinetics of trans-4-methyl-1-cyclohexane carboxylic acid. Biodegradation 20, 125–133. doi:10.1007/s10532-008-9206-2

Peighambardoust, S.J., Rowshanzamir, S., Amjadi, M., 2010. Review of the proton exchange membranes for fuel cell applications, in: International Journal of Hydrogen Energy. pp. 9349–9384. doi:10.1016/j.ijhydene.2010.05.017

Pramanik, S., 2016. Review of biological processes in oil sands: A feasible solution for tailings water treatment. Environ. Rev. 24, 274–284. doi:10.1139/er-2015-0088

Quagraine, E.K., Peterson, H.G., Headley, J. V, 2005. In situ bioremediation of naphthenic acids contaminated tailing pond waters in the athabasca oil sands region--demonstrated field studies and plausible options: a review. J. Environ. Sci. Health. A. Tox. Hazard. Subst. Environ. Eng. 40, 685–722. doi:10.1081/ESE-200046649

Quinlan, P.J., Tam, K.C., 2015. Water treatment technologies for the remediation of naphthenic acids in oil sands process-affected water. Chem. Eng. J. 279, 696–714. doi:10.1016/j.cej.2015.05.062

Rabaey, K., Boon, N., Siciliano, S.D., Verhaege, M., Verstraete, W., 2004. Biofuel cells select for microbial consortia that self-mediate electron transfer. Appl. Environ. Microbiol. 70, 5373–5382. doi:10.1128/AEM.70.9.5373-5382.2004

Rabaey, K., Clauwaert, P., Aelterman, P., Verstraete, W., 2005. Tubular microbial fuel cells for efficient electricity generation. Environ. Sci. Technol. 39, 8077–8082. doi:10.1021/es050986i

Rahimnejad, M., Adhami, A., Darvari, S., Zirepour, A., Oh, S.-E., 2015. Microbial fuel cell as new technology for bioelectricity generation: A review. Alexandria Eng. J. 54, 745–756. doi:10.1016/j.aej.2015.03.031

Ramos-Padrón, E., Bordenave, S., Lin, S., Bhaskar, I. M., Dong, X., Sensen, C. W., ... & Gieg, L. M., 2011. Carbon and sulfur cycling by microbial communities in a gypsum-treated oil sands tailings pond. Environmental science & technology, 45, 439-446. doi:10.1021/es1028487

Ren, L., Siegert, M., Ivanov, I., Pisciotta, J.M., Logan, B.E., 2013. Treatability studies on different refinery wastewater samples using high-throughput microbial electrolysis cells (MECs). Bioresour. Technol. 136, 322–328. doi:10.1016/j.biortech.2013.03.060

Scott, A.C., MacKinnon, M.D., Fedorak, P.M., 2005. Naphthenic acids in athabasca oil sands tailings waters are less biodegradable than commercial naphthenic acids. Environ. Sci. Technol. 39, 8388–8394. doi:10.1021/es051003k

Scott, A.C., Zubot, W., MacKinnon, M.D., Smith, D.W., Fedorak, P.M., 2008. Ozonation of oil sands process water removes naphthenic acids and toxicity. Chemosphere 71, 156–160. doi:10.1016/j.chemosphere.2007.10.051

Shi, Y., Huang, C., Rocha, K.C., El-Din, M.G., Liu, Y., 2015. Treatment of oil sands process-affected water using moving bed biofilm reactors: With and without ozone pretreatment. Bioresour. Technol. 192, 219–227. doi:10.1016/j.biortech.2015.05.068

Shizas, I., Bagley, D.M., 2004. Experimental Determination of Energy Content of Unknown Organics in Municipal Wastewater Streams. J. Energy Eng. 130, 45–53. doi:10.1061/(ASCE)0733-9402(2004)130:2(45)

Siwik, P.L., Van Meer, T., MacKinnon, M.D., Paszkowski, C.A., 2000. Growth of fathead minnows in oilsand-processed wastewater in laboratory and field. Environ. Toxicol. Chem. 19, 1837–1845. doi:10.1002/etc.5620190718

Smith, B.E., Lewis, C.A., Belt, S.T., Whitby, C., Rowland, S.J., 2008. Effects of alkyl chain branching on the biotransformation of naphthenic acids. Environ. Sci. Technol. 42, 9323–9328. doi:10.1021/es801922p

Sonawane, J.M., Yadav, A., Ghosh, P.C., Adeloju, S.B., 2016. Recent advances in the development and utilization of modern anode materials for high performance microbial fuel cells. Biosens. Bioelectron. 90, 558–576. doi:10.1016/j.bios.2016.10.014

Srikanth, S., Kumar, M., Singh, D., Singh, M.P., Das, B.P., 2016. Electro-biocatalytic treatment of petroleum refinery wastewater using microbial fuel cell (MFC) in continuous mode operation. Bioresour. Technol. 221, 70–77. doi:10.1016/j.biortech.2016.09.034

Tharali, A.D., Sain, N., Osborne, W.J., 2016. Microbial fuel cells in bioelectricity production. Front. Life Sci. 9, 252–266. doi:10.1080/21553769.2016.1230787

Veeresh, G.S., Kumar, P., Mehrotra, I., 2005. Treatment of phenol and cresols in upflow anaerobic sludge blanket (UASB) process: A review. Water Res. doi:10.1016/j.watres.2004.07.028

Wang, H., Luo, H., Fallgren, P.H., Jin, S., Ren, Z.J., 2015. Bioelectrochemical system platform for sustainable environmental remediation and energy generation. Biotechnol. Adv. 33, 317–334. doi:10.1016/j.biotechadv.2015.04.003

Watanabe, K., 2008. Recent Developments in Microbial Fuel Cell Technologies for Sustainable Bioenergy. J. Biosci. Bioeng. 106, 528–536. doi:10.1263/jbb.106.528

Watson, V.J., Logan, B.E., 2010. Power production in MFCs inoculated with Shewanella oneidensis MR-1 or mixed cultures. Biotechnol. Bioeng. 105, 489–498. doi:10.1002/bit.22556

Whitby, C., 2010. Microbial naphthenic Acid degradation. Adv. Appl. Microbiol. 70, 93–125. doi:10.1016/S0065-2164(10)70003-4

Yu, N., Xing, D., Li, W., Yang, Y., Li, Z., Li, Y., Ren, N., 2017. Electricity and methane production from soybean edible oil refinery wastewater using microbial electrochemical systems. Int. J. Hydrogen Energy 42, 96–102. doi:10.1016/j.ijhydene.2016.11.116

Zhang, F., Ahn, Y., Logan, B.E., 2014. Treating refinery wastewaters in microbial fuel cells using separator electrode assembly or spaced electrode configurations. Bioresour. Technol. 152, 46–52. doi:10.1016/j.biortech.2013.10.103

Zhang, Y., Sun, J., Hu, Y., Li, S., Xu, Q., 2012. Bio-cathode materials evaluation in microbial fuel cells: A comparison of graphite felt, carbon paper and stainless steel mesh materials. Int. J. Hydrogen Energy 37, 16935–16942. doi:10.1016/j.ijhydene.2012.08.064

APPENDIX A

Gas Chromatography (GC) Calibration Curve

Linear calibration curves for Gas Chromatography were developed using six standard solutions (10, 20, 40, 60, 80 and 100 mg L^{-1}) of either trans-4MCHCA or octanoic acid in modified McKinney's medium. The average retention times were 6.72 ± 0.5, and 5.89 ± 0.5 min. for trans-4MCHCA and octanoic acid, respectively. Calibration was carried out regularly to ensure accuracy and reproducibility of the measurements results. Representative calibration curves for each model NA are presented below.

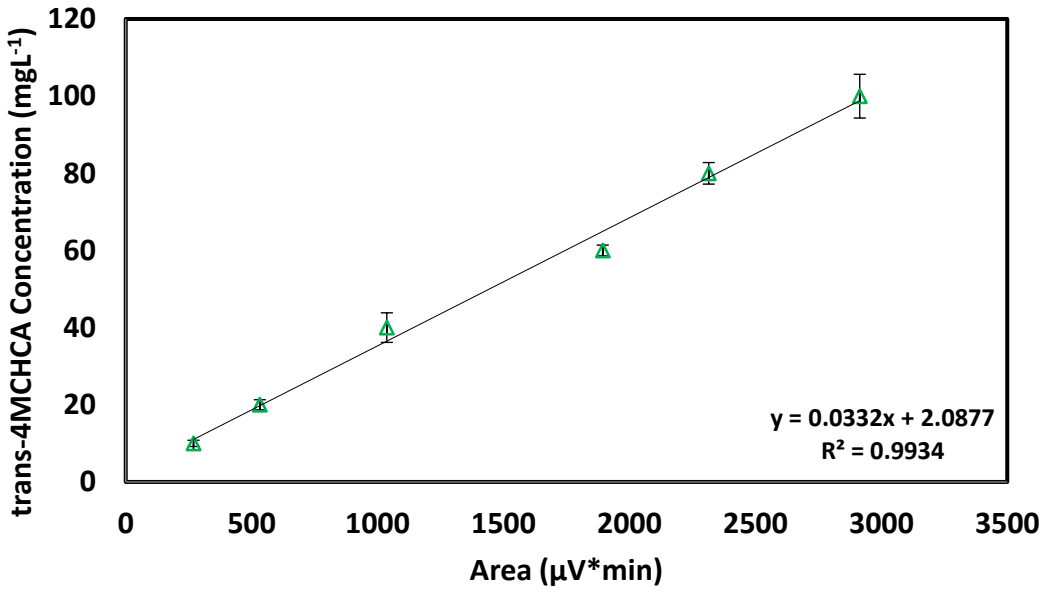

Figure A.1 Calibration curve developed for various trans-4MCHCA concentrations. Error bars represent standard deviations in three trans-4MCHCA concentration readings.

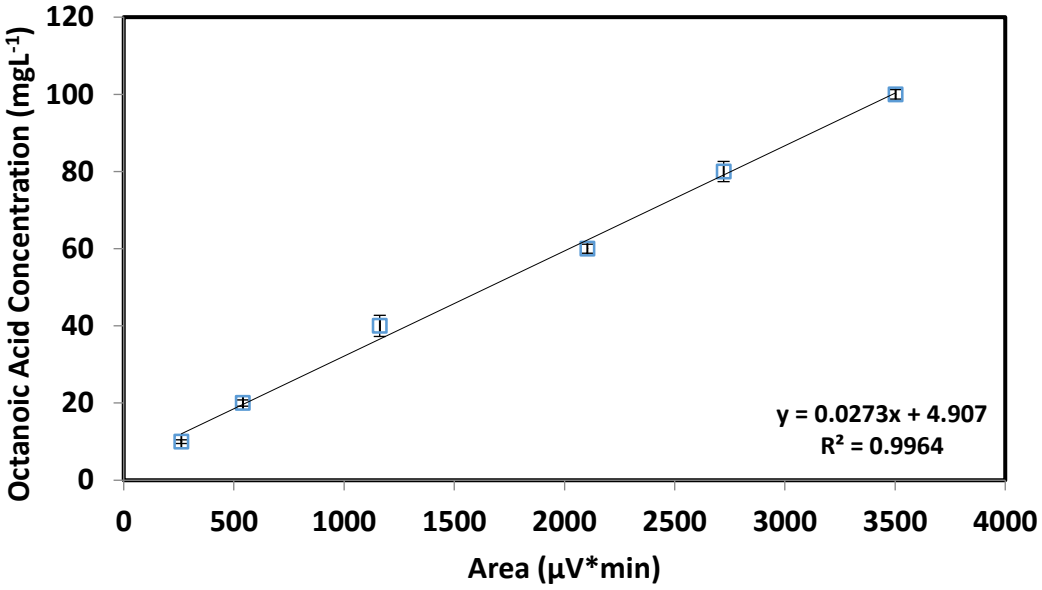

Figure A.2 Calibration curve developed for various octanoic acid concentrations. Error bars represent standard deviations in three octanoic acid concentration readings.

Biomass Calibration Curve

Biomass measurements were obtained from batch operated MFCs with single rod electrodes. Calibration curve for biomass was developed in previous studies in our research group (Dong, 2014) with the linear relationship between Optical Density and biomass dry weight concentration. Figure A.3 shows the biomass calibration curve obtained.

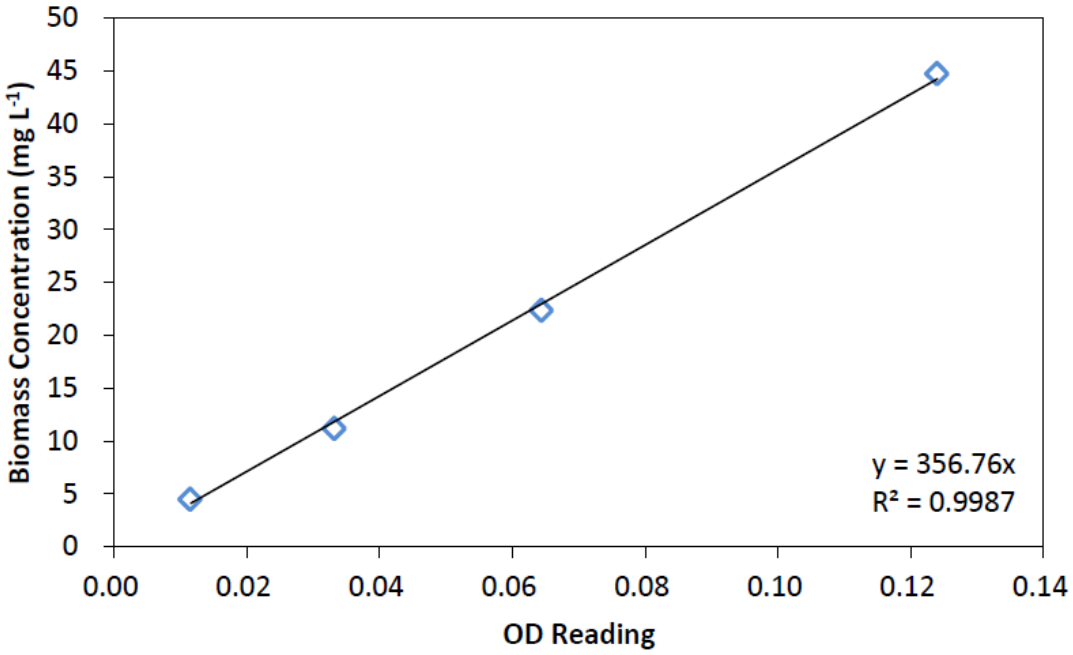

Figure A.3 Biomass Calibration Curve. Reprinted from Anoxic Biodegradation of Naphthenic Acid using Nitrite as an Electron Acceptor, by Dong F., 2014, University of Saskatchewan.

APPENDIX B

Sample of Gas Chromatogram

Figure B.1 shows the chromatogram obtained during co-biodegradation studies. In this chromatogram, the elution times were 5.89 and 6.59 min. for octanoic acid and trans-4MCHCA, respectively.

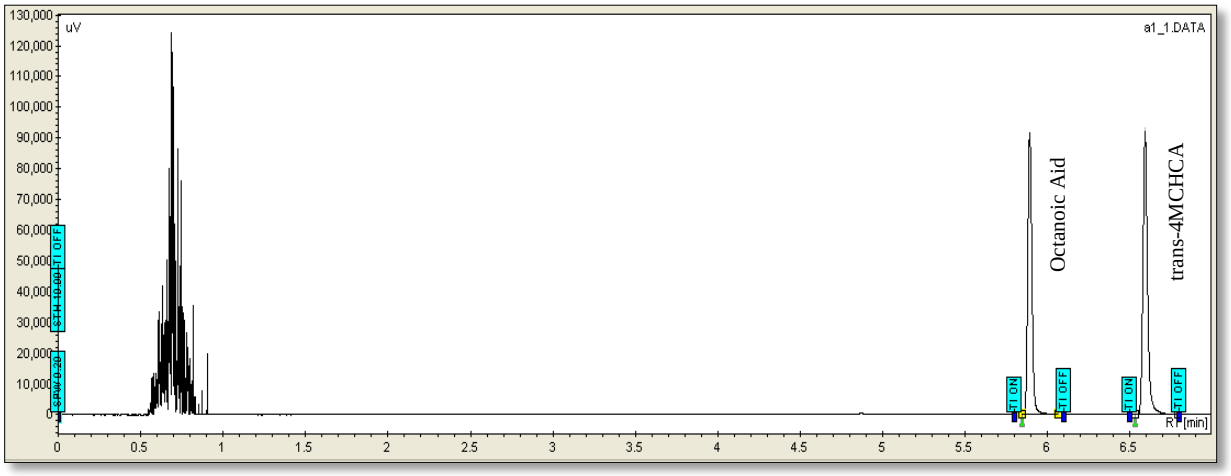

Figure B. 1 The representative GC/FID chromatogram of octanoic acid and trans-4MCHCA.

APPENDIX C

Calculations

The following equations were used to calculate Hydraulic Residence Time (HRT), NAs loading rate, biodegradation rate and removal percentage in continuously operated MFCs with granular electrodes.

$HRT = V/Q$ ……(C.1)

Loading rate: (S_0/HRT) ……(C.2)

Biodegradation rate: $(S_0-S)/HRT$ ……..……(C.3)

Removal percentage: $((S_0-S)/S_0)*100\%$ ……..(C.4)

Where:

Q: volumetric flow rate of the influent and the effluent (mL h^{-1})

S_0: feed NAs concentration (mg L^{-1})

S: residual NAs concentration (mg L^{-1})

V: working volume of the bioreactor (mL)